NASA/TM–2023–104606/Vol. 64

Technical Report Series on Global Modeling and Data Assimilation, Volume 64

Randal D. Koster, Editor

Soil Moisture Active Passive (SMAP) Project Assessment Report for Version 7 of the L4_SM Data Product

Rolf H. Reichle, Qing Liu, Joseph V. Ardizzone, Michel Bechtold, Wade T. Crow, Gabrielle J. M. De Lannoy, John S. Kimball, and Randal D. Koster

March 2023

NASA STI Program ... in Profile

Since its founding, NASA has been dedicated to the advancement of aeronautics and space science. The NASA scientific and technical information (STI) program plays a key part in helping NASA maintain this important role.

The NASA STI program operates under the auspices of the Agency Chief Information Officer. It collects, organizes, provides for archiving, and disseminates NASA's STI. The NASA STI program provides access to the NTRS Registered and its public interface, the NASA Technical Reports Server, thus providing one of the largest collections of aeronautical and space science STI in the world. Results are published in both non-NASA channels and by NASA in the NASA STI Report Series, which includes the following report types:

- TECHNICAL PUBLICATION. Reports of completed research or a major significant phase of research that present the results of NASA Programs and include extensive data or theoretical analysis. Includes compilations of significant scientific and technical data and information deemed to be of continuing reference value. NASA counterpart of peer-reviewed formal professional papers but has less stringent limitations on manuscript length and extent of graphic presentations.

- TECHNICAL MEMORANDUM. Scientific and technical findings that are preliminary or of specialized interest, e.g., quick release reports, working papers, and bibliographies that contain minimal annotation. Does not contain extensive analysis.

- CONTRACTOR REPORT. Scientific and technical findings by NASA-sponsored contractors and grantees.

- CONFERENCE PUBLICATION. Collected papers from scientific and technical conferences, symposia, seminars, or other meetings sponsored or co-sponsored by NASA.

- SPECIAL PUBLICATION. Scientific, technical, or historical information from NASA programs, projects, and missions, often concerned with subjects having substantial public interest.

- TECHNICAL TRANSLATION. English-language translations of foreign scientific and technical material pertinent to NASA's mission.

Specialized services also include organizing and publishing research results, distributing specialized research announcements and feeds, providing information desk and personal search support, and enabling data exchange services.

For more information about the NASA STI program, see the following:

- Access the NASA STI program home page at http://www.sti.nasa.gov

- E-mail your question to help@sti.nasa.gov

- Phone the NASA STI Information Desk at 757-864-9658

- Write to:
  NASA STI Information Desk
  Mail Stop 148
  NASA Langley Research
  Center Hampton, VA 23681-
  2199

NASA/TM–2023–104606/Vol. 64

Technical Report Series on Global Modeling and Data Assimilation, Volume 64

Randal D. Koster, Editor

Soil Moisture Active Passive (SMAP) Project Assessment Report for Version 7 of the L4_SM Data Product

Rolf H. Reichle
Goddard Space Flight Center, Greenbelt, MD

Qing Liu
Science Systems and Applications Inc., Lanham, MD

Joseph V. Ardizzone
Science Systems and Applications Inc., Lanham, MD

Michel Bechtold
KU Leuven, Leuven, Belgium

Wade T. Crow
U.S. Department of Agriculture, Beltsville, MD

Gabrielle J. M. De Lannoy
KU Leuven, Leuven, Belgium

John S. Kimball
University of Montana, Missoula, MT

Randal D. Koster
Goddard Space Flight Center, Greenbelt, MD

National Aeronautics and Space Administration

Goddard Space Flight Center
Greenbelt, Maryland 20771

March 2023

Level of Review: This material has been technically reviewed by technical management.

Available from

NASA STI Program
Mail Stop 148
NASA's Langley Research Center
Hampton, VA 23681-2199

National Technical Information Service
5285 Port Royal Road
Springfield, VA 22161
703-605-6000

TABLE OF CONTENTS

This page intentionally left blank.

EXECUTIVE SUMMARY

This report closely examines Version 7 of the NASA Soil Moisture Active Passive (SMAP) Level 4 Surface and Root Zone Soil Moisture (L4_SM) product, which was first released on 15 November 2022. The assessment includes comparisons of L4_SM soil moisture estimates with in situ measurements from SMAP core validation sites and sparse networks. Also provided is a quasi-global evaluation of the product's anomaly correlation skill relative to the previous version and a model-only version, based on independent satellite radar soil moisture retrievals and an Instrumental Variable approach. The assessment further provides a global evaluation of the internal diagnostics from the ensemble-based data assimilation system that is used to generate the L4_SM product, including observation-minus-forecast (O-F) brightness temperature (Tb) residuals and soil moisture analysis increments. The core validation site comparisons, the assessment of the anomaly correlation skill using independent radar soil moisture retrievals, and the statistics of the assimilation diagnostics are considered primary validation methodologies for the L4_SM product. Comparisons against in situ measurements from regional-scale sparse networks are considered a secondary validation methodology because such in situ measurements are subject to upscaling errors from their native point-scale to the grid-cell scale of the data product. The validation period is April 2015 to March 2022.

The two key changes in the Version 7 L4_SM product relative to earlier versions are (i) improved hydrological process modeling for peatlands (PEATCLSM) and an updated global distribution of peatlands and (ii) the use of climatological L-band soil roughness, scattering albedo, and (seasonally varying) vegetation opacity parameters derived from the SMAP Level 2 soil moisture retrieval product.

An analysis of the time-average surface and root zone soil moisture shows that the global pattern of arid and humid regions is well captured by the Version 7 L4_SM estimates. In peatlands, the Version 7 surface soil moisture is somewhat wetter on average with much increased variability compared to that of Version 6, and the root zone soil moisture is much wetter, owing to the new peatland hydrology module. These changes are also reflected in the surface turbulent fluxes and in the surface and soil temperatures. Because of these climatological differences, the Version 6 and Version 7 products should *not* be combined into a single dataset for use in applications that include peatlands.

Results from the core validation site comparisons indicate that the Version 7 L4_SM product meets its accuracy requirement, which is formulated in terms of the root-mean square (RMS) error after removal of the long-term mean error, i.e., ubRMSE≤0.04 m^3 m^{-3}, where the error is vs. the unknown true soil moisture. Computed directly against core site in situ measurements at the 9-km scale, the average unbiased RMS difference (ubRMSD) of the 3-hourly Version 7 L4_SM data is 0.041 m^3 m^{-3} for surface soil moisture and 0.026 m^3 m^{-3} for root zone soil moisture. When factoring in measurement and upscaling errors of the in situ data, the L4_SM product meets the 0.04 m^3 m^{-3} ubRMSE requirement.

The ubRMSD values of the Version 7 soil moisture are essentially unchanged from those of Version 6. There is a small but consistent increase in the correlation skill of the Version 7 surface and root zone soil moisture, likely owing to the improved seasonal cycle amplitude and phasing of the L-band vegetation opacity parameters derived from the SMAP Level 2 retrieval product.

The Version 7 L4_SM estimates are an improvement compared to estimates from a model-only Open Loop (OL7000) simulation, which demonstrates the beneficial impact of the SMAP Tb data. Overall, L4_SM surface and root zone soil moisture estimates are more skillful than model-only simulation (OL7000) estimates, with statistically significant improvements for surface soil moisture R and anomaly R values (based on 95% confidence intervals). Results from comparisons of the L4_SM product to in situ measurements from more than 400 sparse network sites corroborate the core validation site results.

The new peatland water level output of the Version 7 L4_SM product provides reasonable estimates, as indicated by the validation of retrospective simulations with the L4_SM land model against historic in situ measurements.

The evaluation of the anomaly correlation skill based on independent radar soil moisture retrievals indicates that there is no net skill difference between the Version 6 and Version 7 L4_SM products. This is expected because the key changes in the Version 7 L4_SM algorithm are limited to peatlands and climatological model parameters.

The instantaneous soil moisture analysis increments lie within a reasonable range and result in spatially smooth soil moisture analyses. The long-term mean soil moisture analysis increments make up only a small fraction of the water budget. Regionally, the O-F Tb residuals exhibit only a modest bias (less than 3 K) between the (rescaled) SMAP Tb observations and the L4_SM model forecast, which indicates that the assimilation system is reasonably unbiased. The globally averaged time series standard deviation of the O-F Tb residuals is 5.0 K, which represents a reduction of ~0.1 K from that of the Version 6 product. The globally averaged time series standard deviation is 3.3 K for the observation-minus-analysis Tb residuals, reflecting the impact of the SMAP observations on the L4_SM system. The Tb simulation skill is most improved in peatlands, with average reductions in the typical magnitude of the O-F Tb residuals exceeding 1 K in northern peatlands.

Regionally, the time series standard deviation of the normalized O-F Tb residuals deviates considerably from unity, which indicates that the L4_SM assimilation algorithm tends to over- or underestimate the total (model and observation) error present in the system. There is no net difference in this metric between the Version 6 and Version 7 L4_SM algorithms.

In summary, Version 7 of the L4_SM product is sufficiently mature and of suitable quality for distribution to, and use by, the larger science and application communities.

1 INTRODUCTION

The NASA Soil Moisture Active Passive (SMAP) mission provides space-borne global measurements of the Earth's L-band (1.4 GHz) brightness temperature (Tb) emission from a 685-km, near-polar, sun-synchronous orbit. These observations are primarily sensitive to soil moisture and temperature in the top few centimeters of the soil. SMAP data can therefore be used to enhance our understanding of processes that link the terrestrial water, energy, and carbon cycles, and to potentially extend the capabilities of weather and climate prediction models (Entekhabi et al. 2014).

The suite of SMAP science data products includes the Level 4 Surface and Root Zone Soil Moisture (L4_SM) product, which provides deeper-layer soil moisture estimates that are not available in the Level 2-3 retrieval products. The L4_SM product is based on the assimilation of SMAP Tb observations into the NASA Catchment land surface model (Koster et al. 2000) using a customized version of the Goddard Earth Observing System (GEOS) land data assimilation system (Figure 1; Reichle et al. 2014a, 2017a,b, 2019). This system, which is based on the ensemble Kalman filter (EnKF), accounts for model and observational uncertainty through perturbations of select Catchment model forcing and soil moisture prognostic variables, propagates the surface information from the SMAP instrument to the deeper soil, and ultimately provides global, 3-hourly estimates of soil moisture and other land surface fields without gaps in coverage. The mean publication latency of the L4_SM product is ~2.5 days. This latency is driven by the availability of gauge-based precipitation data used to force the land surface model (Reichle and Liu 2014, 2021; Reichle et al. 2014b, 2021a, 2022a).

The L4_SM product provides surface and root zone soil moisture (along with other geophysical fields) as 3-hourly, time-average fields on the global, cylindrical, 9 km Equal-Area Scalable Earth, version 2 (EASEv2; Brodzik et al. 2012) grid in the "geophysical" (or "gph") output Collection (Reichle et al. 2022b). Moreover, instantaneous soil moisture and soil temperature fields before and after the assimilation update are provided every three hours on the same grid in the "analysis update" (or "aup") output Collection, along with other assimilation diagnostics and error estimates. Time-invariant land model parameters, such as soil porosity, wilting point, and microwave radiative transfer model parameters, are provided in the "land-model-constants" (or "lmc") Collection (Reichle et al. 2022b).

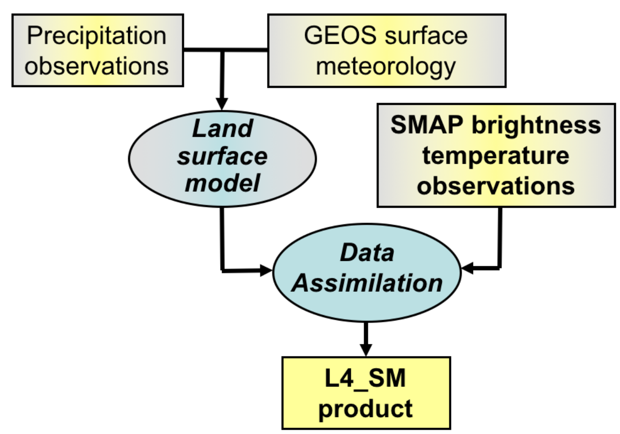

Figure 1. Schematic of the L4_SM algorithm.

For geophysical data products that are based on the assimilation of satellite observations into numerical process models, validation is critical and must be based on quantitative estimates of uncertainty. Direct comparison with independent observations, including ground-based measurements, is a key part of validation. This assessment report provides a detailed description of the status of the L4_SM data quality for the Version 7 release of the L4_SM data product. The L4_SM validation process and data quality of previous versions are discussed by Reichle et al. (2015, 2016, 2017a,b, 2018, 2019, 2021a,b, 2022a) and Colliander et al. (2022).

2 SMAP CALIBRATION AND VALIDATION OBJECTIVES

During the post-launch SMAP calibration and validation (Cal/Val) phase each science product team pursues two objectives:

1. Calibrate, verify, and improve the performance of the science algorithm.
2. Validate the accuracy of the science data product as specified in the science requirements and according to the Cal/Val schedule.

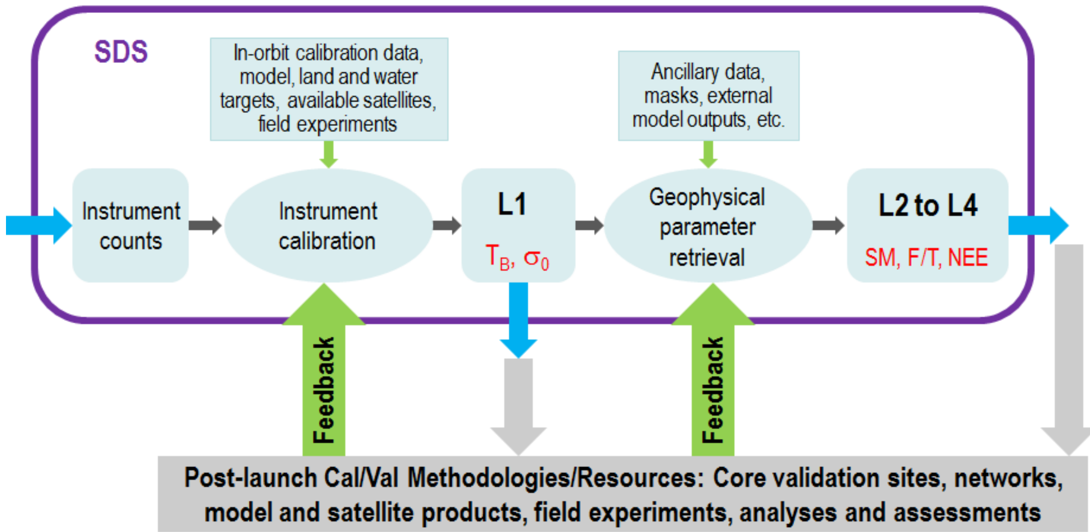

Figure 2. Overview of the SMAP calibration and validation process.

The overall SMAP Cal/Val process is illustrated in Figure 2. This process was first formalized in the SMAP Science Data Cal/Val Plan (Jackson et al. 2014) and the SMAP L2-L4 Data Products Cal/Val Plan (Colliander et al. 2014). Recently, many pioneering aspects of the SMAP Cal/Val process were incorporated into community standards for soil moisture product validation and good practices (Gruber et al. 2020; Montzka et al. 2020). Moreover, Colliander et al. (2022) provide a comprehensive and up-to-date overview of the SMAP project's approach to soil moisture validation. The present assessment report describes how the L4_SM team addressed the Cal/Val objectives for the Version 7 release. The validation approach and procedures that apply specifically to the L4_SM product are further detailed in the Algorithm Theoretical Basis Document for the L4_SM data product (Reichle et al. 2014b).

SMAP established unified definitions to address the mission requirements. These are documented in the SMAP Handbook (Entekhabi et al. 2014), where calibration and validation are defined as follows:

- *Calibration*: The set of operations that establish, under specified conditions, the relationship between sets of values or quantities indicated by a measuring instrument or measuring system and the corresponding values realized by standards.
- *Validation:* The process of assessing by independent means the quality of the data products derived from the system outputs.

To ensure the public's timely access to SMAP data, the mission was required to release validated data products within one year of the beginning of mission science operations. The objectives and maturity of the SMAP validated release products follow the guidance provided by the Committee on Earth Observation

Satellites (CEOS) Working Group on Calibration and Validation (CEOS 2015), which can be summarized as follows (Colliander et al. 2022, their Appendix A):

- Stage 1 Validation: Product accuracy is assessed from a small (typically < 30) set of locations and time periods by comparison with in-situ or other suitable reference data.
- Stage 2 Validation: Product accuracy is estimated over a significant (typically > 30) set of locations and time periods by comparison with reference in situ or other suitable reference data. Spatial and temporal consistency of the product, and its consistency with similar products, has been evaluated over globally representative locations and time periods. Results are published in the peer-reviewed literature.
- Stage 3 Validation: Uncertainties in the product and its associated structure are well quantified over a significant (typically > 30) set of locations and time periods representing global conditions by comparison with reference in situ or other suitable reference data. Validation procedures follow community-agreed-upon good practices. Spatial and temporal consistency of the product, and its consistency with similar products, has been evaluated over globally representative locations and time periods. Results are published in the peer-reviewed literature.
- Stage 4 Validation: Validation results for Stage 3 are systematically updated when new product versions are released and as the interannual time-series expands. When appropriate for the product, uncertainties in the product are quantified using fiducial reference measurements over a global network of sites and time periods (if available).

For the Version 7 release, the L4_SM team has completed all of the above validation stages, including repeated publication of the latest validation results in the peer-reviewed literature (Reichle et al. 2017a,b, 2019, 2021a; Colliander et al. 2022). Consequently, Version 7 of the L4_SM product replaces Version 6. The Cal/Val program will continue over the SMAP mission life span. Incremental improvements are ongoing as more measurements become available from the SMAP observatory. Version 7 data will be replaced in the archive when upgraded product versions become available.

3 L4_SM CALIBRATION AND VALIDATION APPROACH

During the mission definition and development phase, the SMAP Science Team and Cal/Val Working Group identified the metrics and methodologies that would be used for L2-L4 product assessment. These metrics and methodologies were vetted in community Cal/Val Workshops and tested in SMAP pre-launch Cal/Val rehearsal campaigns. The following validation methodologies and their general roles in the SMAP Cal/Val process were identified:

- *Core Validation Sites*: Accurate estimates at matching scales for a limited set of conditions.
- *Sparse Networks*: One point in the grid cell for a wide range of conditions.
- *Satellite Products*: Estimates over a very wide range of conditions at matching scales.
- *Model Products*: Estimates over a very wide range of conditions at matching scales.
- *Field Campaigns*: Detailed estimates for a very limited set of conditions.

The assessment of the L4_SM data product includes comparisons of SMAP L4_SM soil moisture estimates with in situ soil moisture observations from core validation sites and sparse networks. Moreover, independent soil moisture retrievals from satellite radar observations are used to measure the contribution of the SMAP analysis to the anomaly time series correlation skill of the L4_SM product across much of the global land surface. Finally, the assessment includes a global evaluation of the internal diagnostics from the ensemble-based data assimilation system that is used to generate the L4_SM product. This evaluation focuses on the statistics of the observation-minus-forecast (O-F) Tb residuals and the analysis increments.

The core site comparisons, the assessment of the anomaly correlation skill using independent radar soil moisture retrievals, and the statistics of the assimilation diagnostics are considered primary validation methodologies for the L4_SM product. Comparisons against in situ measurements from regional-scale sparse networks are considered a secondary validation methodology because such in situ measurements are subject to upscaling errors from the point-scale to the grid-cell scale of the data product.

Due to their very limited spatial and temporal extent, data from field campaigns play only a tertiary role in the validation of the L4_SM data product. Note, however, that field campaigns are instrumental tools in the provision of high-quality, automated observations from the core validation sites and thus play an important indirect role in the validation of the L4_SM data product.

4 L4_SM ACCURACY REQUIREMENT

There is no formal Level 1 mission requirement for the validation of the L4_SM product, but the L4_SM team self-imposed an accuracy requirement mirroring the one applied to the Level 2 Radar/Radiometer soil moisture (L2_SM_AP) product. Specifically, the L4_SM surface and root zone soil moisture estimates are required to meet the following criterion:

> **ubRMSE ≤ 0.04 m^3 m^{-3}** within the data masks specified in the *SMAP Level 2 Science Requirements* (that is, excluding regions of snow and ice, frozen ground, mountainous topography, open water, urban areas, and vegetation with (above-ground) water content greater than 5 kg m^{-2}),

where ubRMSE is the "unbiased" root-mean square (RMS) error, that is, the RMS error computed after removing long-term mean bias from the data (Entekhabi et al. 2010; Reichle et al. 2015, their Appendix A). (The ubRMSE is the same as the standard deviation of the error.) This criterion applies to the L4_SM instantaneous surface and root zone soil moisture estimates at the 9 km grid-cell scale from the "aup" Collection. It is verified by comparing the L4_SM product to the grid-cell scale in situ measurements from the core validation sites (section 6.2), resulting in the unbiased RMS difference (ubRMSD) metric. The criterion applies to the site-average ubRMSE, which is estimated by averaging across the ubRMSD values for all 9 km core site reference pixels that provide suitable in situ measurements (Reichle et al. 2015). It is important to note that even the high-quality SMAP core site measurements are subject to error. Consequently, the ubRMSD generally overestimates the ubRMSE and therefore is a conservative estimate of the performance of the data product (Chen et al. 2019).

L4_SM output fields other than instantaneous surface and root zone soil moisture are provided as research products (including surface meteorological forcing variables, soil temperature, evaporative fraction, net radiation, etc.) and will be evaluated against in situ observations to the extent possible given available resources.

As part of the validation process, additional metrics, including the mean difference (MD), the time series correlation coefficient (R), and anomaly R values, are also computed for the L4_SM output. This includes computation of the metrics outside of the limited geographic area for which the ubRMSE≤0.04 m^3 m^{-3} validation criterion applies.

For the computation of the *anomaly* R metric, climatological values of soil moisture from a given dataset (i.e., the L4_SM product or the in situ measurements) at a given location are computed for each day of the year using a 31-day smoothing window, thereby generating a local climatological seasonal cycle for that dataset. Anomaly time series are then computed by subtracting this climatological seasonal cycle from the corresponding raw data. The anomaly R metric is derived by computing the correlation coefficient between the L4_SM and the in situ anomaly time series (Reichle et al. 2015).

The validation of the L4_SM product includes additional metrics that are based on the statistics of the O-F Tb residuals and other data assimilation diagnostics (section 6.6). Reichle et al. (2015) provide detailed definitions of all the validation metrics and confidence intervals used here.

5 L4_SM VERSION 7 RELEASE

5.1 Process and Criteria

Since the beginning of the SMAP science data flow on 31 March 2015, the L4_SM team has been conducting frequent assessments of the L4_SM data product and will continue to evaluate the product throughout the life of the SMAP mission. These assessments are based on core validation sites, sparse networks, independent satellite soil moisture retrievals, and assimilation diagnostics, and they capture a wide range of geophysical conditions. The present report summarizes the status of this process for the Version 7 L4_SM product.

The validation of the Version 7 L4_SM product includes comparisons against output from two model-only simulations that are based on the same land surface model and forcing data as the Version 7 L4_SM estimates but are not informed by SMAP Tb observations (Table 1). Any accuracy in these model-only estimates is derived from the imposed meteorological forcing and land model structure and parameter information. The first model-only simulation, the ensemble "Open Loop" (OL7000), employs 24 ensemble members and applies the same forcing and model prognostics perturbations that are also used in the Version 7 L4_SM algorithm, whereas the second model-only simulation, the "Nature Run," version 10.0 (NRv10.0), is a single-member land model simulation without perturbations (Table 1). The OL7000 estimates were prepared for the SMAP period (31 March 2015 to present) and are the primary reference for the model-only skill. The NRv10.0 estimates were generated for the period 1 January 2000 to 31 December 2021 and provide the simulated climatological information required by the L4_SM assimilation algorithm (Reichle et al. 2014b). The NRv10.0 estimates are also used to determine any bias in the ensemble simulations relative to the unperturbed NRv10.0 simulation. Finally, the NRv10.0 estimates are validated against in situ water level measurements in peatlands. The latter are not available in sufficient quantity for validation during the SMAP period, and the NRv10.0 validation provides surrogate information about the Version 7 L4_SM product skill in peatlands.

Table 1. Overview of L4_SM products and model-only simulations.

	No. Ensemble Members	Perturbations	SMAP Tb Assimilation	Version 6	Version 7
L4_SM Product	24	Yes	Yes	**Vv6032**: 31 Mar 2015–29 Jun 2021 **Vv6030**: 30 Jun 2021–13 Nov 2022	**Vv7032**: 31 Mar 2015–30 Sep 2021 **Vv7030**: 1 Oct 2021–present
Open Loop	24	Yes	No	**OL6000**: 31 Mar 2015–13 Nov 2022	**OL7000**: 31 Mar 2015–13 Nov 2022
Nature Run	1	No	No	**NRv9.1**: 1 Jan 1990–31 Dec 2020	**NRv10.0:** 1 Jan 1990–31 Dec 2021

5.2 Processing and Science ID Version

To date, the Version 7 L4_SM product (Reichle et al. 2022c,d,e) has been generated under Science Version ID Vv7032 for 31 March 2015 through 30 September 2021 and Vv7030 thereafter (Table 1), with the minor version change indicating a change in the precipitation inputs (section 5.3).

The Version 7 L4_SM algorithm assimilates operational data from the Version 5 SMAP Tb observations provided in the Level 1C Radiometer Half-Orbit 36 km Brightness Temperature (L1C_TB) product (Chan et al. 2020). The assimilated Version 5 L1C_TB data were generated under several Composite Release IDs (CRIDs), which all produce scientifically equivalent Tb data.

Specifically, the L4_SM Vv7032 algorithm primarily used L1C_TB data with CRID R17000 through 22 April 2021; on 14 days within this period, L1C_TB data with CRID R17030 were also used. From 23 April 2021 through 30 September 2021, Vv7032 primarily used L1C_TB data with CRID R17030; on 27-28 April 2021, L1C_TB data with CRID R17000 were also used.

The Vv7030 algorithm used L1C_TB data with CRID 17030 for 1-25 October 2021. From 26 October 2021 through 14 February 2022, L1C_TB data with CRID R18240 were used. From 15 February 2022 to present, L1C_TB data with CRID R18290 were used, except during the immediate post-safe mode recovery period from 20 to 27 September 2022, when CRID R18240 was used again because a newly implemented sanity check in R18290 conflicted with a post-safe mode deviation of the orbit from the originally planned trajectory.

Some L1C_TB half-orbit granules assimilated into the Version 7 algorithm differ in their minor processing version from those assimilated into Version 6. These minor differences do not represent science changes and are caused by late-arriving L1C_TB granules or reprocessed L1C_TB granules that were not available during Version 6 reprocessing.

The global climatology (section 6.1) and data assimilation diagnostics (section 6.6) are assessed for the 7-year period from **1 April 2015, 0z to 1 April 2022, 0z**. The validation using core site (section 6.2), sparse network (section 6.3), and ASCAT measurements (section 6.5) is conducted for the 6-year period from **1 April 2015, 0z to 1 April 2021, 0z**. The start date matches the first full day when the SMAP radiometer was operating under sufficiently stable conditions following instrument start-up operations. The end date was selected to include the maximum possible number of full years for which data are available for validation. Consequently, L4_SM data with Science Version IDs Vv7032 and Vv7030 were used to prepare this assessment report, along with the corresponding Open Loop (OL7000) data (Table 1). The validation of the water level in peatlands (section 6.4) is conducted using Nature Run (NRv10.0) data from 2008 to 2018, owing to the availability of the in situ measurements. For illustrating select changes from the previous L4_SM product versions, this report also used published Version 6 L4_SM data (Science Version IDs Vv6032 and Vv6030; Reichle et al. 2021c,d,e, 2022a), along with the corresponding Nature Run (NRv9.1) and ensemble Open Loop (OL6000) simulations (Table 1).

Like all previous versions, Version 7 of the L4_SM algorithm ingests only the SMAP L1C_TB radiometer Tb observations, contrary to the originally planned use of downscaled Tb observations from the L2_SM_AP product and landscape freeze-thaw state retrievals from the SMAP Level 2 Radar Half-Orbit 3 km Soil Moisture (L2_SM_A) product. The latter two products are based on SMAP radar observations and are only available for the 10-week period from 13 April to 7 July 2015 because of the failure of the SMAP radar instrument. The decision to again use only radiometer (L1C_TB) inputs for the Version 7 release was made to ensure homogeneity in the longer-term L4_SM data record.

5.3 Summary of Changes from Previous Version

This section provides a summary of algorithm changes between the previous (Version 6) L4_SM algorithm and the current Version 7 assessed here. **The key changes in Version 7** of the L4_SM algorithm are **(i) the new peatland-specific hydrology module and peatland mask used in the Catchment land surface model** and **(ii) the use of climatological L-band radiative transfer model parameters derived from the SMAP Level 2 radiometer soil moisture product.** The complete list of changes from Version 6 to Version 7 is as follows:

1.) An improved treatment of peatlands is used in the Catchment land surface model of the Version 7 L4_SM algorithm. For peatlands, the Catchment model now uses the newly developed PEATCLSM module of Bechtold et al. (2019, 2020). PEATCLSM features completely revised, peatland-specific parameterizations and parameters, replacing the amended TOPMODEL approach of the original Catchment model (Koster et al. 2000) with a microtopography-based approach for peatlands. In addition to the standard Catchment model output variables such as soil moisture and temperature, PEATCLSM produces two peatland-specific output variables: (i) the water level relative to the mean elevation of the peatland surface ("depth_to_water_table_from_surface_in_peat") and (ii) a free surface water flux that represents the change in the free surface water storage when part of the microtopography is flooded during high water level events ("free_surface_water_on_peat_flux"); both are available in the Version 7 "gph" output Collection (Reichle et al. 2022b). See section 7.3 for PEATCLSM assumptions and ongoing development.

2.) The global distribution of peatlands in the Version 7 L4_SM algorithm is based on new information from the PEATMAP database (Xu et al. 2018) being integrated into the blend of the Harmonized World Soil Database (HWSD; version 1.21) and the State Soil Geographic (STATSGO2) soil data (De Lannoy et al. 2014b) that was used exclusively in all previous L4_SM versions. See section 6.1.2 for details.

3.) The Catchment model variables comprising the EnKF state vector for mineral (non-peat) soil in Version 7 remain the same as in Version 6, comprising the "surface excess" and "root zone excess" model prognostic variables. For peatlands, the EnKF state vector in Version 7 additionally includes the "catchment deficit" model prognostic variable.

4.) The Version 7 L4_SM algorithm uses revised parameters in the L-band radiative transfer model that converts the simulated soil moisture and temperature estimates into Tb predictions for the radiance-based L4_SM analysis. Specifically, Version 7 uses a seasonally varying climatology of L-band vegetation opacity derived from the SMAP Enhanced L2 Radiometer Half-Orbit 9 km EASE-Grid Soil Moisture (SPL2SMP_E), Version 5 (R18290) dual-channel algorithm retrieval product (April 2015 – March 2022; O'Neill et al. 2021a,b). Moreover, Version 7 uses the static maps of L-band soil roughness and scattering albedo from the same L2 product. The L2-derived parameters replace the corresponding calibrated values of De Lannoy et al. (2013, 2014a) that were used in previous L4_SM versions. See section 6.1.3 for details.

5.) In Version 7, the Tb scaling parameters are based on seven years of SMAP Tb observations and model (open loop) simulation (April 2015 – March 2022).

6.) In Version 7, the soil moisture climatology underpinning the root zone and profile soil moisture percentile output is based on 21 years of data (2001-2021).

7.) In Version 7, the daily precipitation correction approach using IMERG (Tan et al. 2019) and CPCU observations is applied as in Version 6 (Reichle et al. 2022a), with one minor difference. In Version 7, IMERG-Final (Huffman et al. 2019a) is used through 30 September 2022 before transitioning to IMERG-Late data (Huffman et al. 2019a), which is reflected in the L4_SM Science Version ID changing from Vv7032 to Vv7030. The corresponding transition date from IMERG-Final to IMERG-Late in L4_SM Version 6 was 30 June 2021. (There is no change in the precipitation reference climatology between Versions 6 and 7.)

8.) In Version 7, only lossless compression is applied to the "aup" granules. In Version 6, lossy compression was applied to the "aup" granules; this was found to interfere with the determination of vanishing increments in post-processing. For reference, "bit shaving" lossy compression is applied to "gph" granules in both Versions 6 and 7. Only the 12 most important bits [out of 24] that make up the mantissa of each science data value are retained. The 12 least important bits, which generally do not contain meaningful science information, are modified to enhance compressibility.

6 L4_SM DATA PRODUCT ASSESSMENT

This section provides a detailed assessment of the Version 7 L4_SM data product. First, global patterns and features are discussed, with a focus on the changes in the soil moisture climatology in peatlands (section 6.1). Next, we present comparisons and metrics versus in situ measurements from core validation sites (section 6.2) and sparse networks (section 6.3). This is followed by an assessment versus in situ water level measurements in peatlands (section 6.4). We then assess surface soil moisture skill globally with the help of independent satellite retrievals (section 6.5). Finally, we evaluate various data assimilation diagnostics, including the O-F Tb residuals, soil moisture increments, and data product uncertainty estimates (section 6.6).

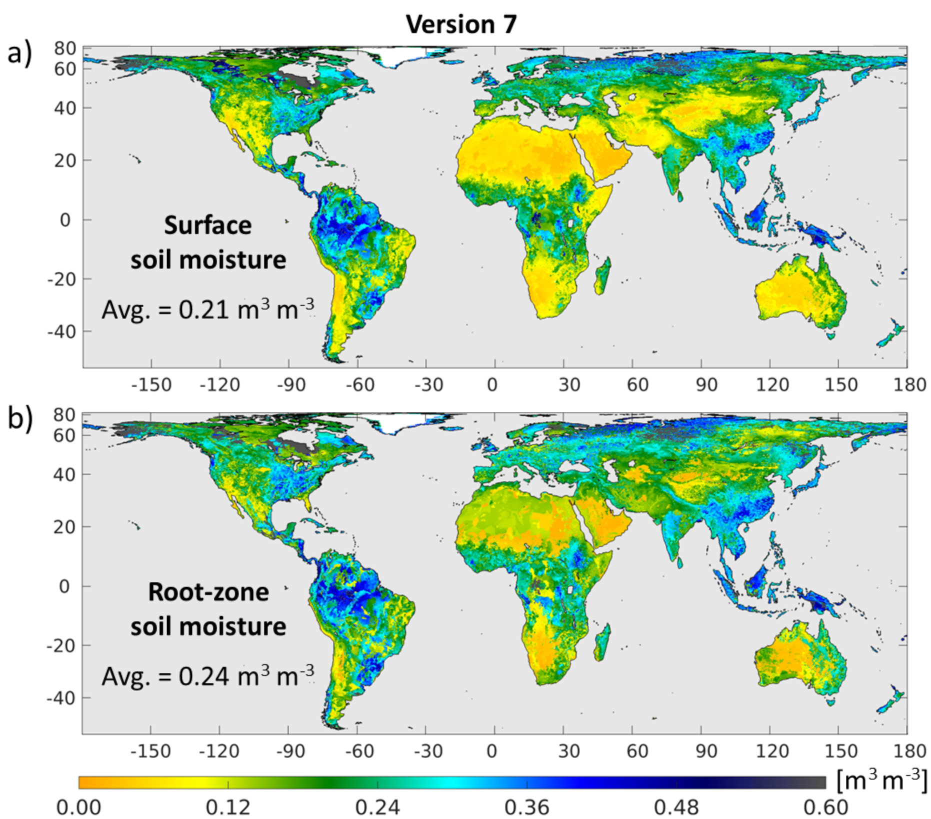

Figure 3. Time-average of Version 7 L4_SM (a) surface and (b) root zone soil moisture for April 2015 – March 2022. White shading indicates no-data-values (including lakes and permanently glaciated surfaces).

6.1 Global Patterns and Features

6.1.1 Global Soil Moisture

Figure 3 shows the time-averages for Version 7 surface and root zone soil moisture (April 2015 – March 2022). The global patterns are as expected – arid regions such as the southwestern US, the Sahara Desert, the Arabian Peninsula, the Middle East, southern Africa, and central Australia exhibit generally dry surface and root zone soil moisture conditions, whereas the tropics (Amazon, central Africa, and Indonesia) and high-latitude regions show wetter conditions. The global patterns of soil moisture are further impacted by soil texture, which is noticeable, for example, in the coarse-scale pattern of root zone soil moisture in the Sahara Desert, where little is known about the spatial distribution of mineral soil fractions. Areas with highly organic peat soil include portions of Alaska, the region along the southern edge of Hudson Bay, portions of northern Eurasia, the Cuvette Centrale region in central Congo, and portions of Indonesia. In the land model, the soils in these regions are assigned a high porosity value and show persistently wetter conditions than seen in other areas.

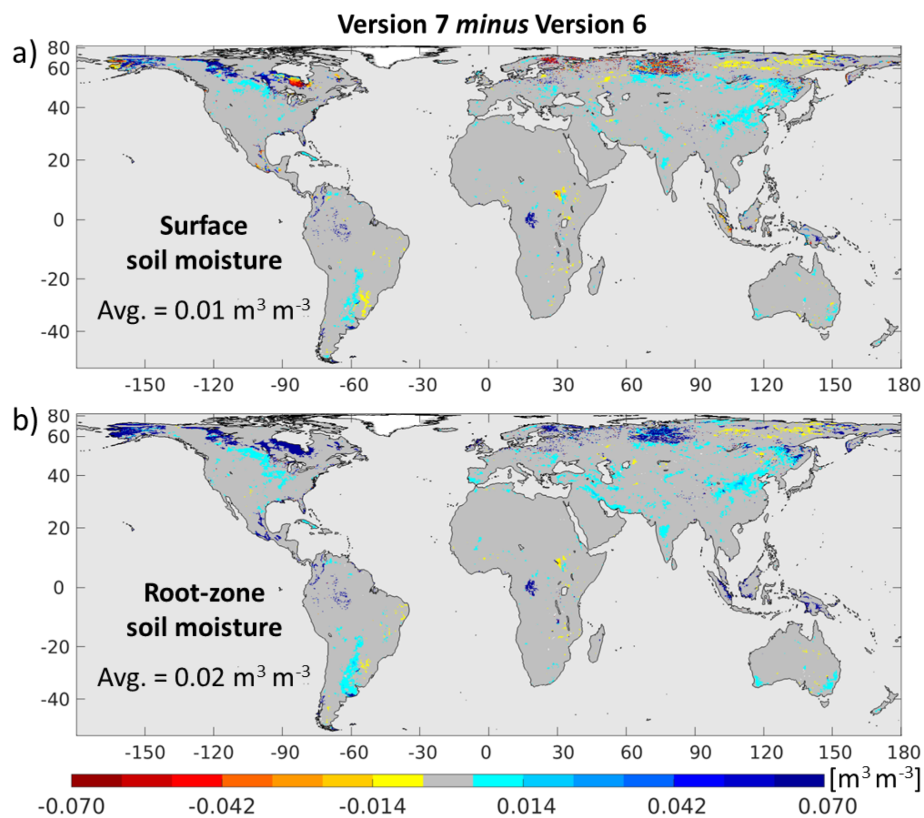

Figure 4. As in Figure 3, but for Version 7 minus Version 6.

The precipitation forcing in L4_SM Versions 6 and 7 is identical except for July-September 2021, when the L4_SM daily precipitation corrections are based on the satellite-gauge IMERG-Final product in Version 7 and on the satellite-only IMERG-Late product in Version 6 (section 5.3). When averaged across the 7-year validation period, however, these precipitation differences (not shown) are negligible and therefore do not result in meaningful differences in time-average soil moisture between the Version 6 and 7 products. In fact, outside of peatlands there are only a few regions, primarily in the Americas and Asia, with small differences in time-average soil moisture of around ±0.01 $m^3 m^{-3}$ between Version 7 and Version 6 (Figure 4). These differences are related to small shifts in the updated Tb scaling parameters and to the change in the L-band radiative transfer model parameters (section 5.3). Averaged across the globe, the time-average surface (root zone) soil moisture increases only slightly by 0.01 (0.02) $m^3 m^{-3}$ in Version 7 compared to that of Version 6, with the global mean differences dominated by the changes in the peatlands.

6.1.2 Peatlands

The total land area simulated in L4_SM is ~130 million km^2 (excluding lakes and permanently glaciated surfaces, notably all of Antarctica and ~80% of Greenland). Of this area, 5.22 million km^2 (4.0%) are simulated as peatland in Version 7 and 3.38 million km^2 (2.6%) are simulated as peatland in Version 6, which amounts to a 54% increase in peatland area in Version 7 compared to Version 6.

The global distribution of peatlands in the Version 7 algorithm and the differences in peatland coverage between Versions 6 and 7 are illustrated in Figure 5. Regions simulated as peatlands in both L4_SM versions (dark gray shading, 3.20 million km^2) are concentrated in the high northern latitudes, Central America, and Indonesia. Compared to Version 6, the integration of the PEATMAP database in Version 7 greatly expands the peatland coverage across the high latitudes and the Tropics (magenta shading, 2.02 million km^2). There are also small patches of land that are simulated as peatland only in Version 6, primarily scattered across high-latitude Eurasia, and are simulated as mineral soil in Version 7 (yellow shading, 0.17 million km^2).

As expected, the total area simulated as peatland in Version 6 closely matches the HWSD v2.1 estimate of 3.32 million km^2 (Xu et al. 2018, their Table 2). Less obviously, the total area simulated as peatland in Version 7 considerably exceeds the PEATMAP estimate of 4.23 million km^2 (Xu et al. 2018, their Table 2), with ~1 million km^2 of peatland area in Version 7 determined from the HWSD v2.1 and STATSGO blend alone that is not considered peatland in PEATMAP. For example, the HWSD v2.1 and STATSGO blend used in Version 6 indicates significant histosol coverage in northwestern Alaska and across portions of Mexico; these regions are not considered peatlands in PEATMAP (Xu et al. 2018, their Figure 1) but are retained in the Version 7 peatland mask based on the information from HWSD v2.1 and STATSGO. Some of these differences can be explained by the fact that PEATMAP is largely a compilation of national maps, with country-specific peatland criteria such as, for example, the minimum thickness of the soil organic layer. Our approach for designating peatlands based on soil texture from HWSD v2.1 and STATSGO uses the soil organic carbon (SOC) content in just the top 30 cm layer and includes soils with SOC of 8.72-17% (by weight; De Lannoy et al. 2014b). While such soils may not be classified as peatlands according to PEATMAP criteria, they are still hydrologically similar to and often located on the margins of the peatlands in PEATMAP. In our modeling system, using the PEATCLSM hydrology module for such soils is more appropriate than using the standard Catchment hydrology.

Changes from peatland in Version 6 to mineral soil in Version 7 (that is, the small speckles of yellow shading in Figure 5) are primarily the result of a minor revision in the pre-processing of the HWSD v2.1 and STATSGO soil texture. Through Version 6, a grid cell was considered a peatland if the highest SOC class was the dominant class (out of four SOC classes), even if the land area fraction associated with the highest SOC class was less than 50%. In Version 7, a grid cell is simulated as a peatland only if the highest soil organic carbon class covers at least 50% of the grid cell's land area (or if so indicated by PEATMAP).

The peatland distribution in the Version 7 L4_SM algorithm merely represents the presence of peat soil and therefore includes both natural and managed (e.g., drained) peatlands. Peatland drainage is not simulated in the PEATCLSM module of Bechtold et al. (2019) that is used in L4_SM Version 7, which likely results in a wet bias in PEATCLSM soil moisture in drained peatlands. Since the SMAP Tb observations are rescaled to the model's Tb climatology prior to their assimilation, the L4_SM Tb analysis does not correct for such a bias. Consequently, Version 7 L4_SM soil moisture estimates are likely biased wet in drained peatlands, which are mainly located in Europe and Southeast Asia. See section 7.3 for ongoing PEATCLSM development.

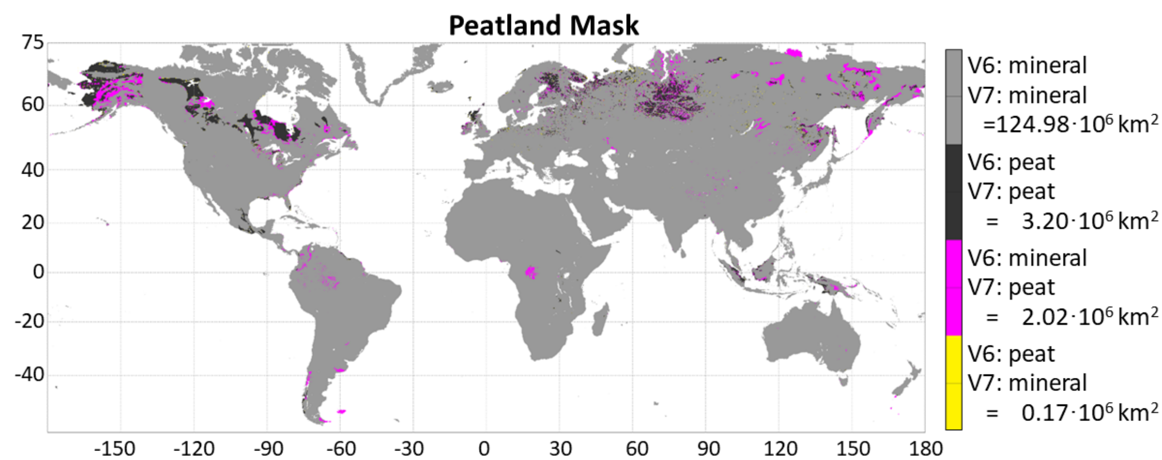

Figure 5. Peatland vs. mineral soil in L4_SM Version 6 (V6) and Version 7 (V7). Shading indicates grid cells with (light gray) mineral soil in both V6 and V7, (dark gray) peatland in both V6 and V7, (magenta) mineral soil in V6 and peatland in V7, and (yellow) peatland in V6 and mineral soil in V7. The latter category occurs in very small patches primarily across high-latitude Eurasia. White shading indicates no-data-values (including oceans, lakes, and permanently glaciated surfaces). The Miller projection is chosen for enhanced detail in the high latitudes. Peatlands poleward of 75 N (not shown) comprise only 460 km^2 in V6 and 3 km^2 in V7.

Figure 6 shows the time-average Version 7 soil moisture in more detail for select peatland regions, including across high-latitude North America, high-latitude western Eurasia, and the Cuvette Central in the Congo. Together, the peatlands in these regions capture 66% of the total area simulated as peatland in Version 7. Typical time-average values range from 0.4 to 0.8 m^3 m^{-3} for surface soil moisture and from 0.8 to 0.9 m^3 m^{-3} for root zone soil moisture.

The peatland-specific algorithm changes in Version 7 entail considerable changes in the time-average peatland soil moisture compared to Version 6 (Figure 7). The time-average surface soil moisture in peatlands is typically wetter in Version 7 by ~0.1-0.3 m^3 m^{-3}, but there are also peatlands where the Version 7 surface soil moisture is drier than that of Version 6 by ~0.1 m^3 m^{-3}. Root zone soil moisture in peatlands is universally wetter by up to 0.7 m^3 m^{-3} in Version 7 compared to Version 6.

The largest increases in time-average soil moisture are seen in regions that are simulated as mineral soil in Version 6 and as peatland in Version 7. One example of such a region is the Cuvette Centrale in the Congo, where the true extent of tropical peatland carbon stocks was discovered only recently (Dargie et al. 2017). Here, time-average root zone soil moisture values increase from ~0.25 m^3 m^{-3} (not shown), which is typical for mineral soil, to ~0.85 m^3 m^{-3} (Figure 6f), which is typical of peatlands, thereby representing a dramatic increase of ~0.6 m^3 m^{-3} (Figure 7f). The increase in surface soil moisture in such regions is typically smaller but still considerable (Figure 7e).

For regions that are simulated as peatlands in both Versions 6 and 7, the change in the peatland porosity from 0.80 m^3 m^{-3} in Version 6 to 0.93 m^3 m^{-3} in Version 7 implies a general increase in root zone soil moisture from Version 6 to Version 7 (Figure 7b,d). For surface soil moisture, however, the peatland-specific processes encoded in the new PEATCLSM hydrology module generally produce somewhat drier long-term average values of *relative* soil saturation. Because of the larger porosity value used in Version 7, this means that peatland surface soil moisture can be drier or wetter in Version 7 than in Version 6 (Figure 7a,c).

The revisions in the peatland hydrology also impact the time series variability of soil moisture. In Version 7 peatlands, the time series standard deviation ranges from 0.05 to 0.15 m^3 m^{-3} for surface soil moisture (Figure 8a,c,e) and from 0.02 to 0.1 m^3 m^{-3} for root zone soil moisture (Figure 8b,d,f). Variability is generally lower in the high-latitude peatlands and higher in the mid-latitude and tropical peatlands. Surface soil moisture variability increased considerably in Version 7 compared to Version 6 (Figure 9a,c,e), and now better reflects the typical swings between very wet and very dry surface conditions seen in peatlands. On average, root zone soil moisture variability is nearly the same in Versions 6 and 7 in high-latitude peatlands (Figure 9b,d). The tropical Cuvette Centrale region, however, sees a considerable increase in root-zone soil moisture variability from Version 6 to Version 7 (Figure 9f). The differences seen in Figure 9 are very similar to those between the Nature Run simulations corresponding to Version 6 (NRv9.1) and Version 7 (NRv10.0; not shown), which indicates that the soil moisture variability changes in the Version 7 L4_SM product are dominated by the revisions of the peatland hydrology and global distribution in the land model and are not caused by the addition of the catchment deficit model prognostic variable to the EnKF state vector in peatlands (section 5.3).

Because of the large differences in the peatland soil moisture, **the Version 6 and Version 7 products should *not* be combined into a single dataset for use in applications that include regions with peatlands in either Version 6 or Version 7**.

The peatland changes in Version 7 are also reflected in the estimated latent heat and total runoff fluxes (Figure 10). In high-latitude peatlands, latent heat fluxes typically decrease by a few W m^{-2} in Version 7 compared to Version 6 (Figure 10a,c), despite the net increase in soil moisture (Figure 7a-d), which reflects the revised peatland hydrology encoded in the new PEATCLSM module and the fact that latent heat fluxes in the high latitudes are primarily limited by the radiation forcing. In the Cuvette Centrale peatlands, the latent heat flux increases by 18.1 W m^{-2} on average (Figure 10e), presumably because of the dramatic increase in soil moisture there (Figure 7e,f). There are no meaningful differences between Versions 6 and 7 in surface temperature, soil temperature, and net radiation forcing (not shown). Consequently, changes in the sensible heat fluxes are opposite those in the latent heat fluxes (not shown). Moreover, changes in runoff are also generally opposite those in the latent heat fluxes; total runoff (including surface runoff and baseflow) increased by ~0.5-1 mm d^{-1} from Version 6 to Version 7 in high-latitude peatlands (Figure 10b,d) but decreased by ~0.4 mm d^{-1} in the Cuvette Centrale peatlands (Figure 10f). Note that these "research" output fields are not subject to formal validation requirements.

Finally, Figures 11 and 12 illustrate the time series mean and variability of peatland water level. Since water level was not output for the Version 6 L4_SM product, the figures show estimates derived from the corresponding Nature Run simulations for Version 6 (NRv9.1) and Version 7 (NRv10.0) (Table 1), with statistics computed for the validation period. It should be noted that in the standard Catchment model hydrology used for peatlands in NRv9.1, the water level diagnostic is a fairly crude approximation of the actual water level (hence the omission of water level output in the Version 6 and earlier L4_SM products). We use the Version 6 diagnostic here primarily to illustrate the contrast with the more realistic peatland water level output available from the Version 7 system. The mean peatland water level in NRv9.1 ranges from near 0 m to below -3 m, with regional averages of -1 to -2 m (Figure 11a-c). In stark contrast, mean peatland water levels in NRv10.0 are much closer to the surface, typically ranging from -0.05 to -0.5 m (Figure 11d-f). The time series variability of peatland water levels ranges from close to 0 m to 0.8 m in NRv9.1 and from 0.05 m to 0.2 m in NRv10.0. As will be shown in section 6.4, the shallower and less variable water levels in the Version 7 system provide much more realistic descriptions of peatland hydrology than the deeper and more variable water levels of Version 6.

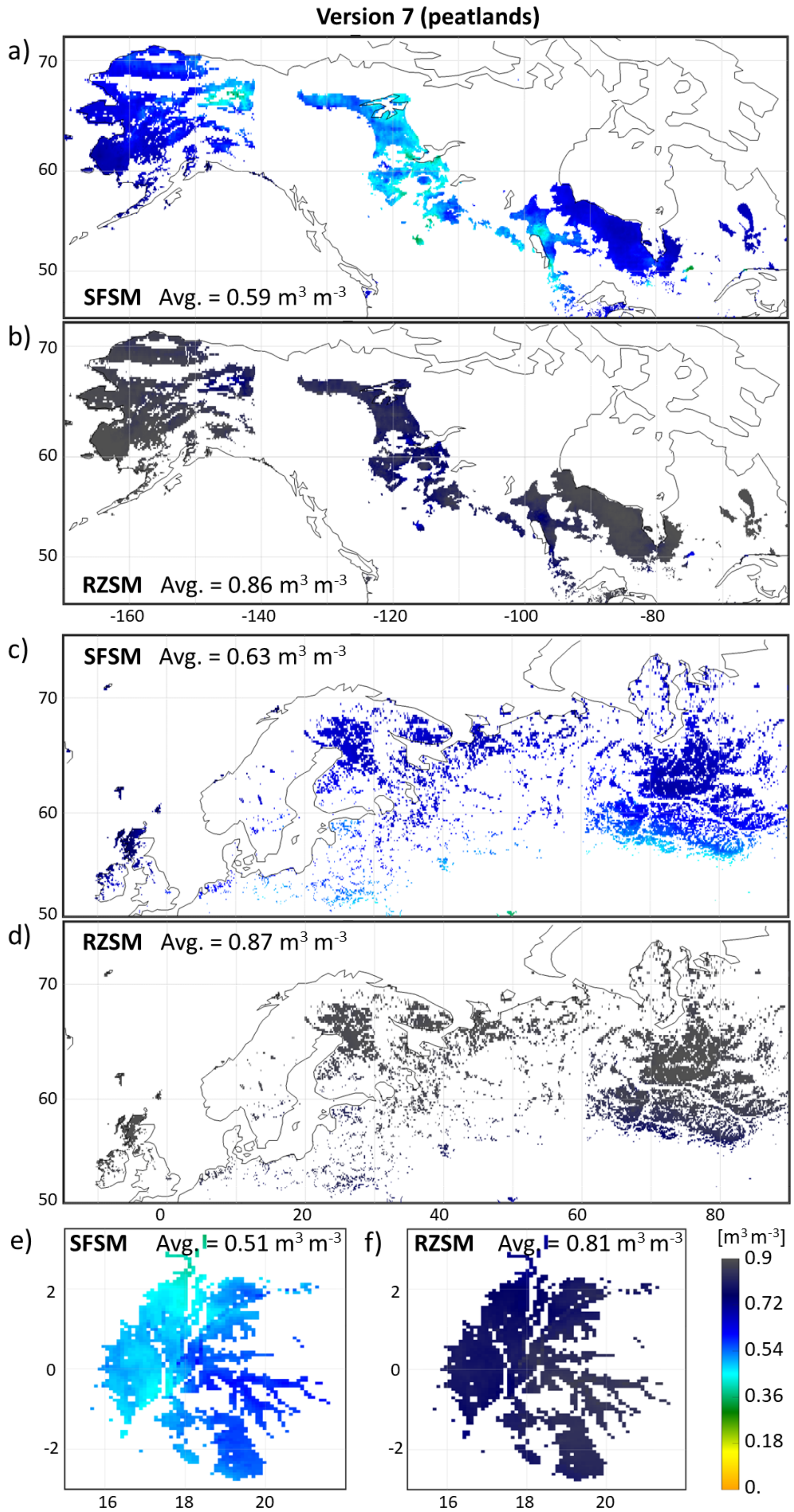

Figure 6. Time-average (April 2015 – March 2022) of Version 7 L4_SM (a,c,e) surface soil moisture (SFSM) and (b,d,f) root zone soil moisture (RZSM) in the peatlands of (a,b) high-latitude North America, (c,d) high-latitude western Eurasia, and (e,f) the Cuvette Centrale (Congo).

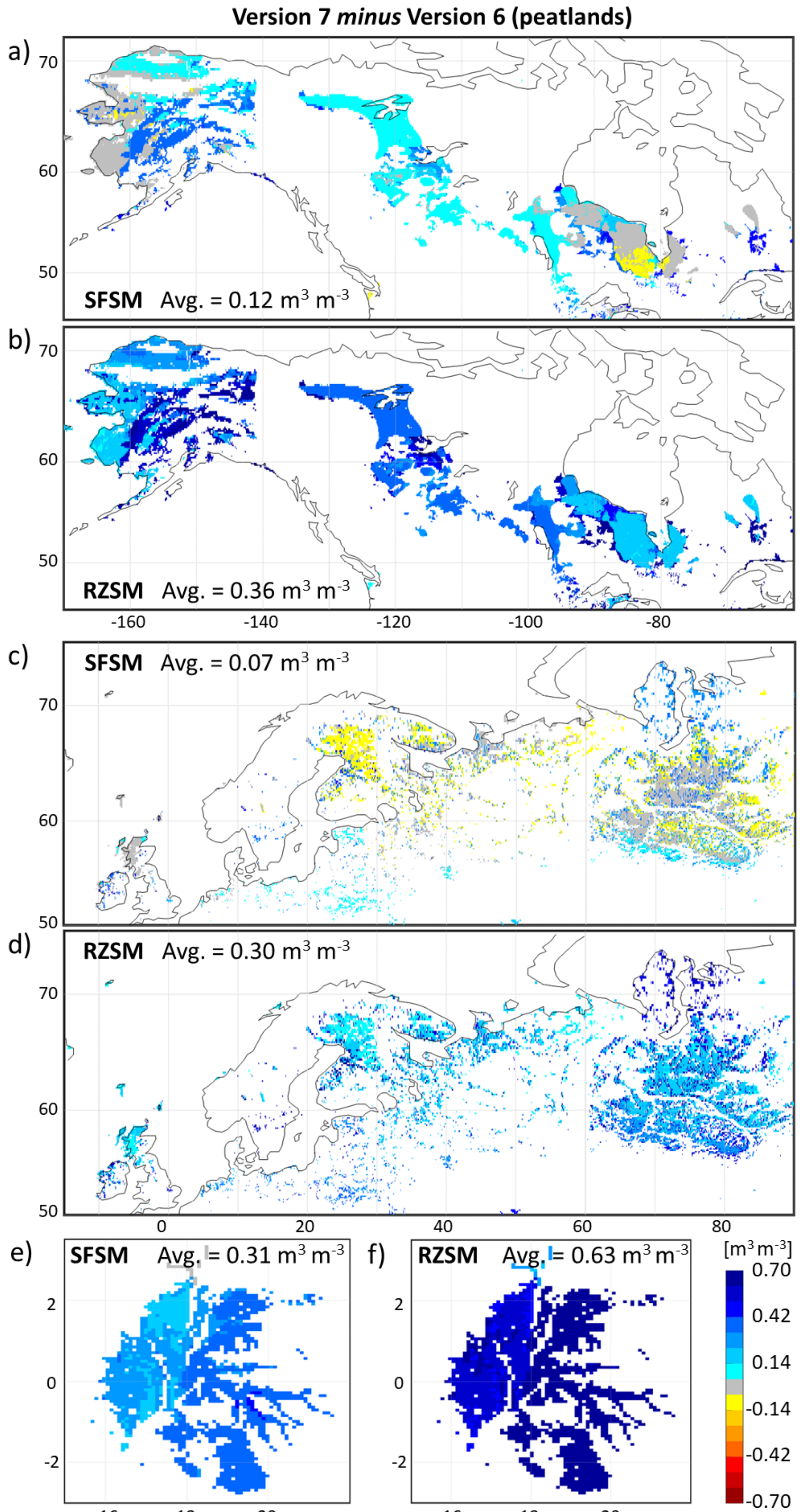

Figure 7. As in Figure 6, but for the Version 7 minus Version 6 difference in soil moisture using the Version 7 peatland mask (Figure 5).

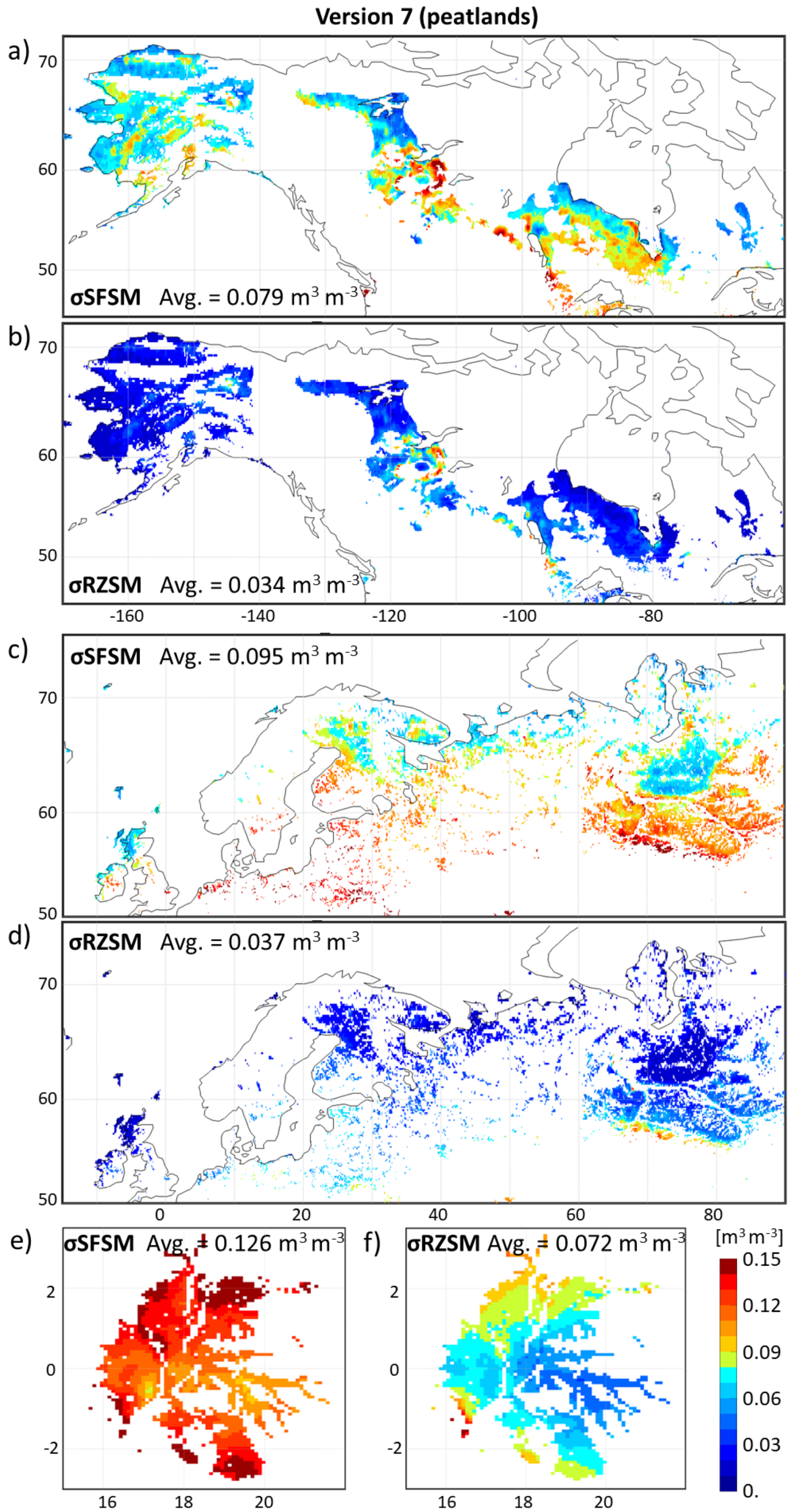

Figure 8. As in Figure 6, but for the time series standard deviation (σ) of SFSM and RZSM.

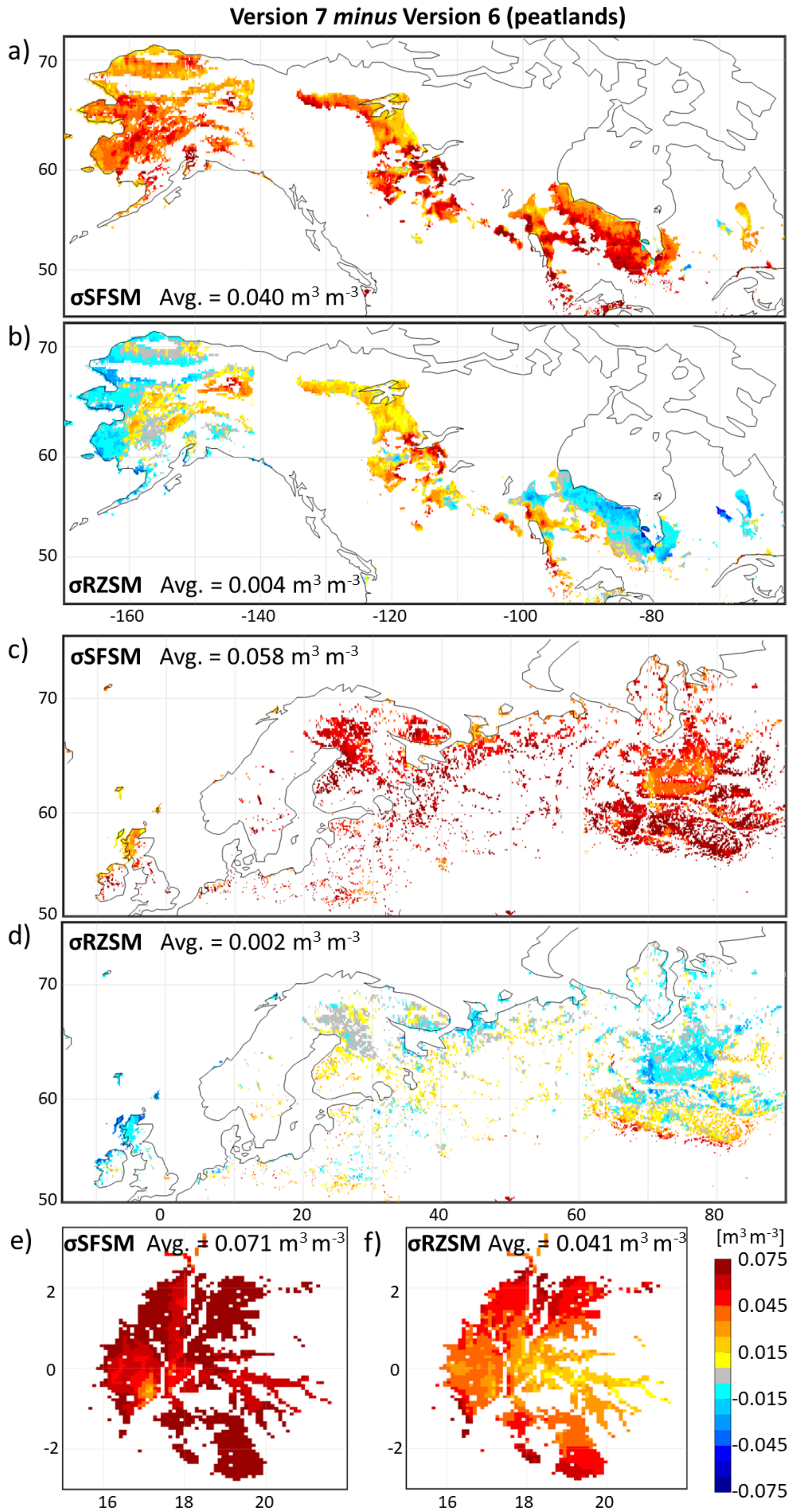

Figure 9. As in Figure 6, but for the Version 7 minus Version 6 difference in the time series standard deviation (σ) of soil moisture using the Version 7 peatland mask (Figure 5).

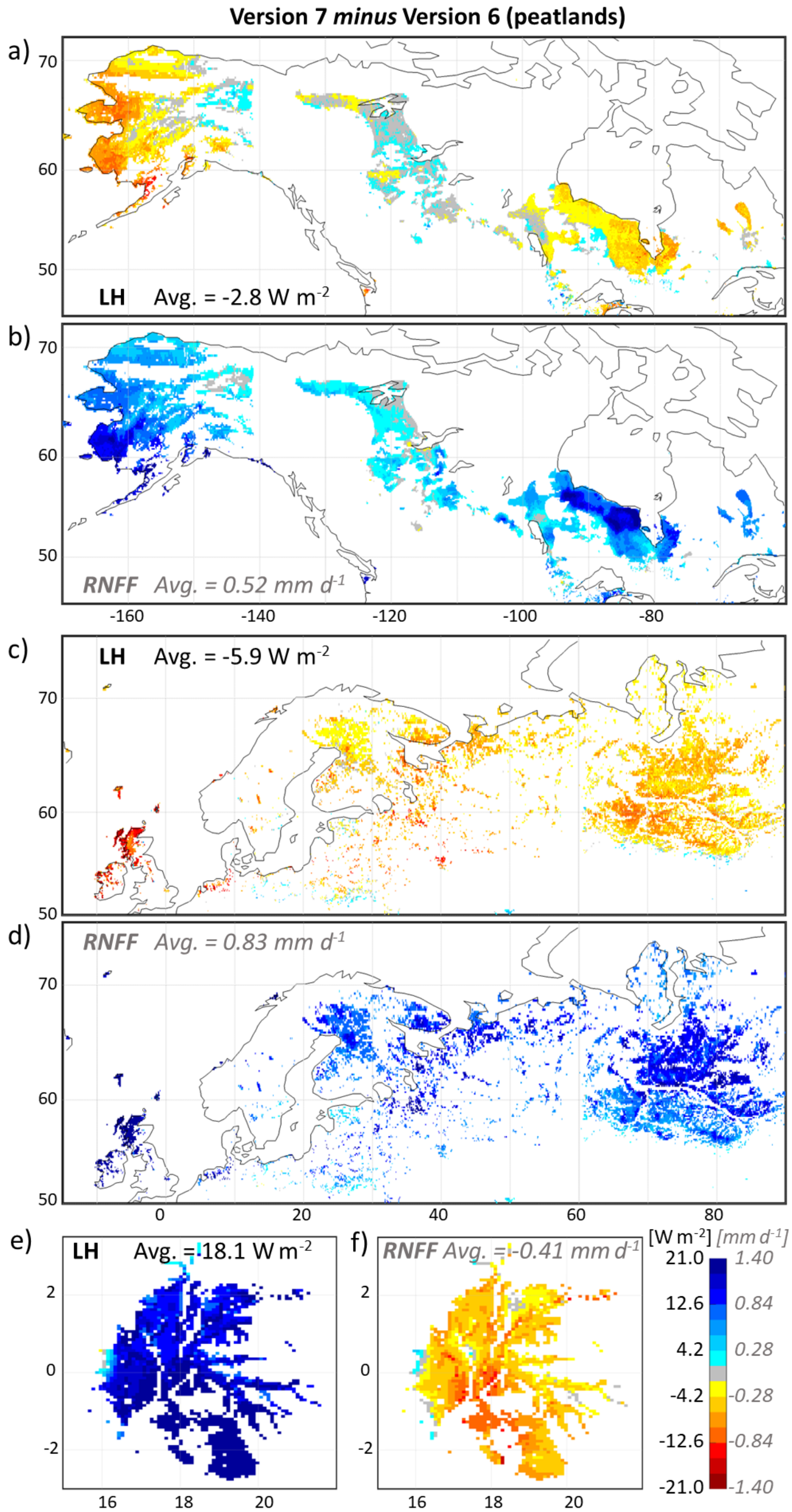

Figure 10. Time-average (April 2015 – March 2022) of Version 7 minus Version 6 differences in L4_SM (a,c,e) latent heat flux (LH) and (b,d,f) total runoff (RNFF) in the peatlands of (a,b) high-latitude North America, (c,d) high-latitude western Eurasia, and (e,f) the Cuvette Centrale (Congo) using the Version 7 peatland mask.

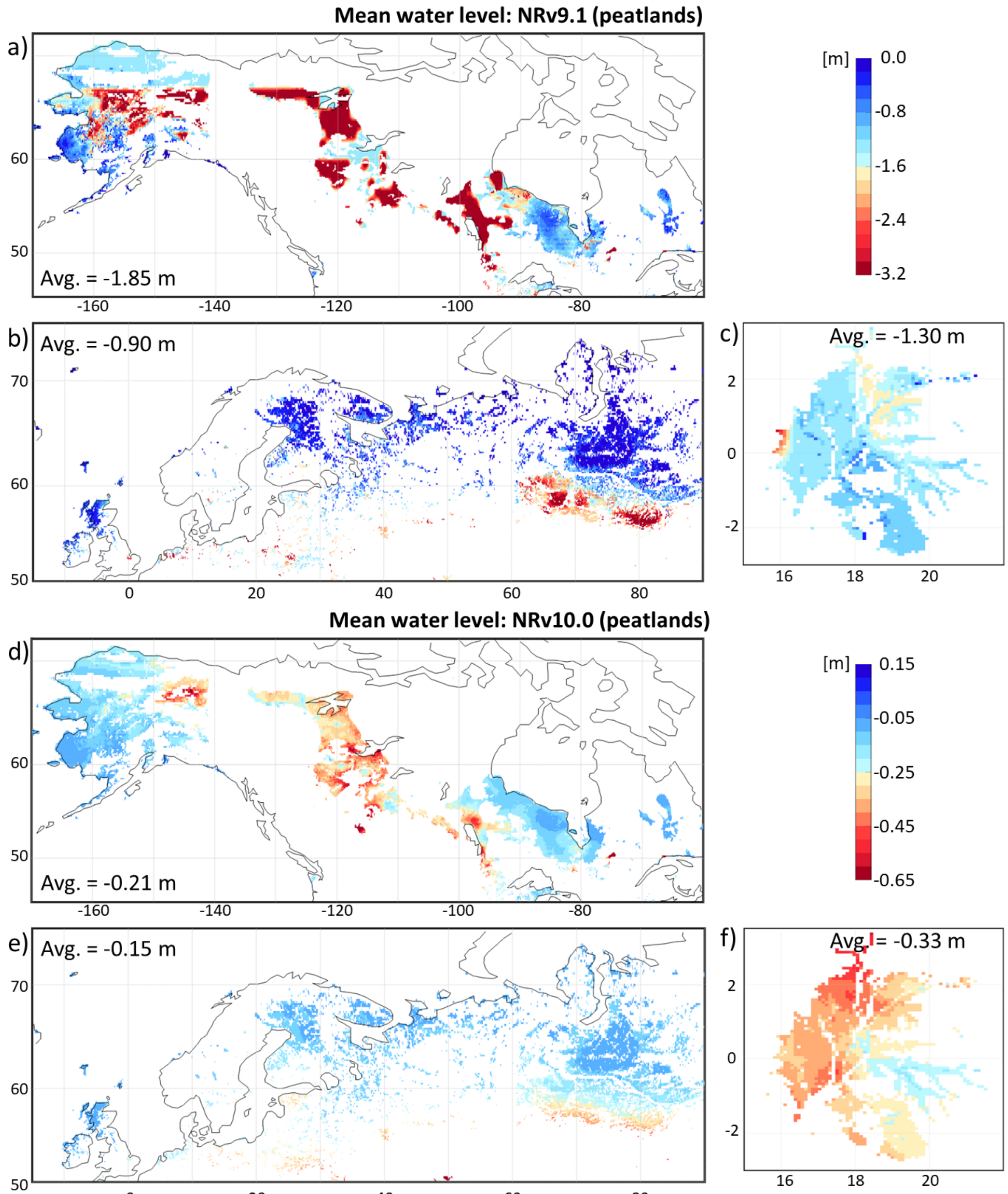

Figure 11. Time-average (April 2015 – March 2022) of water level for (a-c) NRv9.1 and (d-f) NRv10.0 in the peatlands of (a,d) high-latitude North America, (b,e) high-latitude western Eurasia, and (c,f) the Cuvette Centrale (Congo) using the NRv10.0 (i.e., Version 7) peatland mask. Note the difference in the color scale for (a-c) NRv9.1 and (d-f) NRv10.0. More negative (red) values indicate water levels that are deeper in the ground.

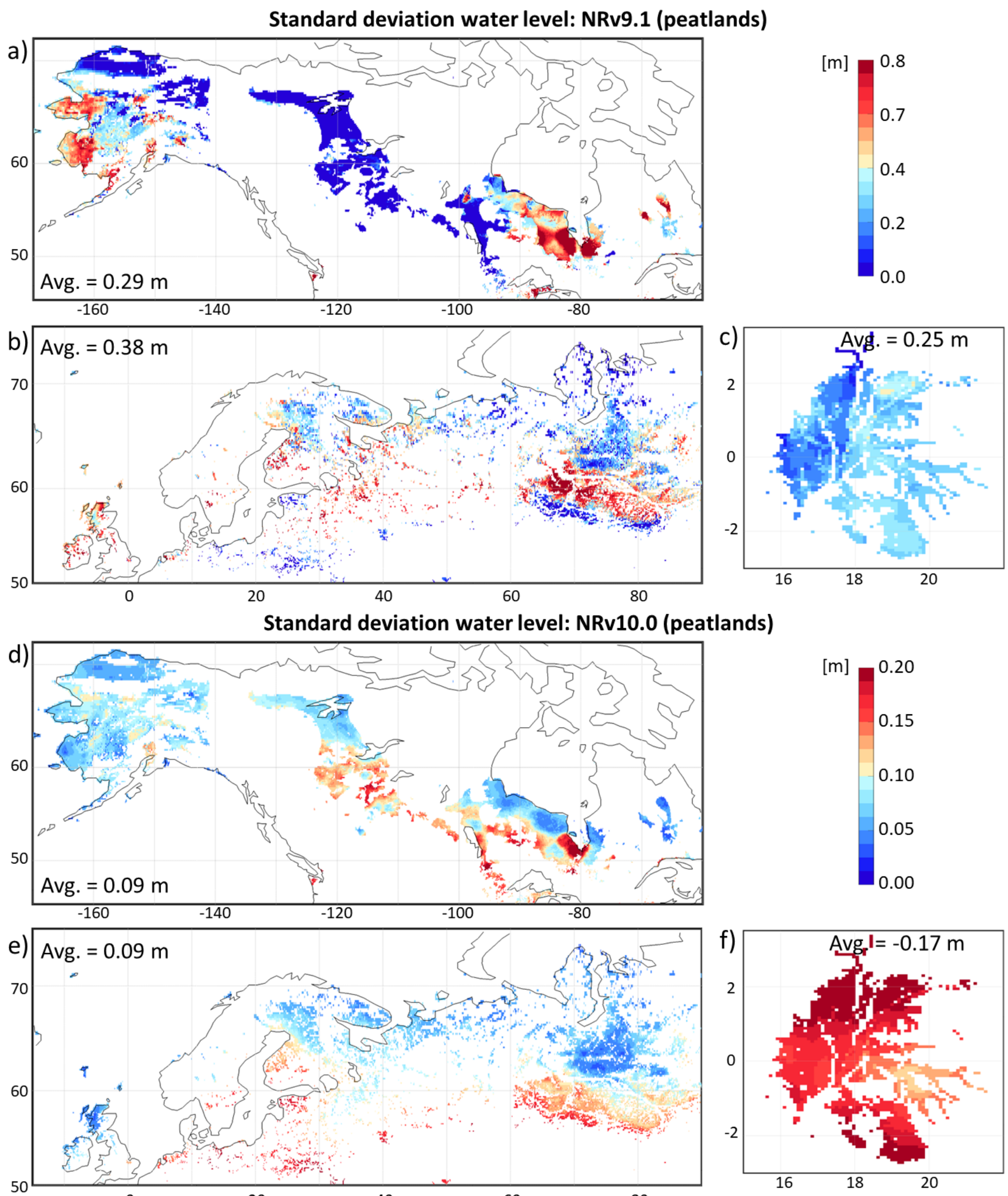

Figure 12. As in Figure 11, but for the time series standard deviation (April 2015 – March 2022) of water level. Note the difference in the color scale for (a-c) NRv9.1 and (d-f) NRv10.0.

6.1.3 L-band Radiative Transfer Model Parameters

This section illustrates the changes in the L-band radiative transfer model (RTM) parameters used in Version 7. The RTM converts the simulated soil moisture and temperature estimates into Tb predictions and is a key element in the radiance-based L4_SM analysis. As mentioned above (section 5.3), Version 7 uses L-band RTM parameters derived from the SMAP Enhanced L2 Radiometer Half-Orbit 9 km EASE-Grid Soil Moisture (SPL2SMP_E), Version 5 (R18290) dual-channel algorithm retrieval product (April 2015 – March 2022; O'Neill et al. 2021a,b). The L2 algorithm jointly retrieves soil moisture and L-band vegetation opacity, using static maps of L-band soil roughness and scattering albedo also estimated from SMAP Tb observations in two separate pre-processing steps (Chaubell et al. 2020). The same soil roughness and scattering albedo maps are used in the Version 7 L4_SM algorithm. Moreover, Version 7 uses a seasonally varying, 8-day climatology of the L-band vegetation opacity derived from the L2 product. Vegetation opacity retrievals from both ascending and descending passes are used to compute the climatology, provided the retrieval quality flag indicates successful soil moisture retrieval, the surface flag indicates non-frozen soil and ice/snow-free surface conditions, and the H- and V-polarization Tb quality flags indicate acceptable Tb observation quality. The 8-day vegetation opacity climatology is further smoothed using a centered 24-day window. Finally, the Version 7 soil roughness, scattering albedo, and vegetation opacity parameters are gap-filled using averages from a 5-by-5 grid cell neighborhood (without iterative filling) to mitigate gaps in the spatially distributed Tb analysis. The L-band parameters derived from the L2 product replace the corresponding calibrated values derived from multi-angular SMOS Tb observations (De Lannoy et al. 2013, 2014a) that were used in previous L4_SM versions.

The L-band soil roughness is illustrated in Figure 13. In Version 6, soil roughness varied with soil moisture (De Lannoy et al. 2013), and Figure 13a shows the soil roughness associated with the NRv9.1 time-average soil moisture for the validation period. In contrast, the Version 7 soil roughness is prescribed from the L2 retrieval product and is time-invariant (Figure 13b). The global average soil roughness decreases from 0.79 in Version 6 to 0.63 in Version 7. There are both similarities and clear differences between the global patterns of soil roughness in the two versions. In both versions, the Sahara Desert, the Arabian Peninsula, and central Australia exhibit among the lowest values, and larger values are seen in topographically complex mountain ranges such as the Andes and the Himalayas. Stark differences between the soil roughness in the two versions exist, for example, in the Eurasian high latitudes and in the tropical forests. Moreover, the Version 6 soil roughness exhibits a spatially noisy pattern in densely vegetated regions because of the poor sensitivity of the satellite Tb observations to L-band soil emission in these regions, which results in an ill-posed calibration.

Similarities and differences are also seen in the L-band scattering albedo of the two versions (Figure 13c,d). In both versions, the scattering albedo is, as expected, generally higher in vegetated regions than in arid and bare regions. The stark contrast between high and low albedo values in Version 6, however, is considerably more muted in Version 7. For the scattering albedo, the calibration used in Version 6 is ill-posed in the absence of vegetation and thus results in noisy parameter estimates, e.g., in the Sahara Desert (Figure 13c). Moreover, the SMOS Tb observations used in the Version 6 parameter calibration are adversely affected by radio-frequency interference, which is prevalent across much of southern and central Eurasia. Therefore, in Version 6 the L-band RTM parameters in these regions were filled using vegetation class-average values, which can be seen in the very coarse spatial pattern in the Version 6 scattering albedo in these regions (Figure 13c). In contrast, the Version 7 scattering albedo varies smoothly across the globe, with the lowest values in bare regions (Figure 13d).

The L-band vegetation opacity in the RTM is prescribed as a seasonally varying climatology in both Version 6 and Version 7. In Version 6, the seasonal cycle of the vegetation opacity is determined by optical data, specifically, the leaf area index (LAI; De Lannoy et al. 2013). In Version 7, the vegetation opacity seasonal cycle is computed from the SMAP L2 retrievals and thus from L-band data, which is more directly related to the required L-band vegetation opacity. Figure 14 illustrates the global pattern of the climatological vegetation opacity for two 8-day periods, one in January and one in July. In Version 6, the January 9-16 vegetation opacity values are less than 0.2 across almost the entire Northern Hemisphere mid- and high latitudes, with a global average value of 0.26 (Figure 14a). In Version 7, by contrast, the January 9-16 vegetation opacity values reach up to 0.8 in the forested regions of western and eastern North America and central and eastern Europe, reflecting the presence of some water in the vegetation during winter (Figure 14b) and resulting in a higher global average value of 0.35. Note also that in Version 7 the vegetation opacity remains undefined in the coldest regions, owing to the lack of L2 retrievals under frozen or snow-covered surface conditions. The Southern Hemisphere patterns of the vegetation opacity in the two versions are more alike, although the transition between the highest and lowest values appears somewhat smoother in Version 7 (Figure 14a,b). The vegetation opacity patterns for July 20-27 show relatively similar patterns for the two versions, again with smoother transitions between high and low values in Version 7 (Figure 14c,d).

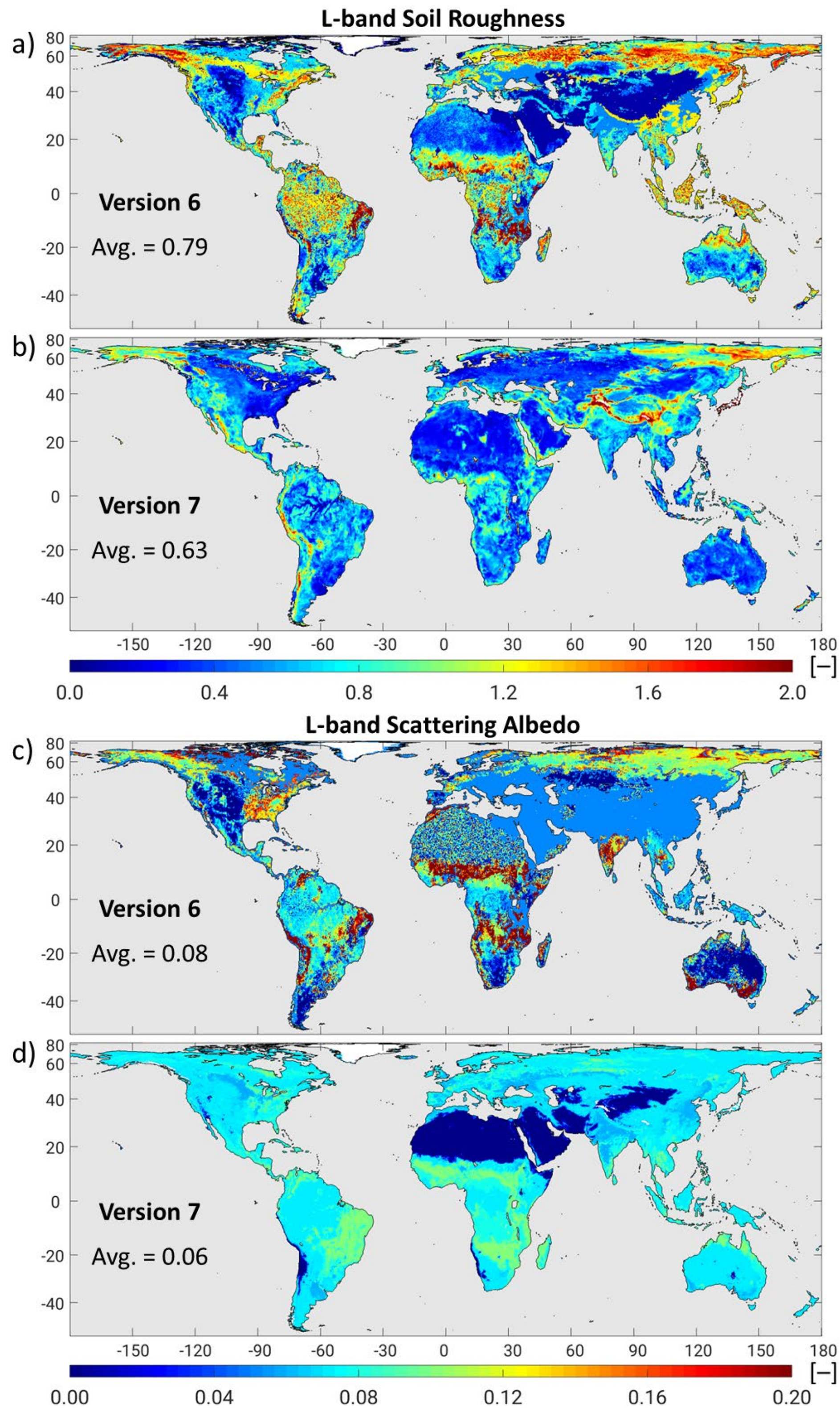

Figure 13. L-band (a,b) soil roughness and (c,d) scattering albedo in (a,c) Version 6 and (b,d) Version 7. Roughness is parameterized in Version 6 as a function of soil moisture (De Lannoy et al. 2013); panel (a) shows roughness computed from NRv9.1 time-average soil moisture for April 2015 – March 2022. White shading indicates no-data-values.

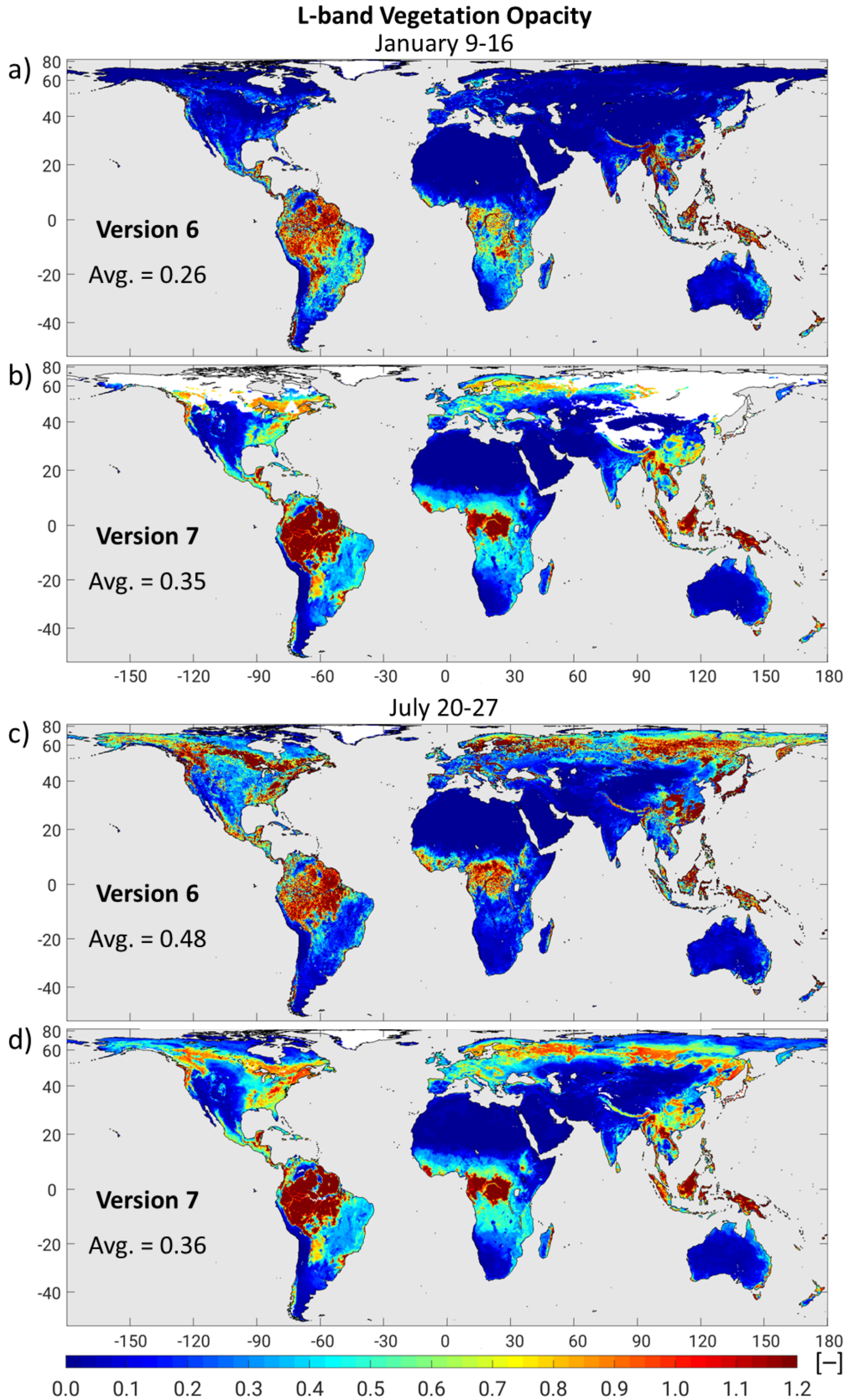

Figure 14. Climatological L-band vegetation opacity for (a,b) January 9-16 and (c,d) July 20-27 in (a,c) Version 6 and (b,d) Version 7. White shading indicates no-data-values.

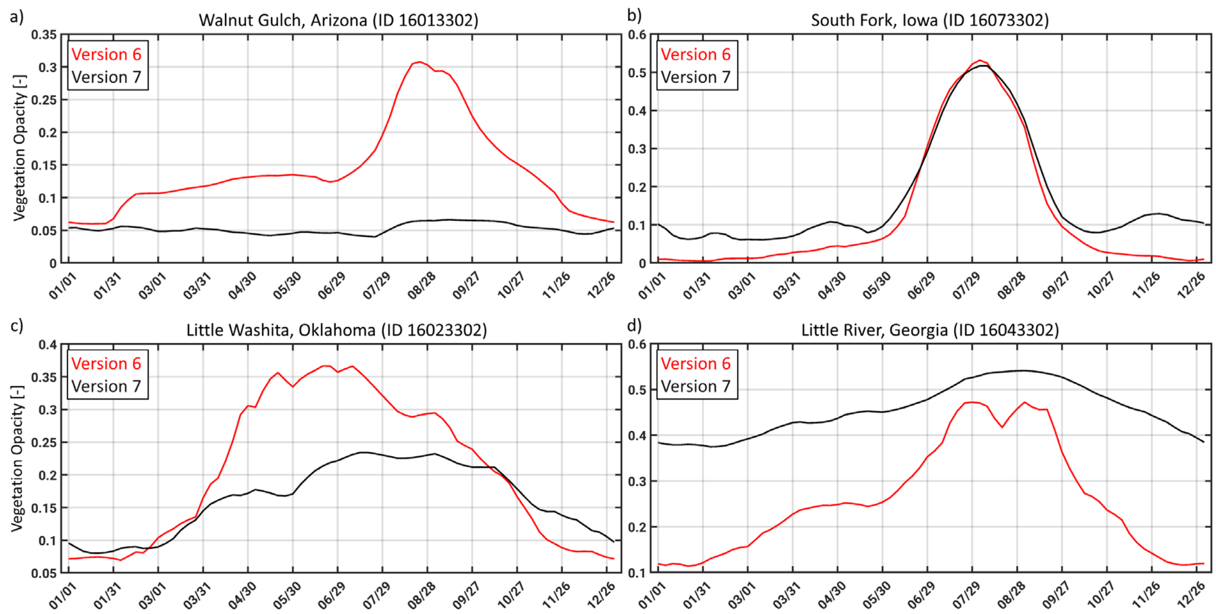

Figure 15. Climatological L-band vegetation opacity at (a) Walnut Gulch, (b) South Fork, (c) Little Washita, and (d) Little River. Note the different ordinate scales. See section 6.2 for site details.

For further illustration, Figure 15 shows the seasonal cycle of the climatological vegetation opacity in the two versions at four SMAP core validation sites (see section 6.2 for details). There is a distinct difference in the seasonal cycle of the vegetation opacity at Walnut Gulch, Arizona, with Version 6 exhibiting a peak up to 0.3 during the August and September monsoon season, whereas the Version 7 vegetation opacity remains fairly constant at ~0.05 (Figure 15a). At South Fork, Iowa, the vegetation opacity during the summer growing season is nearly identical between the two versions, but outside of the growing season the vegetation opacity practically vanishes in Version 6 whereas it bottoms out at ~0.1 in Version 7 (Figure 15b). At Little Washita, Oklahoma, both the phasing and the peak values of the vegetation opacity differ between the two versions, with Version 6 showing a higher peak at ~0.35 that occurs during May-July whereas the Version 7 peak is lower at ~0.25 and occurs during July-September (Figure 15c). At Little River, Georgia, the Version 6 vegetation opacity is ~0.1 during the winter and exhibits a late summer peak of ~0.45, whereas the Version 7 vegetation opacity barely drops below 0.4 during the winter and peaks at ~0.55 during the summer (Figure 15d).

In the absence of independent vegetation opacity measurements, it is difficult to determine directly whether the Version 6 or Version 7 vegetation opacity is more correct. The seasonal cycle and dynamic range of the vegetation opacity, however, impact the simulated Tb in the L4_SM algorithm, which is verified below through an examination of the Tb O-F residuals (section 6.6). They also impact the L4_SM soil moisture estimates, which are validated below against in situ measurements (sections 6.2 and 6.3).

6.2 Core Validation Sites

This section provides an assessment of the L4_SM soil moisture estimates using data from SMAP core validation sites, which provide estimates of soil moisture and soil temperature at the scale of 9 km and 33 km grid cells based on locally dense networks of in situ sensors (Colliander et al. 2017a,b, 2022). The 6-year period from **1 April 2015, 0z to 1 April 2021, 0z** is used for the core site validation because more recent in situ measurements are available for only a small minority of the sites.

6.2.1 Method

Since the core site in situ measurements used here are identical to those used in the Version 6 assessment report, this subsection is essentially the same as section 6.2.1 of Reichle et al. (2022a) with only very minor edits.

Like the assessments for Versions 4, 5, and 6 of L4_SM (Reichle et al. 2018, 2019, 2021b, 2022a), the present report uses reference pixel data on the 33 km EASEv2 grid (defined through suitable aggregation of the 3 km EASEv2 grid), instead of the 36 km reference pixels used in earlier assessments (Reichle et al. 2015, 2016, 2017a). Additional details about the processing of the data and the validation methodology can be found in Reichle et al. (2015, their section 6.2.1).

The status of the core validation sites is reviewed periodically. The set of core sites that provide data for this assessment of the L4_SM product are listed in Table 2, with details of the 9 km and 33 km reference pixels that are used here shown in Table 3. The validation is based on a total of 48 reference pixels from 19 different core validation sites. Surface soil moisture measurements are available for all 48 reference pixels, which include 18 reference pixels at the 33 km scale from 18 different sites and 30 reference pixels at the 9 km scale from 18 different sites. For root zone soil moisture, measurements are available for only 20 reference pixels from 8 different core sites, including 8 reference pixels at the 33 km scale from 8 different sites and 12 reference pixels at the 9 km scale from 7 different sites. The 9 km reference pixels for root zone soil moisture belong to the core validation sites of Little Washita (Oklahoma), Fort Cobb (Oklahoma), Little River (Georgia), South Fork (Iowa), Tonzi Ranch (California), Kenaston (Saskatchewan), and TxSON (Texas). The same 7 sites plus Yanco (Australia) provide root zone soil moisture data at the 33 km scale. This very limited set obviously lacks the diversity to be fully representative of global conditions, but we are not aware of any other comparable datasets. Finally, note that Table 2 lists the land cover at Yanco as grassland (Colliander et al. 2022), which is more appropriate than the cropland/natural mosaic classification reported in earlier L4_SM assessment reports.

The metrics at a given site are computed from 3-hourly data, provided at least 480 measurements, or about 2 months of data, are available for the site after quality control. The computation of the anomaly R value (section 4) further requires estimates of the 6-year mean seasonal cycle, for which we required a minimum of at least 240 measurements for a given 31-day smoothing window across the 6-year validation period. This requirement implies that the anomaly R metric is available for surface (root zone) soil moisture at only 17 (7) reference pixels at the 33 km scale. At the 9 km scale, the anomaly R metric is available whenever the other metrics are also available.

Table 3 also lists the depths of the deepest sensors that contribute to the in situ root zone soil moisture measurements. The measurements from the individual sensors are vertically averaged with weights that are proportional to the spacing of the depth of the sensors within the 0-100 cm layer depth of the L4_SM root zone soil moisture estimates. At all reference pixels except Little River and Yanco, the deepest sensors are at 40-50 cm depth. At Little River and Yanco, the deepest sensors are at 30 cm and 75 cm, respectively, with Yanco's second-deepest sensors being installed at 45 cm depth. In all cases, the deepest sensors are therefore weighted most strongly in the computation of the vertical average. To compute the vertically averaged root zone soil moisture at a given time from a given sensor profile, all sensors within the profile must provide measurements that pass the automated quality control.

Table 2. Soil moisture core validation sites used in the present assessment.

Site Name	***Country***	***Climate Regime***	***Land Cover***	***Number of 9-km (33-km) Reference Pixels***		***Reference***
				Surface Soil Moisture	***Root zone Soil Moisture***	
REMEDHUS	Spain	Temperate	Croplands	2 (1)	- (-)	Sanchez et al. 2012; Gonzalez-Zamora et al. 2015
Reynolds Creek	USA (Idaho)	Arid	Grasslands	2 (1)	- (-)	Seyfried et al. 2001
Yanco	Australia (New South Wales)	Arid	Grasslands	2 (1)	- (1)	Panciera et al. 2014
Carman	Canada (Manitoba)	Cold	Croplands	1 (1)	- (-)	McNairn et al. 2015
Ngari	Tibet	Cold	Barren / sparse	- (1)	- (-)	Wen et al. 2014
Walnut Gulch	USA (Arizona)	Arid	Shrub open	3 (1)	- (-)	Keefer et al. 2008
Little Washita	USA (Oklahoma)	Temperate	Grasslands	3 (1)	2 (1)	Cosh et al. 2006
Fort Cobb	USA (Oklahoma)	Temperate	Grasslands	2 (1)	2 (1)	Cosh et al. 2014
Little River	USA (Georgia)	Temperate	Cropland / natural mosaic	1 (1)	1 (1)	Bosch et al. 2007
St Josephs	USA (Indiana)	Temperate	Croplands	1 (1)	- (-)	Heathman et al. 2012
South Fork	USA (Iowa)	Cold	Croplands	3 (1)	3 (1)	Coopersmith et al. 2015
Monte Buey	Argentina	Temperate	Croplands	1 (1)	- (-)	Thibeault et al. 2015
Tonzi Ranch	USA (California)	Temperate	Savannas woody	1 (1)	1 (1)	Clewley et al. 2017; Moghaddam et al. 2016
Kenaston	Canada (Saskatchewan)	Cold	Croplands	2 (1)	1 (1)	Rowlandson et al. 2015; Tetlock et al. 2019
Valencia	Spain	Cold	Savannas woody	1 (-)	- (-)	Juglea et al. 2010; Khodayar et al. 2019
Niger	Niger	Arid	Grassland	1 (1)	- (-)	Galle et al. 2018
Benin	Benin	Tropical	Savannas	1 (1)	- (-)	Galle et al. 2018
TxSON	USA (Texas)	Temperate	Grasslands	2 (1)	2 (1)	Caldwell et al. 2018
HOBE	Denmark	Temperate	Croplands	1 (1)	- (-)	Bircher et al. 2012; Jensen and Refsgaard 2018
All Sites				***30 (18)***	***12 (8)***	

Table 3. Soil moisture core validation site reference pixels used in the present assessment. The 33 km reference pixels are shown in boldface. See Table 2 for core validation site characteristics.

	Reference Pixel										
Site Name (Abbreviation)	***ID***	***Latitude [degree]***	***Longitude [degree]***	***Horizontal Scale [km]***	***Depth of Deepest Sensor [m]***	***Number of Sensors (Surface Soil Moisture)***			***Number of Sensors (Root Zone Profiles)***		
						Min.	***Mean***	***Max.***	***Min.***	***Mean***	***Max.***
REMEDHUS (RM)	**03013302**	**41.29**	**-5.46**	**33**	**0.05**	**8**	**12.1**	**15**	n/a	n/a	n/a
	03010903	41.42	-5.37	9	0.05	4	4.0	4	n/a	n/a	n/a
	03010908	41.32	-5.27	9	0.05	4	4.0	4	n/a	n/a	n/a
Reynolds Creek (RC)	**04013302**	**43.19**	**-116.75**	**33**	**0.05**	**7**	**7.0**	**7**	n/a	n/a	n/a
	04010907	43.19	-116.72	9	0.05	4	4.0	4	n/a	n/a	n/a
	04010910	43.09	-116.81	9	0.05	4	4.0	4	n/a	n/a	n/a
Yanco (YC)	**07013301**	**-34.86**	**146.16**	**33**	**0.75**	**8**	**19.0**	**23**	**7**	**15.6**	**23**
	07010902	-34.72	146.13	9	0.05	8	8.5	9	n/a	n/a	n/a
	07010916	-34.98	146.31	9	0.05	8	10.0	11	n/a	n/a	n/a
Carman (CR)	**09013301**	**49.60**	**-97.98**	**33**	**0.05**	**8**	**17.9**	**20**	n/a	n/a	n/a
	09010906	49.67	-97.98	9	0.05	8	9.9	11	n/a	n/a	n/a
Ngari (NG)	**12033301**	**32.50**	**79.96**	**33**	**0.05**	**6**	**6.0**	**6**	n/a	n/a	n/a
Walnut Gulch (WG)	**16013302**	**31.75**	**-110.03**	**33**	**0.05**	**8**	**14.9**	**18**	n/a	n/a	n/a
	16010906	31.72	-110.09	9	0.05	8	9.1	11	n/a	n/a	n/a
	16010907	31.72	-109.99	9	0.05	8	9.8	11	n/a	n/a	n/a
	16010913	31.83	-110.90	9	0.05	6	6.0	6	n/a	n/a	n/a
Little Washita (LW)	**16023302**	**34.86**	**-98.08**	**33**	**0.45**	**8**	**10.4**	**12**	**8**	**8.9**	**12**
	16020905	34.92	-98.23	9	0.05	4	4.0	4	n/a	n/a	n/a
	16020906	34.92	-98.14	9	0.45	4	4.0	4	4	4.0	4
	16020907	34.92	-98.04	9	0.45	4	4.0	4	4	4.0	4
Fort Cobb (FC)	**16033302**	**35.38**	**-98.64**	**33**	**0.45**	**8**	**10.4**	**11**	**8**	**9.4**	**11**
	16030911	35.38	-98.57	9	0.45	4	4.0	4	4	4.0	4
	16030916	35.29	-98.48	9	0.45	4	4.0	4	4	4.0	4
Little River (LR)	**16043302**	**31.67**	**-83.60**	**33**	**0.30**	**8**	**17.2**	**19**	**8**	**15.7**	**18**
	16040901	31.72	-83.73	9	0.30	8	8.0	8	6	6.2	8
St Josephs (SJ)	**16063302**	**41.39**	**-85.01**	**33**	**0.05**	**8**	**8.3**	**9**	n/a	n/a	n/a
	16060907	41.45	-84.97	9	0.05	7	7.0	7	n/a	n/a	n/a
South Fork (SF)	**16073302**	**42.42**	**-93.41**	**33**	**0.50**	**8**	**16.6**	**19**	**8**	**11.8**	**16**
	16070909	42.42	-93.53	9	0.50	4	4.0	4	4	4.0	4
	16070910	42.42	-93.44	9	0.50	4	4.0	4	4	4.0	4
	16070911	42.42	-93.35	9	0.50	4	4.0	4	4	4.0	4
Monte Buey (MB)	**19023301**	**-32.91**	**-62.51**	**33**	**0.05**	**8**	**9.8**	**12**	n/a	n/a	n/a
	19020902	-33.01	-62.49	9	0.05	5	5.0	5	n/a	n/a	n/a
Tonzi Ranch (TZ)	**25013301**	**38.45**	**-120.95**	**33**	**0.40**	**8**	**12.8**	**20**	**8**	**14.0**	**10**
	25010911	38.43	-120.95	9	0.40	8	14.4	26	8	18.0	11
Kenaston (KN)	**27013301**	**51.47**	**-106.48**	**33**	**0.50**	**8**	**25.7**	**30**	**8**	**22.7**	**30**
	27010910	51.39	-106.51	9	0.05	8	8.0	8	n/a	n/a	n/a
	27010911	51.39	-106.42	9	0.50	8	12.5	14	8	11.4	14
Valencia (VA)	41010906	39.57	-1.26	9	0.05	7	7.0	7	n/a	n/a	n/a
Niger (NI)	**45013301**	**13.57**	**2.66**	**33**	**0.05**	**6**	**6.0**	**6**	n/a	n/a	n/a
	45010902	13.57	2.66	9	0.05	4	4.0	4	n/a	n/a	n/a
Benin (BN)	**45023301**	**9.83**	**1.73**	**33**	**0.05**	**7**	**7.0**	**7**	n/a	n/a	n/a
	45020902	9.77	1.68	9	0.05	5	5.0	5	n/a	n/a	n/a
TxSON (TX)	**48013301**	**30.35**	**-98.73**	**33**	**0.50**	**8**	**28.1**	**29**	**8**	**22.8**	**24**
	48010902	30.43	-98.81	9	0.50	8	9.6	10	8	8.7	10
	48010911	30.28	-98.73	9	0.50	8	14.4	15	8	13.4	14
HOBE (HB)	**67013301**	**55.97**	**9.10**	**33**	**0.05**	**8**	**11.2**	**15**	n/a	n/a	n/a
	67010901	55.97	9.10	9	0.05	5	5.0	5	n/a	n/a	n/a

Across the reference pixels listed in Table 3, the average number of individual surface soil moisture sensors that contribute to a given 33 km reference pixel ranges between 6.0 and 28.1, with a mean value of 13.4. The corresponding number of sensor profiles for root zone soil moisture ranges between 8.9 and 22.8, with a mean value of 15.1. At the 9 km scale, 13 of the 31 reference pixels are based on just 4 individual sensor profiles, while most of the rest of the 9 km reference pixels consist of about 10 sensor profiles each. The mean number of surface soil moisture sensors per 9 km reference pixel is 6.7, and the corresponding number of root zone profiles is 7.1. The sampling density (sensors per unit area) is therefore higher for the 9 km reference pixels than for the 33 km reference pixels.

For most reference pixels, individual sensor profiles occasionally drop out temporarily. If the sensor that drops out is installed in a particularly wet or a particularly dry location (relative to reference pixel average conditions), not having this sensor contribute to the reference pixel average will result in an artificial discontinuity in the time series of the reference pixel average soil moisture. In the assessment of Version 4 and earlier L4_SM products, this effect was mitigated only for reference pixels with 8 or fewer individual sensor profiles; for these reference pixels, quality-controlled in situ measurements from all contributing sensor profiles needed to be available for the computation of the reference pixel average.

As in the Version 5 and 6 assessments, the processing of the in situ measurements for the present Version 7 assessment includes an additional safeguard against discontinuities caused by temporary sensor dropout. In the revised processing used here, the time series from each individual sensor is first converted from volumetric soil moisture units into standard-normal deviates, based on the time series mean and variance of the measurements at the individual sensor. Next, a normalized reference pixel average time series is computed by averaging the standard-normal deviate time series from the available individual sensors at any given time. Finally, the resulting normalized reference pixel average time series is converted back into volumetric units based on the reference pixel average of the soil moisture climatologies from the individual sensors. By averaging the measurements from the individual sensors in the normalized space, the reference pixel average time series in volumetric units is less sensitive to the dropping out of sensors that are installed in a particularly wet or dry location (relative to reference pixel average conditions).

Core site metrics are provided separately for the 9 km and 33 km reference pixels. Metrics are computed directly against the (reference pixel average) in situ measurements. Because the latter contain measurement error, we present the metrics as the mean *difference* (MD), RMS *difference* (RMSD), and unbiased RMS *difference* (ubRMSD), along with the correlation and anomaly correlation. Because of the in situ measurement error, the primary metrics of interest – that is, the RMSE and ubRMSE – are less than the RMSD and ubRMSD, respectively. Similarly, the (anomaly) correlation vs. the true soil moisture exceeds the (anomaly) correlation that is directly determined against the imperfect in situ measurements.

Summary metrics are obtained by averaging across the metrics from all individual reference pixels at the given scale. For the 9 km metrics, we first average each metric across the 9 km reference pixels within each site, separately for each site and weighted by the number of measurements that contribute to the metric at a given 9 km reference pixel. Second, we average the resulting individual site-average metrics across all sites. This approach gives equal weight to each site and differs from the straight average over all 9 km reference pixels that was used in earlier assessments (Reichle et al. 2015, 2016, 2017a), which somewhat arbitrarily gave more weight to sites that had more 9 km reference pixels. (We computed summary metrics using both methods and found the results to be close. That is, the conclusions remain the same regardless of how exactly the average metric is computed.)

Statistical uncertainty in the ubRMSD, R, and anomaly R metrics is estimated using 95% confidence intervals, which are computed at each site based on the number of samples in the time series (with a correction for temporal autocorrelation). We refer to changes in metrics as statistically significant whenever the confidence intervals do not overlap. It is important to keep in mind that the confidence intervals are themselves uncertain and only provide practical guidance as to whether the skill differences may be meaningful. Statistical uncertainty estimates for the MD are not provided because the upscaling error is considerably larger for the bias than for the second-order metrics (Chen et al. 2019).

Finally, in situ measurements are used for validation only when the model (or assimilation) estimates indicate non-frozen and snow-free conditions (Reichle et al. 2015, their section 6.2.1). Because the soil temperature and snow states differ somewhat between the L4_SM product and the model-only (Open Loop) simulation examined here, in situ measurements were used only if both datasets indicate favorable validation conditions. This cross-masking ensures that the metrics are directly comparable across both datasets.

6.2.2 Results

In this section, we investigate the summary metrics for soil moisture at the core validation sites. These metrics are illustrated in Figures 16 and 17. For completeness, the soil moisture and soil temperature performance metrics for each site are provided in the Appendix (Tables A1-A8).

Probably the most important result is that the Version 7 L4_SM surface and root zone soil moisture data meet the accuracy requirement (section 4) of ubRMSE ≤ 0.04 m^3 m^{-3}. Specifically, the ubRMSD of the Version 7 L4_SM product at the 9 km (33 km) scale is 0.041 (0.038) m^3 m^{-3} for surface soil moisture and 0.026 (0.023) m^3 m^{-3} for root zone soil moisture (Figure 16a). As mentioned earlier, the ubRMSD is impacted by in situ measurement errors, which results in an overestimation of the ubRMSE. When factoring in the measurement error of the reference pixel-average in situ observations, which Chen et al. (2019) estimate to be at least ~0.01-0.02 m^3 m^{-3} (in terms of ubRMSE), the Version 7 L4_SM surface and root zone soil moisture meet the product accuracy requirement.

Next, we compare the skill of the Version 7 L4_SM product to that of the Version 6 product. The ubRMSD at the 9 km (33 km) scale is 0.040 (0.037) m^3 m^{-3} in Version 6, which is slightly better than in Version 7; for root zone soil moisture, on the other hand, the ubRMSD at the 9 km (33 km) scale is 0.027 (0.024) m^3 m^{-3} in Version 6, which is slightly worse than in Version 7 (Figure 16a). On balance, the ubRMSD results for Version 7 are therefore neutral compared to Version 6. Moreover, the Version 7 product has a slightly larger average MD than Version 6 for surface and root-zone soil moisture (Figure 16b), and the absolute MD metrics are neutral on balance (Figure 16c).

The Version 7 product has slightly but consistently better correlation skill for both surface and root zone soil moisture than the Version 6 product, although the changes are not statistically significant at the 5% level, as indicated by the overlapping 95% confidence intervals (Figure 17a). For surface soil moisture, the correlation at the 9 km (33 km) scale is 0.78 (0.79) in Version 7 and 0.76 (0.78) in Version 6; for root zone soil moisture, the correlation at the 9 km (33 km) scale is 0.78 (0.83) in Version 7 and 0.76 (0.82) in Version 6. For the anomaly correlation skill, results are neutral on balance, with a very slight improvement in the Version 7 surface soil moisture and a similarly slight degradation in the Version 7 root zone soil moisture. The small but consistent increase in correlation (but not anomaly correlation) skill is consistent with the introduction in Version 7 of the seasonally varying climatology of vegetation opacity derived from the SMAP L2 radiometer retrieval product. The latter is based on L-band observations and thus better represents the required microwave vegetation opacity than the vegetation opacity climatology that was derived from optical data in previous L4_SM versions.

It is not surprising that the skill of the Version 6 and 7 products is generally very similar. None of the core validation sites are in peatlands, so the core site skill metrics are not informative about the peatland changes in Version 7. Moreover, the impact of the microwave radiative transfer model parameter revisions in Version 7 is limited because the Tb scaling approach is designed to correct for mean differences in the simulated and observed Tb. In any case, both L4_SM versions use only climatological microwave radiative transfer model parameters; consequently, errors in interannual variations are similar in the two versions.

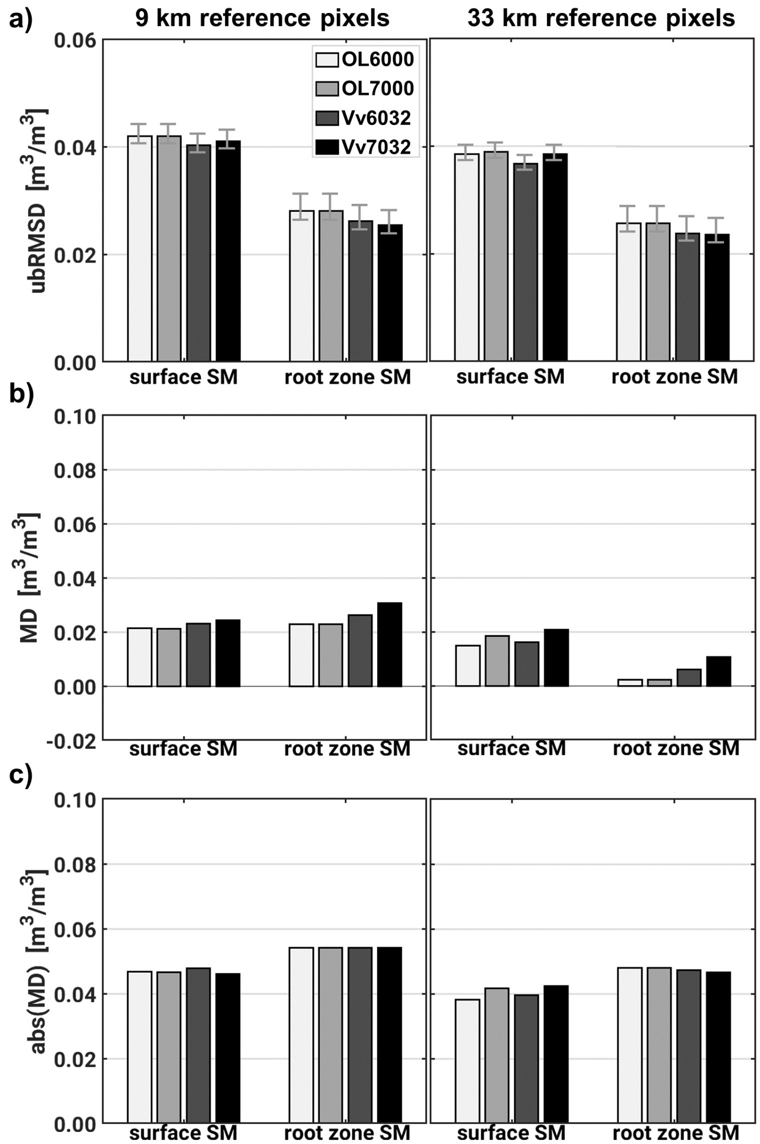

Figure 16. Surface and root zone soil moisture (a) ubRMSD, (b) MD and (c) absolute MD averaged across (left) 9 km and (right) 33 km core site reference pixels for the Version 6 Open Loop (OL6000), the Version 7 Open Loop (OL7000), the Version 6 L4_SM (Vv6032) product, and the Version 7 L4_SM (Vv7032) product for April 2015 – March 2021. Error bars for ubRMSD indicate 95% confidence intervals.

Next, we compare the skill of the Version 7 L4_SM product to that of the corresponding model-only Open Loop (OL7000) estimates. The ubRMSD for surface and root zone soil moisture skill at the 9 km and the 33 km scales is slightly lower for the Version 7 L4_SM product than for the Open Loop (Figure 16a), demonstrating the positive impact of assimilating SMAP Tb observations. For example, at the 9 km scale the surface soil moisture ubRMSD is 0.041 m^3 m^{-3} for the Version 7 L4_SM surface soil moisture and 0.042 m^3 m^{-3} for OL7000. However, the ubRMSD improvement of the L4_SM product over the model-only simulation is not statistically significant at the 5% level. The average MD values for surface and root zone soil moisture tend to be somewhat worse for the Version 7 product than for the model-only (OL7000) estimates (Figure 16b), but these differences are much smaller than the (considerable) upscaling uncertainty (Chen et al. 2019). The average absolute MD values are the essentially the same for the Version 7 product and OL7000 (Figure 16c).

Considerable and across-the-board improvements in terms of R (Figure 17a) and anomaly R (Figure 17b) skill are seen in the Version 7 L4_SM soil moisture over the model-only Open Loop estimates. The improvements range from 0.04 to 0.12 and are statistically significant for surface soil moisture at both the 9 km and 33 km scales. The improvements in the correlation metrics reflect the L4_SM product's emphasis on accurately estimating temporal variations in soil moisture.

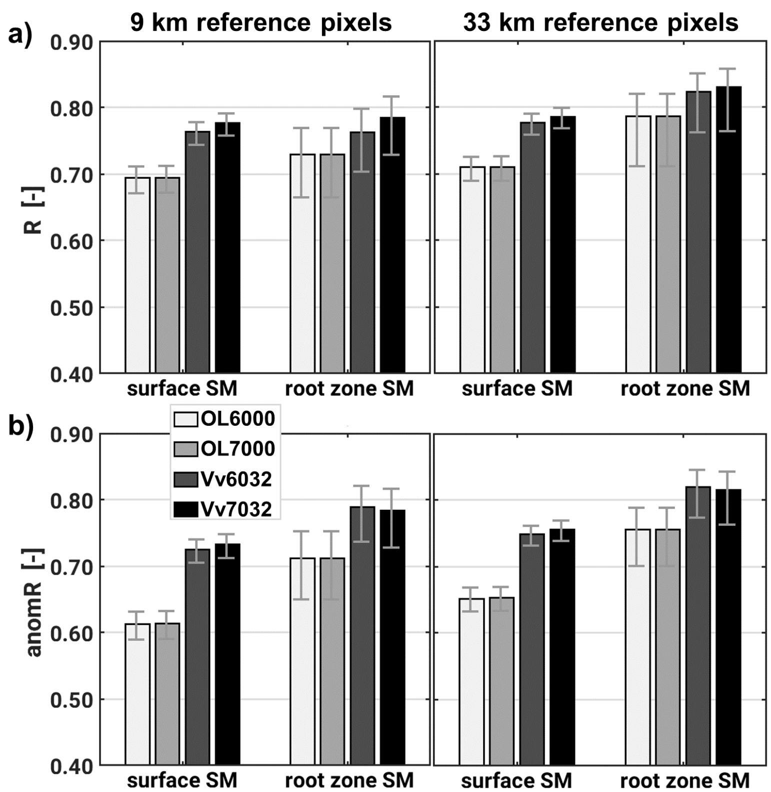

Figure 17. As in Figure 16, but for (a) time series correlation coefficient (R) and (b) anomaly R. Error bars indicate 95% confidence intervals.

Next, we compare the skill values at 9 km to those at 33 km. In both versions, the L4_SM and Open Loop skill values at 33 km are better for all metrics than the corresponding values at 9 km (Figures 16 and 17), which is consistent with the fact that the model forcing data and the assimilated SMAP Tb observations are all at resolutions of about 30 km or greater. The information used to downscale the assimilated information primarily stems from the land model parameters, which are at the finer, 9 km resolution; this information is expected to have a modest impact at best. It is therefore not a surprise that the estimates at 33 km are more skillful than those at 9 km.

Finally, we compare the skill of the surface estimates to that of the root zone estimates. Across both versions and both scales, for nearly all metrics and for both the L4_SM and Open Loop estimates, the skill of the root zone soil moisture estimates is better than that of the surface estimates. This result makes sense because there is much more variability in surface soil moisture. It is important to keep in mind, however, that the root zone metrics are computed from only a subset of the sites used for the computation of the surface metrics.

For completeness, Tables A1-A8 list the ubRMSD, MD, R, and anomaly R metrics vs. core site in situ measurements at the 9 km and 33 km scales for each reference pixel; metrics are provided for surface soil moisture, root zone soil moisture, surface soil temperature at 6am local time, and surface soil temperature at 6pm local time for the both the Version 6 and Version 7 Open Loop simulations and L4_SM products. Note that the OL6000 and Version 6 metrics listed in the present report can differ slightly from the values listed in Tables A1-A8 of the Version 6 assessment report (Reichle et al. 2022a). These slight differences occur because we cross-mask the two simultaneously validated products for above-freezing conditions in both products; that is, the Version 6 metrics are computed after cross-masking with Version 7 data in the present report and after cross-masking with Version 5 data in Reichle et al. 2022a.

For surface soil temperature, there are no meaningful differences in the average metrics between the Open Loop estimates and the L4_SM product or between the two versions. For additional discussion of surface soil temperature skill, the reader is referred to (Reichle et al. 2018). For reference, Table A9 also lists the Version 7 L4_SM metrics categorized by land cover, as shown for Version 5 in Table XII of Colliander et al. (2022).

6.3 Sparse Networks

This section provides an assessment of the L4_SM soil moisture estimates using in situ measurements from additional regional and continental-scale networks. Unlike the SMAP core sites, the networks used in this subsection usually have just one sensor (or profile of sensors) located within a given 9 km EASEv2 grid cell; hereinafter, we refer to these networks as “sparse” networks (Colliander et al. 2022). The point-scale measurements from sparse networks are, of course, generally not representative of the grid cell average conditions estimated by the L4_SM algorithm. On the other hand, sparse networks offer in situ measurements in a larger variety of environments and provide data quasi-operationally with short latency. One disadvantage of the sparse network measurements is that they typically require some manual quality control to identify and address artificial breaks in the time series of the measurements, which is a labor-intensive process. Here, the 6-year period from **1 April 2015, 0z to 1 April 2021, 0z** is used for validation using the same quality-controlled measurements that were used in the Version 6 assessment report (Reichle et al. 2022a). Extending the quality-controlled in situ record beyond April 2021 is left for future work. See Reichle et al. (2015) for further discussion of the advantages and limitations of using sparse networks in the L4_SM validation process.

6.3.1 Method

Since the sparse network measurements used here are identical to those used in the Version 6 assessment report, this subsection is essentially the same as section 6.3.1 of Reichle et al. (2022a) with only minor edits.

This assessment report focuses on metrics obtained from a direct comparison of the L4_SM product to in situ measurements, that is, metrics derived without using triple collocation approaches that attempt to correct for errors in the in situ measurements (Gruber et al. 2016; Chen et al. 2017). The values of the time series correlation metrics provided here are thus lower than those that would be obtained with the aid of triple collocation, and they are therefore conservative estimates of the true skill. Note also that the *relative* performance of the products under investigation does not depend on the use of triple collocation approaches (Dong et al. 2020).

The skill of the L4_SM estimates was computed using all available in situ measurements (after quality control) at 3-hourly time steps, and this skill was compared to that of the model-only Open Loop estimates. For sparse networks, we used the same requirements for the minimum number of data values as for core validation sites (section 6.2). Note that quality control generally excludes in situ measurements when the ground is frozen (see Reichle et al. 2015, their Appendix C). Instantaneous L4_SM data from the "aup" Collection and corresponding Open Loop data were taken directly from the standard 9 km EASEv2 grid cell that includes the sensor location (that is, the data product estimates are not interpolated bilinearly or otherwise to the precise location of the in situ sensor locations). Metrics were computed for surface and root zone soil moisture against in situ measurements from the USDA Soil Climate Analysis Network (SCAN), the NOAA US Climate Reference Network (USCRN), the Oklahoma (OK) Mesonet, the OZNet-Murrumbidgee network, and the SMOSMania network (Table 4). The average metrics were computed based on a clustering algorithm that assigns the weights given to each location based on the density of sites in the surrounding region (De Lannoy and Reichle 2016). As for the core site metrics, statistical uncertainty estimates in the form of 95% confidence intervals are provided for the second-order metrics (ubRMSD, R, and anomaly R) but not for the MD metrics because the upscaling error for the latter is considerably larger (Chen et al. 2019).

Measurements used for L4_SM validation cover most of the contiguous United States (SCAN, USCRN, OK Mesonet), parts of the Murrumbidgee basin in Australia (OZNet), and an area in south-western France (SMOSMania). The in situ measurements from the sparse network sites were subjected to extensive automated and manual quality control procedures by the L4_SM team following Liu et al. (2011), which removed spikes, temporal inhomogeneities, oscillations, and other artifacts that are commonly seen in these automated measurements. In our experience, the manual inspection and quality control is an indispensable step in the process. Table 4 also lists the number of sites with sufficient data after quality control.

Table 4. Overview of sparse networks, with indication of the sensor depths, number of sites, and data periods used here. Values in parentheses indicate the number of sites for which the anomaly R metric was computed. The anomaly R metric was only available for sites with sufficient data to compute a seasonally varying climatology. Count of USCRN (OK Mesonet) sites includes 4 (1) site(s) with undetermined IGBP land cover classification.

Network	Region	Sensor Depths (m)	Number of Sites				Period (MM/DD/YYYY)	Reference
			Surface		Root Zone			
SCAN	USA	0.05, 0.10, 0.20, 0.50	135	(134)	108	(106)	04/01/2015 - 03/31/2021	Schaefer et al. 2007
USCRN	USA	0.05, 0.10, 0.20, 0.50	111	(111)	78	(76)	04/01/2015 - 03/31/2021	Bell et al. 2013; Diamond et al. 2013
OK Mesonet	Okla. USA	0.05, 0.25, 0.60	118	(116)	77	(76)	04/01/2015 - 05/01/2018	McPherson et al. 2007
OZNet	Australia	0.04, 0.45	43	(43)	19	(19)	04/01/2015 - 09/01/2020	Smith et al. 2012
SMOSMania	France	0.05, 0.20	21	(21)	21	(21)	04/01/2015 - 12/31/2019	Calvet et al. 2007
All Networks			***428***	***(425)***	***303***	***(298)***		

A total of 428 sites provided surface soil moisture measurements, and 303 provided root zone soil moisture measurements. Most of the sites are in the continental United States, including more than 100 each in the USCRN and SCAN networks, and another 118 sites in Oklahoma alone from the OK Mesonet. The OZNet network contributes 43 sites with surface soil moisture measurements, of which 19 sites also provide root zone measurements. Finally, 21 sites with surface and root zone soil moisture measurements were used from the SMOSMania network. Three (five) sites do not have enough surface (root zone) soil moisture measurements for the computation of the climatology that is needed to determine the anomaly R skill.

Table 4 also lists the sensor depths that were used to compute the in situ root zone soil moisture. As with the core validation sites, vertical averages for SCAN, USCRN, and OK Mesonet are weighted by the spacing of the sensor depths within the 0-100 cm layer corresponding to the L4_SM estimates, and the average is only computed if all sensors within a given profile provide measurements after quality control. For SCAN and USCRN sites, some measurements at 100 cm depth are available, but these deeper layer measurements are not of the quality and quantity required for L4_SM validation and are therefore not used here. For OZNet and SMOSMania, in situ root zone soil moisture is given by the measurements at the 45 cm and 20 cm depth, respectively; that is, no vertical average is computed.

6.3.2 Results

Figure 18 shows the Open Loop and L4_SM metrics for Versions 6 and 7 averaged across all sparse network sites. As for the core site validation, the sparse network ubRMSD for surface soil moisture is slightly larger in Version 7 than in Version 6; for root zone soil moisture, the two versions have nearly identical ubRMSD skill (Figure 18a). The Version 7 product also has a slightly larger average MD than Version 6 for surface and root-zone soil moisture (Figure 18b). The sparse network correlation skill, however, is consistently improved in Version 7 compared to Version 6 (Figure 18c), and the anomaly correlation skill is neutral, with a slight improvement in Version 7 for surface soil moisture and a slight degradation for root zone soil moisture (Figure 18d). Generally, the performance differences between the two versions are small, with skill changes that are consistent across the surface and root zone metrics seen only for the correlation, owing to the improved L-band vegetation opacity parameters in Version 7. The sparse network correlation results thus corroborate the core site validation results (Figures 16 and 17). As with the core site validation, this is not surprising. Like the core sites, none of the sparse network sites is located in peatlands, and the Tb scaling approach limits the impact of the updated but still climatological parameters in the Version 7 microwave radiative transfer model (section 6.2.2).

Compared to the Open Loop estimates, both L4_SM product versions have generally lower ubRMSD and higher R and anomaly R values, with improvements that are statistically significant at the 5% level for the surface soil moisture correlation metrics (Figure 18c,d). This again demonstrates the additional information contributed by the assimilation of the SMAP Tb observations in the L4_SM system and corroborates the core site validation results.

As with the core site validation results, the ubRMSD and MD values vs. the sparse network measurements are smaller (better) for root zone soil moisture than for surface soil moisture (Figure 18a,b), which again reflects the fact that root zone soil moisture generally varies less in time than surface soil moisture.

Like the core sites, the sparse network sites are in regions with high-quality precipitation measurements, owing to the generally dense gauge network in CONUS, Western Europe, and southeastern Australia (Reichle et al. 2021a, their Figure 1c). Larger improvements from the assimilation of SMAP observations are generally seen where the precipitation forcing is based on fewer gauges (section 6.5).

Overall, the evaluation of skill for the sparse network sites yields results that are very similar to those obtained for the core validation sites. The beneficial impact of assimilating SMAP Tb observations is greatest for surface soil moisture, with smaller improvements in root zone soil moisture estimates. Finally, it is important to keep in mind that the skill metrics presented here underestimate the true skill because these metrics are based on a direct comparison against in situ measurements (which themselves are subject to error). Therefore, the sparse network ubRMSD values suggest that the L4_SM estimates would meet the formal accuracy requirement across a very wide variety of surface conditions, beyond those that are covered by the relatively few core validation sites that have been available to date for formal verification of the accuracy requirement. One caveat, however, is that the sparse network results do not provide an entirely independent validation because SCAN and USCRN measurements were used to calibrate an earlier version

(NRv7.2) of the model (Reichle et al. 2018). Nevertheless, the sparse network results provide additional confidence in the conclusions drawn from the core validation site comparisons.

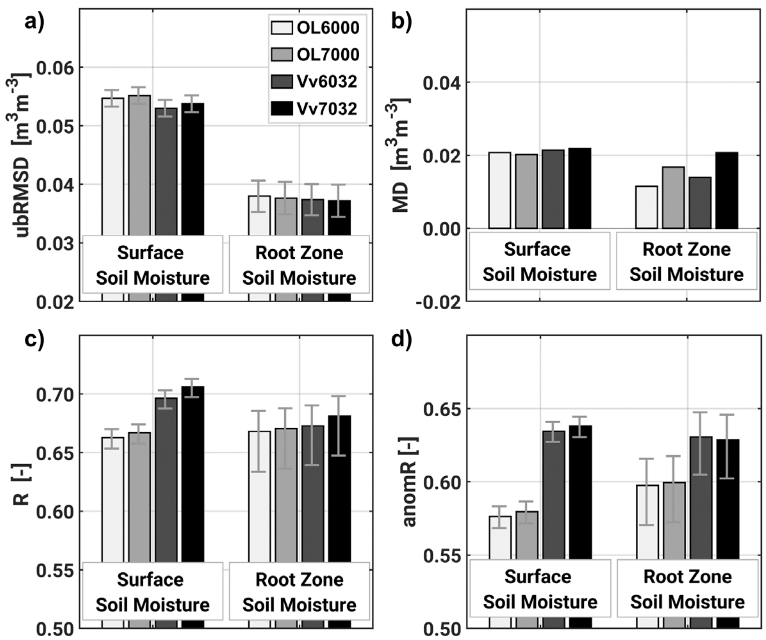

Figure 18. Skill metrics for Version 6 and Version 7 Open Loop (OL6000 and OL7000, resp.) estimates and the Version 6 and Version 7 L4_SM products (Vv6032 and Vv7032, resp.) over the sparse network sites listed in Table 4 for April 2015 – March 2021. (a) ubRMSD, (b) MD, (c) time series correlation coefficient (R), and (d) anomaly R. Error bars for ubRMSD, R, and anomaly R indicate 95% confidence intervals.

6.4 Water Level in Peatlands

In situ measurements of peatland water level are available for 18 point-scale locations at 7 different sites (Table 5). Three of the sites are in Canada (CA_FOM, CA_JB, CA_URSA), and one site each is in Estonia (EE_kaev), Finland (FI_LOM), Poland (PO_BPN), and Russia (RU_MU). The 18 different point-scale locations fall into 12 distinct 9-km EASEv2 grid cells. Of the 18 point-scale locations, 11 are in fens (which are fed by surface and/or groundwater as well as precipitation) and 7 are in bogs (which are purely rain-fed). At each site, between 5 and 10 years of data are available. Most of the measurements were taken before the launch of SMAP, with just 1-3.5 years of overlap with the SMAP period, depending on the location. Moreover, water level output is not available in the Version 6 L4_SM product (section 6.1.2). Here, we therefore validate the water level estimates from the Nature Run simulations of Version 6 (NRv9.1) and Version 7 (NRv10.0) (Table 1).

Table 5. Characteristics of peatland sites with in situ water level measurements.

Site ID	Country	Latitude [degree]	Longitude [degree]	9-km EASEv2 Index Latitude	9-km EASEv2 Index Longitude	Peatland Type	Measurement Period
CA_FOM_SAL	Canada	56.5747	-111.2773	132	736	Fen	Jan 2012 - Sep 2017
CA_JB_F	Canada	52.7144	-84.1985	164	1026	Fen	Jan 2008 - Jul 2016
CA_JB_G	Canada	52.7105	-84.1723	164	1026	Fen	Jan 2008 - Jul 2016
CA_JB_Bog1	Canada	52.7457	-83.9750	164	1028	Bog	Jan 2008 - Jul 2018
CA_JB_Fen1	Canada	52.7492	-83.9522	164	1028	Fen	Jan 2008 - Jul 2017
CA_URSA_171_1	Canada	55.9809	-115.1885	137	694	Bog	May 2010 - Oct 2018
CA_URSA_171_15	Canada	55.9844	-115.1903	137	694	Fen	May 2010 - Oct 2018
EE_kaev_222	Estonia	58.8773	26.2217	115	2208	Bog	Jan 2008 - Dec 2016
EE_kaev_225	Estonia	58.8789	26.2163	115	2208	Bog	Jan 2008 - Dec 2016
FI_LOM	Finland	67.9972	24.2092	56	2187	Fen	May 2008 - Sep 2017
PO_BPN_126	Poland	53.3490	22.5718	159	2169	Fen	Nov 2009 - May 2017
PO_BPN_162	Poland	53.2853	22.6056	159	2170	Fen	Nov 2009 - May 2017
PO_BPN_177	Poland	53.5986	22.7509	157	2171	Fen	Nov 2009 - Jun 2017
PO_BPN_179	Poland	53.6635	22.8162	156	2172	Fen	May 2010 - May 2017
PO_BPN_191	Poland	53.5855	22.8338	157	2172	Fen	May 2010 - Jun 2017
RU_MU_p02	Russia	60.8920	68.6824	100	2663	Bog	Jun 2008 - Oct 2018
RU_MU_france1	Russia	60.8928	68.6826	100	2663	Bog	Oct 2012 - Oct 2018
RU_MU_france2	Russia	60.8939	68.6824	100	2663	Bog	Oct 2012 - Oct 2018

Figures 19 and 20 show the water level skill metrics for the 18 point-scale locations along with the (cluster-based) average metrics across all locations, only fens, and only bogs. The ubRMSD values range from 0.11 to 0.74 m for NRv9.1 and from 0.06 to 0.22 m for NRv10.0 (Figure 19a). The average ubRMSD across all locations is 0.34 m for NRv9.1 and drops to 0.13 m for NRv10.0. The contrast in performance is even starker for the MD (Figure 19b). For NRv9.1, the MD is universally negative and ranges from -0.30 to -3.36 m, with an average MD of -1.52 m. That is, the water level estimates in NRv9.1 are much too deep. For NRv10.0, the MD ranges from -0.29 to 0.23 m, with an average MD of just -0.08 m. The time series correlation ranges from -0.10 to 0.55 for NRv9.1 and from -0.19 to 0.77 for NRv10.0, with average correlations of 0.21 for NRv9.1 and 0.42 for NRv10.0 (Figure 20a). Similarly, the anomaly correlation ranges from -0.02 to 0.66 for NRv9.1 and from -0.02 to 0.70 for NRv10.0, with average correlations of 0.16 for NRv9.1 and 0.36 for NRv10.0 (Figure 20b). With just a few exceptions at individual locations, the peatland water level estimates from the Version 7 system (NRv10.0) clearly outperform those from the Version 6 system (NRv9.1) in all skill metrics.

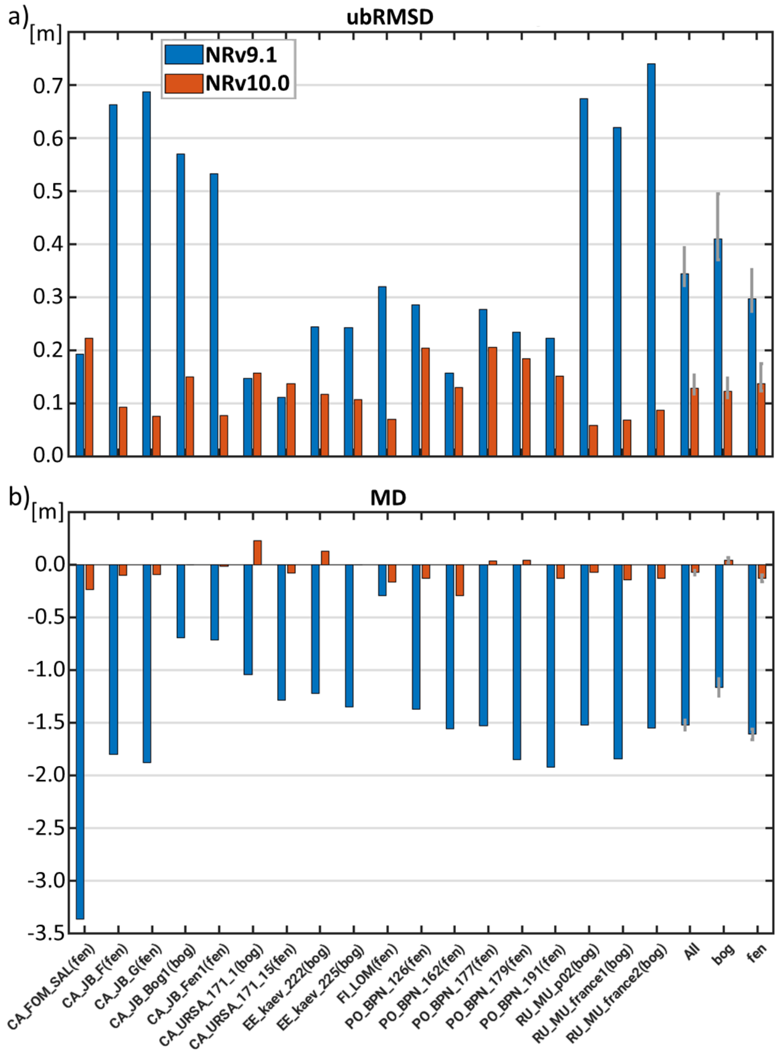

Figure 19. (a) ubRMSD and (b) MD of peatland water level from the (blue bars) NRv9.1 and (red bars) NRv10.0 Nature Run simulations. Metrics computed vs. in situ measurements for 2008–2018. The three rightmost pairs of bars show metrics averaged over all 18 sites, the 7 bog sites, and the 11 fen sites, respectively. Error bars for multi-site average ubRMSD metrics indicate 95% confidence intervals. See Table 5 for site locations and characteristics.

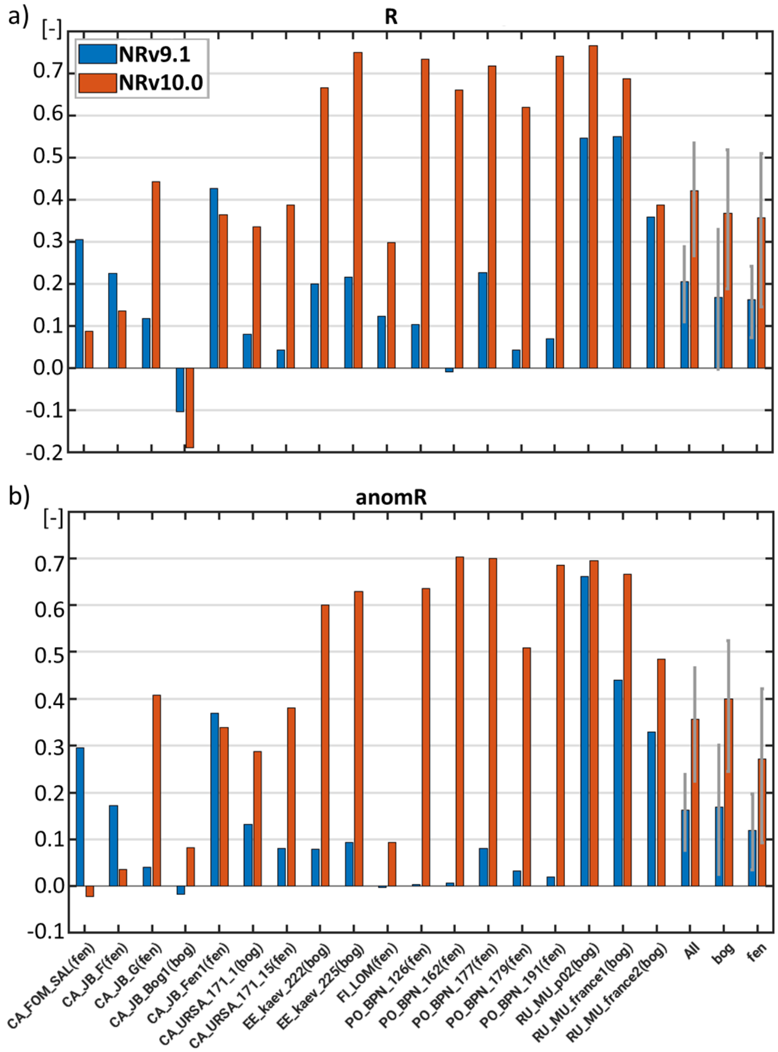

Figure 20. As in Figure 19, but for (a) time series correlation (R) and (b) anomaly R. Error bars for multi-site average metrics indicate 95% confidence intervals.

6.5 Satellite Soil Moisture Retrievals

Reichle et al. (2021a) quantified the contribution of the SMAP Tb analysis to the anomaly time series correlation skill of the L4_SM surface soil moisture based on the single instrumental variable (IV) method and independent soil moisture retrievals from the Advanced Scatterometer (ASCAT; Wagner et al. 2013), an active microwave (radar) instrument. In a nutshell, the IV method obtains the difference in skill (vs. the unknown true soil moisture) between the L4_SM and model-only estimates through the respective sample correlation skill values vs. the independent ASCAT satellite observations. This ASCAT-based IV approach was validated at the SMAP core validation sites using the grid cell-scale in situ measurements (Reichle et al. 2021a, their Figure 4). Their findings apply to the Version 4 L4_SM product.

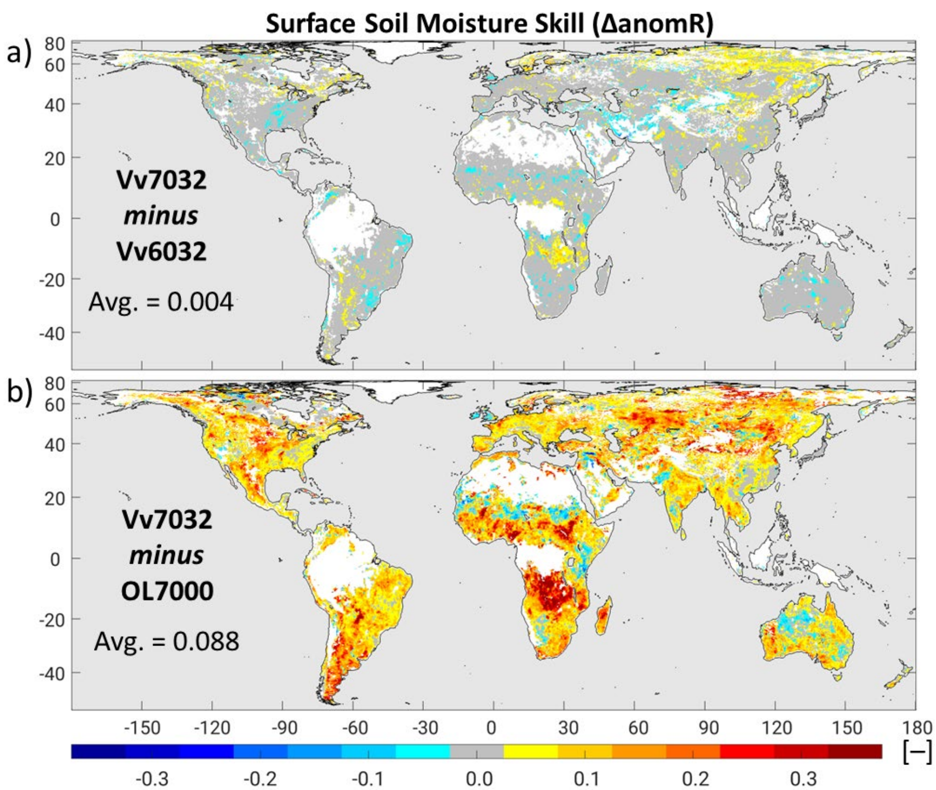

Figure 21. Difference in surface soil moisture anomaly R skill between (a) the Version 7 and Version 6 L4_SM products (Vv7032 minus Vv6032) and (b) the Version 7 L4_SM product and Open Loop simulation (Vv7032 minus OL7000). Skill difference was estimated using the single instrumental variable method and ASCAT soil moisture retrievals for April 2015 – March 2021. White shading indicates no-data-values, including lakes, permanently glaciated surfaces, and regions where reliable ASCAT observations are not available for the assessment. The latter regions encompass peatlands. Note that the L4_SM and Open Loop data used here are from the "gph" Collection because the different lossy compression strategies in the Version 6 and Version 7 "aup" granules would adversely impact the results (not shown).

Here, we apply the IV approach to determine the skill differences between the L4_SM products and the Open Loop simulations of Versions 6 and 7 using ASCAT soil moisture retrievals for April 2015 to March 2021. Figure 21a shows the surface soil moisture anomaly R difference between the Version 7 and Version 6 L4_SM products. Generally, the skill differences between the two versions are minimal, with a global average anomaly R difference of just 0.004. This is expected because the updated parameters in the Version 7 radiative transfer model are still climatological averages, as in Version 6; consequently, errors in interannual variations of soil moisture remain largely the same in the two versions. Moreover, the skill difference map is not informative about the peatland-specific changes in Version 7 because reliable ASCAT soil moisture retrievals are not available for peatlands.

The anomaly R skill difference between the Version 7 L4_SM product and the corresponding Open Loop simulation is shown in Figure 21b. This map illustrates the improvement in anomaly R skill from the assimilation of the SMAP Tb observations; the increase in skill is largest in otherwise data-sparse regions, including much of South America, Africa, and Central Asia. In the global average, the assimilation of the SMAP Tb observations improves the surface soil moisture anomaly R skill by 0.09 in Version 7. The anomaly R improvement from the SMAP Tb assimilation in Version 7 (Figure 21b) is essentially the same as that in Version 6 (Reichle et al. 2022a, their Figure 13a) because there is little skill difference between the Version 6 and 7 L4_SM products (Figure 21a) and virtually no skill difference between the Version 6 and 7 Open Loop simulations (not shown).

6.6 Data Assimilation Diagnostics

This section provides an evaluation of the L4_SM data assimilation diagnostics, including the statistics of the observation-minus-forecast (O-F) Tb residuals, the observation-minus-analysis (O-A) residuals, and the analysis increments. Because the L4_SM algorithm assimilates Tb observations, the O-F and O-A diagnostics are in terms of Tb (that is, in "observation space"). The analysis increments are, strictly speaking, in the space of the Catchment model prognostic variables that make up the "state vector", including the "surface excess", "root zone excess", and "top-layer ground heat content" (Reichle et al. 2014b). For peatlands only, the "state vector" also includes the "catchment deficit" variable (section 5.3). For the discussion below, the soil moisture excess and deficit increments have been converted into equivalent volumetric soil moisture content in units of m^3 m^{-3} and into water flux terms in units of mm d^{-1}.

A key element of the analysis update is the downscaling and inversion of the observational information from the 36 km grid of the assimilated Tb observations into the modeled geophysical variables on the 9 km grid, based on the simulated error characteristics, which vary dynamically and spatially. An example and illustration of a single analysis update can be found in Reichle et al. (2017b, their section 3b).

6.6.1 Observation-Minus-Forecast Residuals

Figure 22a shows the total number of L1C_TB observations that were assimilated at each grid cell in Version 7 during the assessment period (April 2015 – March 2022). This count includes H- and V-pol observations from ascending and descending orbits. The average data count (per 36 km grid cell) across the globe is approximately 2,780 for the 7-year (2,557-day) period. Few or no SMAP Tb observations are assimilated in high-elevation and mountainous areas (including the Rocky Mountains, the Andes, the Himalayas, and Tibet), in the vicinity of lakes (such as in northern Canada), and next to major rivers (including the Amazon and the Congo). In the high latitudes, the much shorter warm (nonfrozen) season also results in lower counts of assimilated Tb observations, although this is somewhat mitigated by SMAP's polar orbit, which results in more frequent revisit times there. The remaining gaps in coverage might reflect a lack of sufficient numbers of SMAP observations to provide the required climatological information for the computation of the (seasonally varying) Tb scaling parameters during the times of the year when conditions are suitable for a soil moisture analysis. Note, however, that the L4_SM product provides soil moisture estimates everywhere, even if in some regions the L4_SM estimates are not based on the assimilation of SMAP observations and rely only on the information in the model and forcing data.

In the global average, the count of assimilated observations for Version 7 decreased minimally, by 7.9 per 36 km grid cell (~0.3%), from that of Version 6 (Figure 22b). This is expected because the major (science) version of the assimilated L1C_TB observations has not changed between the Version 6 and Version 7 L4_SM algorithms (section 5.2), and the minor differences in the assimilated SMAP Tb observations should not impact the data counts. The decrease in the number of assimilated SMAP observations in Version 7 is concentrated in small regions, including portions of the Amazon, southern Iraq, and pockets of northern Pakistan and northern India. In these regions, the number of assimilated SMAP observations drops by up to ~10%. These drops are primarily caused by gaps in the seasonally varying vegetation opacity climatology derived from the SMAP L2 data.

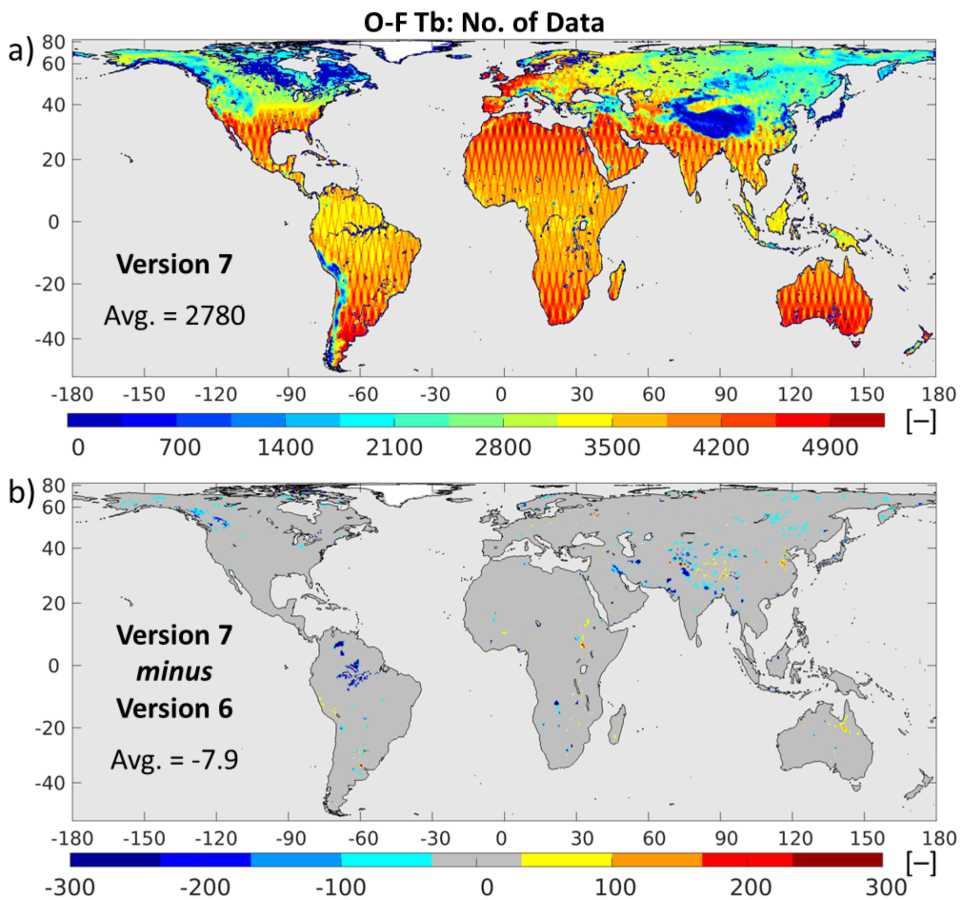

Figure 22. (a) Number of L1C_TB observations assimilated in the Version 7 L4_SM algorithm during the 7-year validation period (April 2015 – March 2022). (b) Number of L1C_TB observations assimilated in Version 7 minus that in Version 6 during the same period. Data counts include H-pol and V-pol data from ascending and descending half-orbits. White shading indicates no-data-values.

Next, Figure 23a shows the global distribution of the time-average O-F Tb residuals (or bias) for Version 7; values are typically small and mostly range from -1 to 3 K, with an overall O-F Tb bias of just 0.13 K and a mean absolute bias of just 0.25 K. Compared to Version 6, the global average of the absolute bias decreased slightly (by 0.04 K), with regional differences in the absolute bias falling mostly within ±0.5 K (Figure 23b). A corresponding graphic (not shown) for the 6-year period from 1 April 2015 to 31 March 2021 indicates that the absolute bias increased slightly (by 0.06 K) from Version 6 to Version 7, which is consistent with the fact that the Tb scaling parameters were computed from the 6-year period for Version 6 and from the 7-year validation period for Version 7.

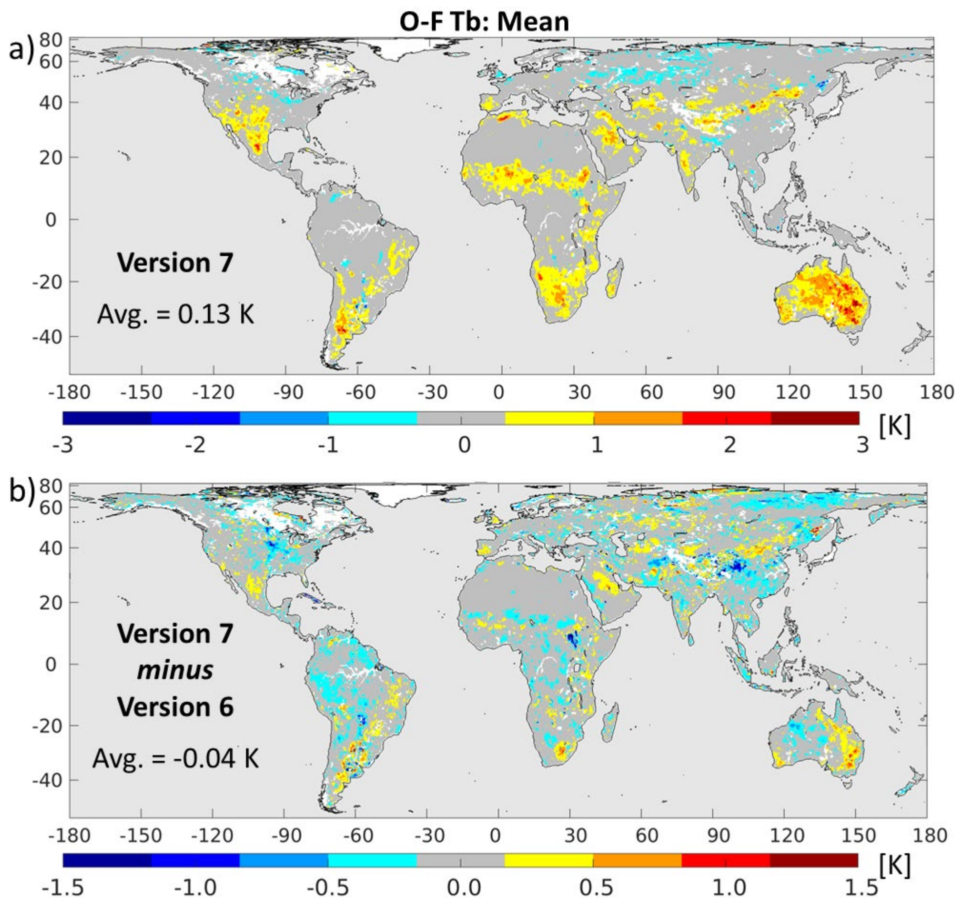

Figure 23. (a) Time-average of the O-F Tb residuals from the Version 7 L4_SM algorithm for April 2015 – March 2022. (b) Absolute value of time-average O-F Tb for Version 7 minus that of Version 6 during the same period; blue colors indicate that the mean of the Version 7 O-F Tb residuals is closer to the perfect value of zero than that of the Version 6 residuals. White shading indicates no-data-values.

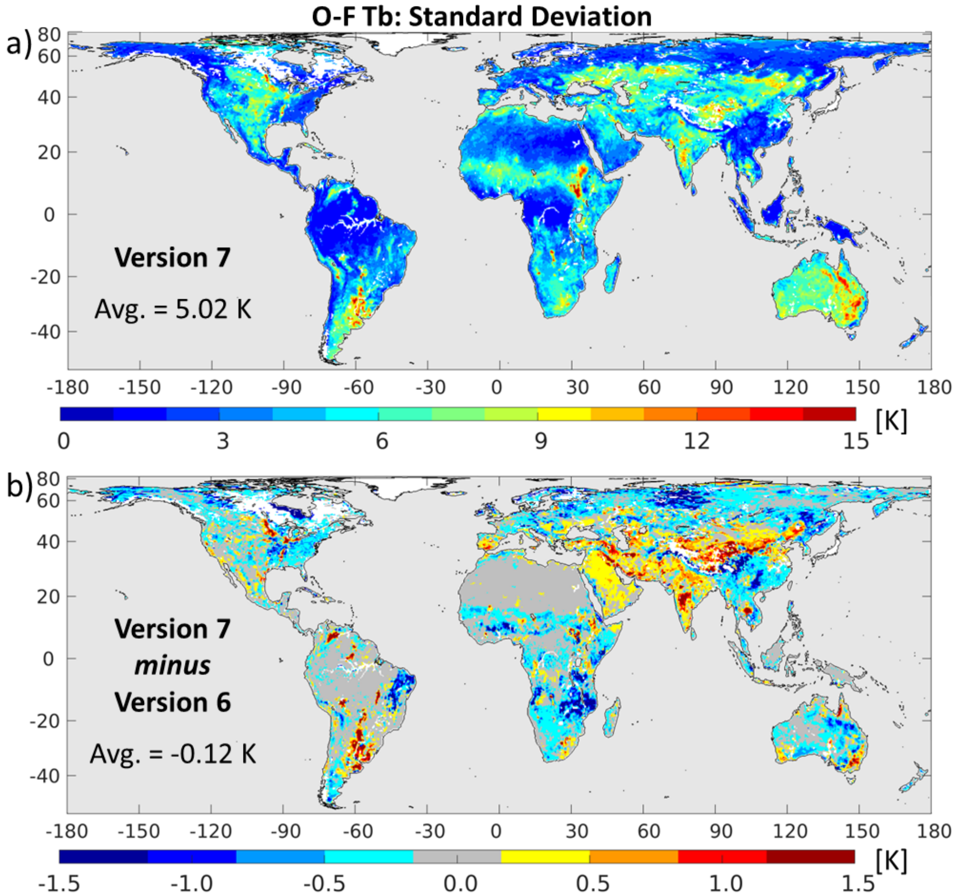

Figure 24. As in Figure 23, but for the standard deviation of the O-F Tb residuals. Blue colors in (b) indicate improved Tb simulation skill in Version 7 compared to Version 6.

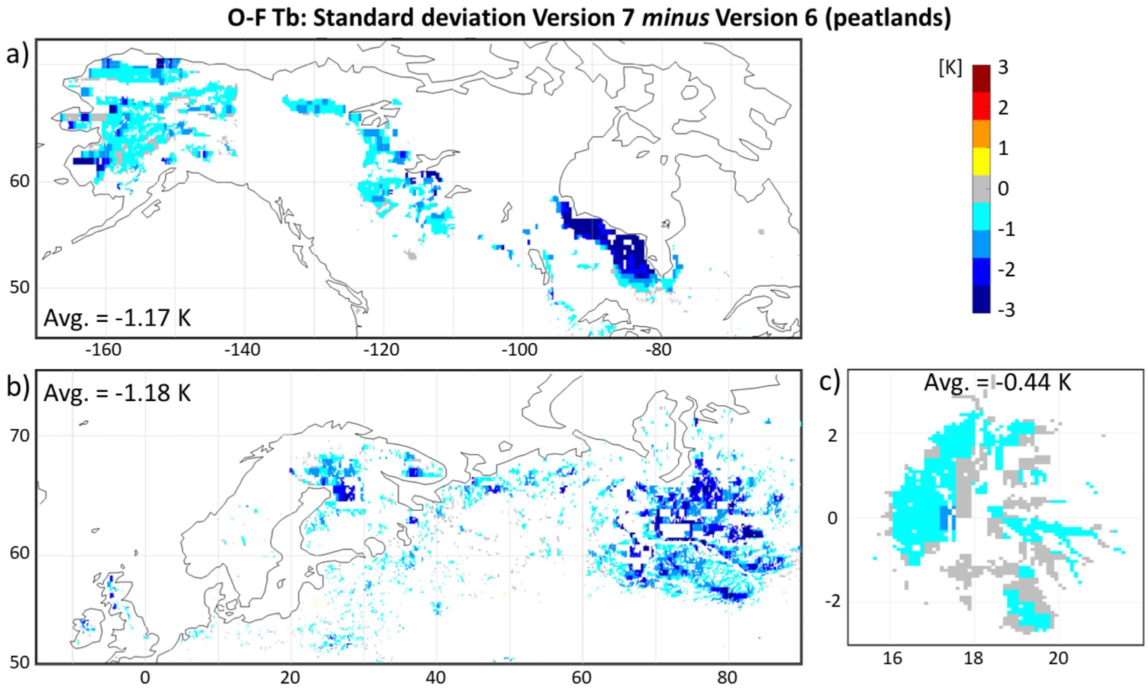

Figure 25. As in Figure 24b, but for peatlands only in (a) high-latitude North America, (b) high-latitude western Eurasia, and (c) the Cuvette Centrale (Congo) using the Version 7 peatland mask. Blue colors in (b) indicate improved Tb simulation skill in Version 7 compared to Version 6.

The time series standard deviation of the O-F Tb residuals ranges from a few Kelvins to around 15 K in a handful of small regions (Figure 24a). Higher values are found in central North America, southern South America, southern Africa, the Sahel, central Asia, India, and Australia. These regions have sparse or modest vegetation cover and typically exhibit strong variability in soil moisture conditions. The O-F Tb residuals are generally smallest in more densely vegetated regions, including the eastern United States, the Amazon basin, and tropical Africa. Small values are also found in the high latitudes, including Alaska and Siberia, and in the Sahara Desert. The global (spatial) average of the O-F Tb standard deviation is just 5.0 K in Version 7, compared to 5.1 K in Version 6. That is, the Version 7 modeling system is slightly better able to predict the observed Tb just prior to each analysis, particularly across much of Africa, China, and the high latitudes, although some degradation in this metric is seen in Argentina, the Arabian Peninsula, the Middle East, India, and portions of central Asia (Figure 24b). The improvements are strongest in peatlands (Figure 25). This is true especially in northern peatlands, where the O-F Tb residuals are smaller by ~1 K in Version 7 than in Version 6 (Figure 25a,b). For reference, the spatially averaged time series standard deviation of the O-A Tb residuals is 3.3 K in Version 7 and essentially matches that of the Version 6 system (not shown).

Finally, Figure 26a shows the standard deviation of the <u>normalized</u> O-F Tb residuals (*stddev_norm*), which measures the consistency between the simulated errors and the actual errors. Specifically, the O-F Tb residuals are normalized with the standard deviation of their expected total error, which is the sum (in a covariance sense) of the error in the observations (including instrument errors and errors of representativeness) and the error in the Tb model forecasts (Reichle et al. 2015, their Appendix B). The parameters that determine the expected error standard deviations are key inputs to the ensemble-based L4_SM assimilation algorithm. If they are chosen such that the expected errors are fully consistent with the actual errors, the metric shown in Figure 26a should be unity everywhere. If the *stddev_norm* metric is less than one, the actual errors are overestimated by the assimilation system, and if the metric is greater than one, the actual errors are underestimated.

The global average of the *stddev_norm* metric in Version 7 is 0.99, which suggests that, on average, the simulated error standard deviation nearly matches that of the actual errors (Figure 26a). This is essentially unchanged from Version 6 (Reichle et al. 2022a, their Figure 17a). As in Version 6, however, the Version 7 *stddev_norm* metric varies greatly across the globe (Figure 26a). Typical values are either too low or too high. In the Amazon basin, tropical Africa, Indonesia, parts of Southeast Asia, and portions of the high northern latitudes, *stddev_norm* values are around 0.5 or less, and thus the actual errors there are considerably overestimated by the modeling system. Conversely, *stddev_norm* values range from 1.25 to 2.5 in much of central North America, Argentina, the Sahel, southern Africa, India, central Asia, and Australia, meaning that the actual errors in these regions are considerably underestimated.

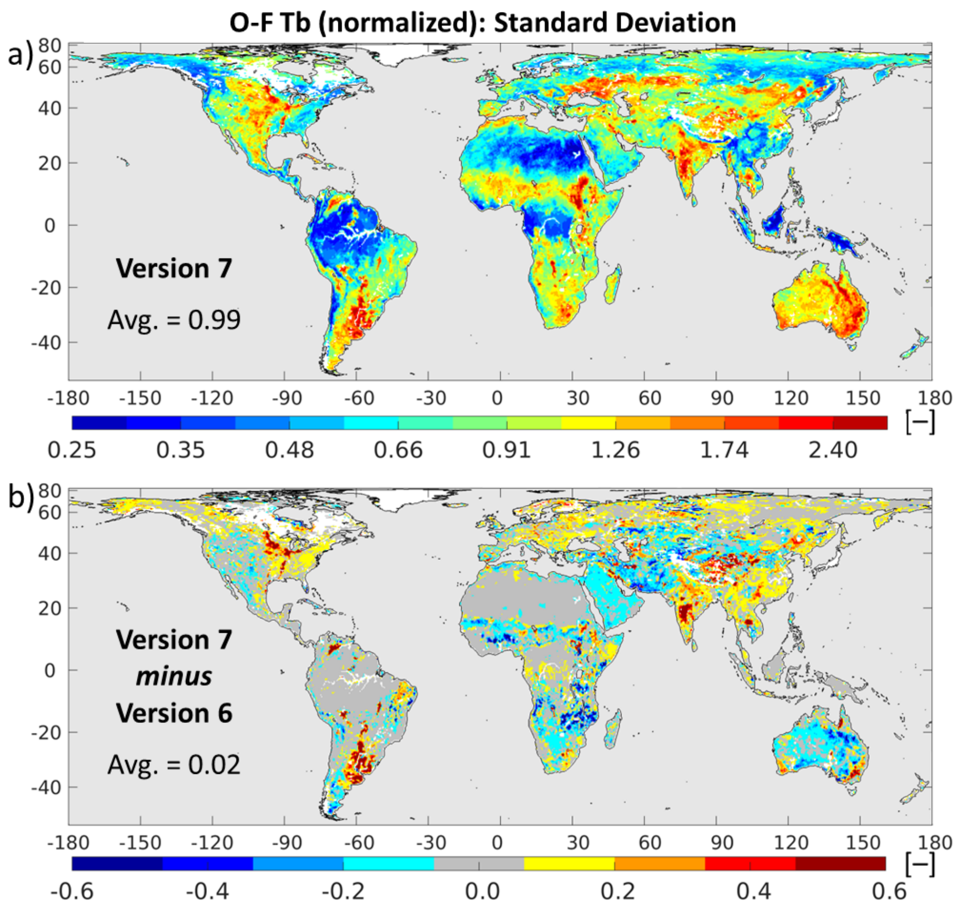

Figure 26. (a) Time series standard deviation of the normalized O-F Tb residuals (*stddev_norm*) from the Version 7 L4_SM algorithm for April 2015 – March 2022. (b) Absolute deviation of Version 7 *stddev_norm* from unity minus that of Version 6 during the same period; blue colors indicate that *stddev_norm* is closer to the perfect value of unity in Version 7 than in Version 6. White shading indicates no-data-values.

Finally, Figure 26b compares the absolute deviation of *stddev_norm* from unity between Version 7 and Version 6. In the Sahel, southern Africa, the Arabian Peninsula, the Middle East, and central Australia, the consistency of the simulated and actual errors is improved in Version 7 compared to Version 6. However, the opposite is true in the eastern half of North America, Argentina, and large portions of Eurasia. In the global average, the absolute difference of the *stddev_norm* metric from the perfect value of unity increased by 0.02 in Version 7 compared to Version 6. More work is needed to further improve the calibration of the input parameters that determine the model and observation errors in the L4_SM system.

6.6.2 Increments

The number of times an analysis increment is applied at a given 9 km EASEv2 grid cell during the validation period depends on the count of assimilated observations in the vicinity (that is, within the 1.25-degree "localization" radius of influence; Reichle et al. 2017b). For simplicity, we compute the number of increments, separately for each 9 km grid cell, by counting the number of times the absolute analysis-minus-forecast difference in the 3-hourly analysis update output exceeded 10^{-5} m^3 m^{-3} for surface soil moisture or 0.001 K for surface temperature[1].

The average number of increments in Version 7 is 0.78 per day over the 7-year validation period, which means that there are approximately four increments applied every five days on average, either from an ascending or a descending overpass. The overall pattern of the increments count (Figure 27a) follows that of the count of the assimilated Tb observations (Figure 22a). There is little difference in the number of increments between Version 7 and Version 6 (Figure 27b), which is expected given the similarity of the count of the assimilated SMAP Tb observations in the two versions (Figure 22b).

The time-average of the analysis increments for surface and root zone soil moisture is shown in Figure 28a and c, respectively. In the global average, these net increments are only -0.023 mm d^{-1} for surface soil moisture and 0.053 mm d^{-1} for root zone soil moisture (or -8.4 and 19 mm per year, respectively). Regionally, however, the net increments can be up to ~0.5 mm d^{-1} and constitute a non-negligible fraction of the water balance. Generally, the pattern of the net soil moisture increments reflects the long-term average of the O-F Tb residuals (Figure 23a). They are largest in the central US, eastern South America, Africa, India, portions of mid-latitude Eurasia, and eastern Australia. Interestingly, the net surface soil moisture increments are generally negative (i.e., drying) while the mean root zone soil moisture increments are generally positive (i.e., wetting). The magnitude of the net increments in Version 7 is generally similar to that of Version 6 for surface soil moisture (Figure 28b). The differences in magnitude are a bit larger for the net increments in root zone soil moisture (Figure 28d; note the different color scale). For both surface and root zone soil moisture, the global average of the magnitude of the net increments in the two versions is nearly identical.

---

[1]In Version 6, this approach produces noisy results when the published analysis and forecast fields are used, owing to the lossy compression of the published Version 6 aup files. To compute the statistics of the Version 6 increments, we therefore used intermediate binary data that were written before the lossy compression. These data can be made available upon request.

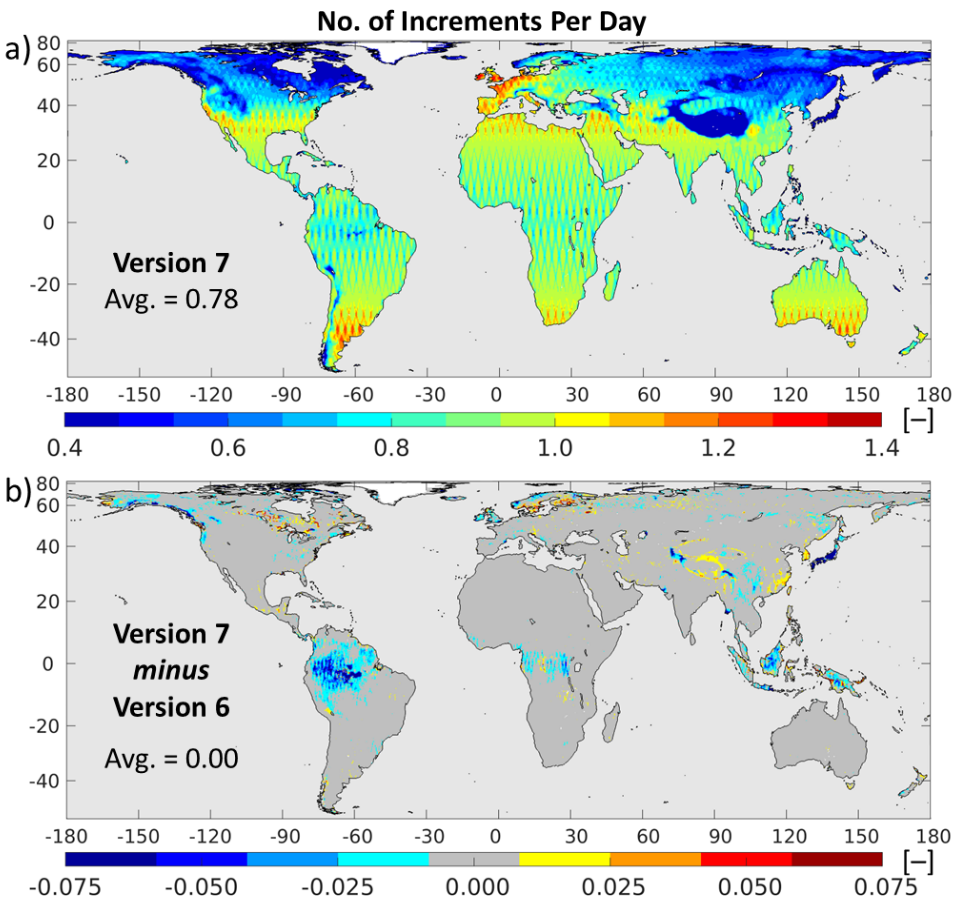

Figure 27. (a) Average number of increments per day generated by the Version 7 L4_SM algorithm during April 2015 – March 2022. (b) Average number of increments generated in Version 7 minus that in Version 6 during the same period. The results apply equally to all elements of the control vector, including the model prognostic variables related to surface soil moisture, root zone soil moisture, surface temperature, and top-layer soil temperature. White shading indicates no-data-values.

Finally, Figure 29 shows the time series standard deviation of the increments in surface and root zone soil moisture. This metric measures the typical magnitude of instantaneous increments. Typical increments in surface soil moisture are on the order of 0.02-0.03 $m^3\ m^{-3}$ in the central US, Argentina, the Sahel, southern Africa, India, portions of central Asia, and most of Australia (Figure 29a). In the same regions, root zone soil moisture increments are typically on the order of 0.002-0.006 $m^3\ m^{-3}$ (Figure 29c). In densely vegetated regions, in particular the tropical forests, surface and root zone soil moisture increments are generally negligible, reflecting the fact that in those areas the measured SMAP Tb observations are mostly sensitive to the dense vegetation and are only marginally sensitive to soil moisture. Compared to Version 6, the typical magnitude of the instantaneous increments in Version 7 is largely unchanged for both surface and root zone soil moisture outside of peatlands (Figure 29b and d). In peatlands, the typical magnitude of the Version 7 root zone soil moisture increments increases by 0.001-0.002 $m^3\ m^{-3}$ (Figure 30), which stems from the addition of the catchment deficit variable to the EnKF state vector for peatlands (section 5.3).

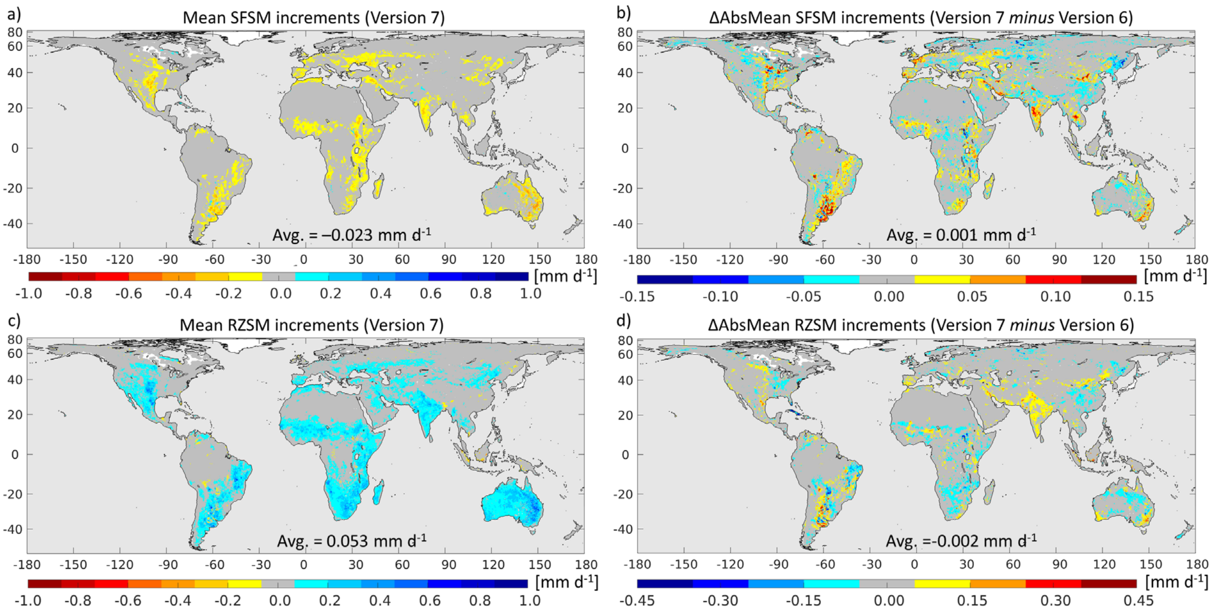

Figure 28. Time-average analysis increments for (a) surface and (c) root zone soil moisture from the Version 7 L4_SM algorithm for Apr 2015 – March 2022 in equivalent flux units (mm d^{-1}). Absolute value of time-average increments for Version 7 minus that of Version 6 during the same period for (b) surface and (d) root zone soil moisture; blue colors in (b) and (d) indicate that the time-average of the Version 7 increments is closer to the perfect value of zero than that of the Version 6 increments. Note the different color scales in (b) and (d). White shading indicates no-data-values.

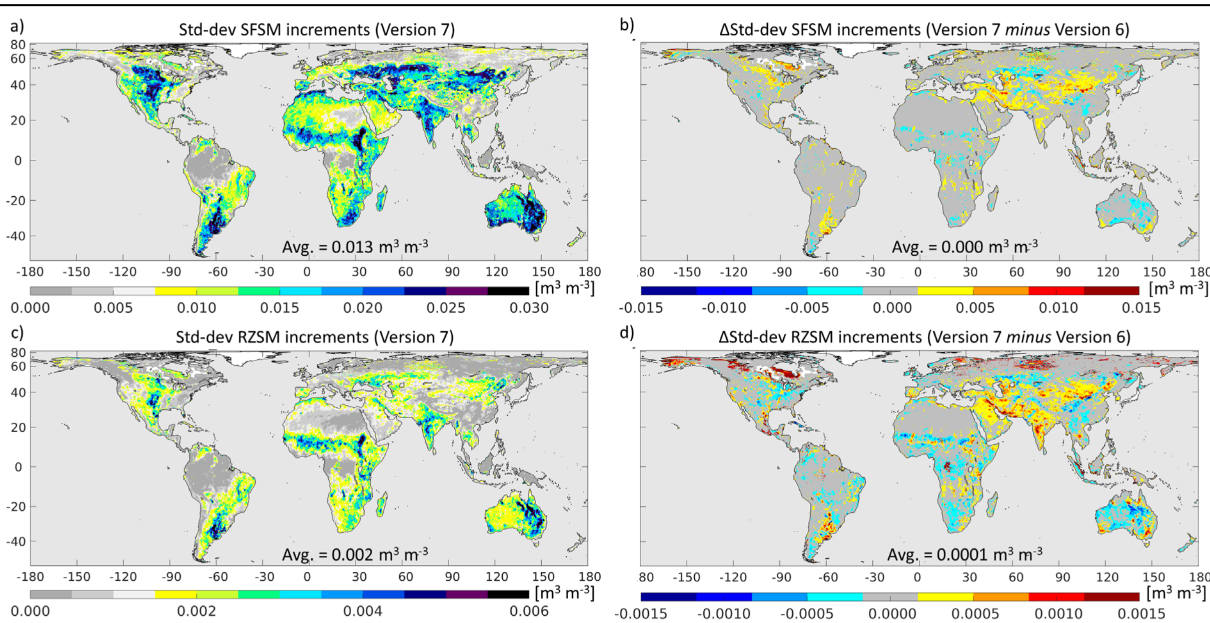

Figure 29. As in Figure 28, but for time series standard deviation of the increments in volumetric soil moisture units (m^3 m^{-3}). Blue colors in (b) and (d) indicate that the standard deviation of the increments is smaller in Version 7 than in Version 6.

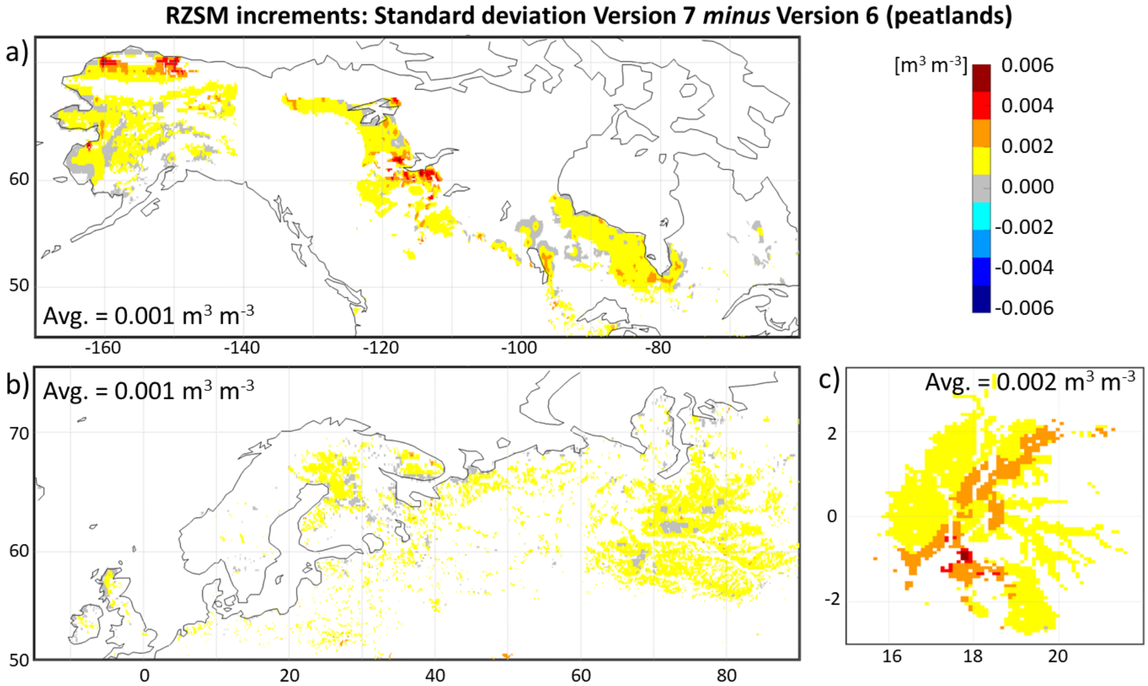

Figure 30. As in Figure 29d, but zoomed into the peatlands of (a) high-latitude North America, (b) high-latitude western Eurasia, and (c) the Cuvette Centrale (Congo) using the Version 7 peatland mask. Yellow and red colors indicate that the standard deviation of the RZSM increments is larger in Version 7 than in Version 6. Note the difference in color scale compared to Figure 29d.

6.6.3 Uncertainty Estimates

The L4_SM data product also includes error estimates for key output variables, including surface and root zone soil moisture as well as surface and soil temperature. These uncertainty estimates vary dynamically and geographically because they are computed as the standard deviation of a given output variable across the ensemble of land surface states at a given time and location. (The ensemble is an integral part of the ensemble Kalman filter employed in the L4_SM algorithm, and the ensemble average provides the estimate of the variable under consideration (Reichle 2008).) By construction, the uncertainty estimates represent only the random component of the uncertainty. Bias and other structural errors such as errors in the dynamic range are not included.

Figure 31 shows the time-average soil moisture uncertainty estimates for the 7-year validation period. Across the globe, surface soil moisture uncertainty typically ranges from 0.02 to 0.05 m^3 m^{-3} in Version 7, with larger uncertainties in regions where the lowest number of SMAP Tb observations are assimilated (Figure 22a), including northwestern North America, northeastern Asia, and the Tibetan Plateau, which are subject to frozen or snow-covered conditions for a large part of the year. The less frequent Tb analysis in these regions implies less reduction in ensemble spread. The uncertainty in root zone soil moisture exhibits a similar pattern, albeit with uncertainty estimates typically ranging from 0.01 to 0.03 m^3 m^{-3} (Figure 31b). The lower uncertainty estimates in root zone soil moisture primarily reflect the fact that root zone soil moisture is less variable in time than surface soil moisture.

Outside of peatlands, the estimated uncertainties for soil moisture and soil temperature of Version 7 are very close to those of Version 6 (not shown). Across peatlands, in contrast, there is a marked increase in the uncertainty for surface soil moisture in Version 7 from that of Version 6 (Figure 32a,c,e). In northern peatlands, the surface soil moisture uncertainty in Version 7 roughly doubles in value from that in Version 6, with increases of up to ~0.04 $m^3 m^{-3}$. Differences in root zone soil moisture uncertainty between Version 7 and Version 6 are mixed, with some regions seeing an increase in uncertainty and others seeing a decrease of up to ~0.01 $m^3 m^{-3}$ in magnitude (Figure 32b,d,f). The revised peatland hydrology in Version 7 tends to increase the surface soil moisture variability (Figure 10); therefore, peatland surface soil moisture in Version 7 is more sensitive to the meteorological forcing data and to the applied perturbations, resulting in a greater ensemble spread.

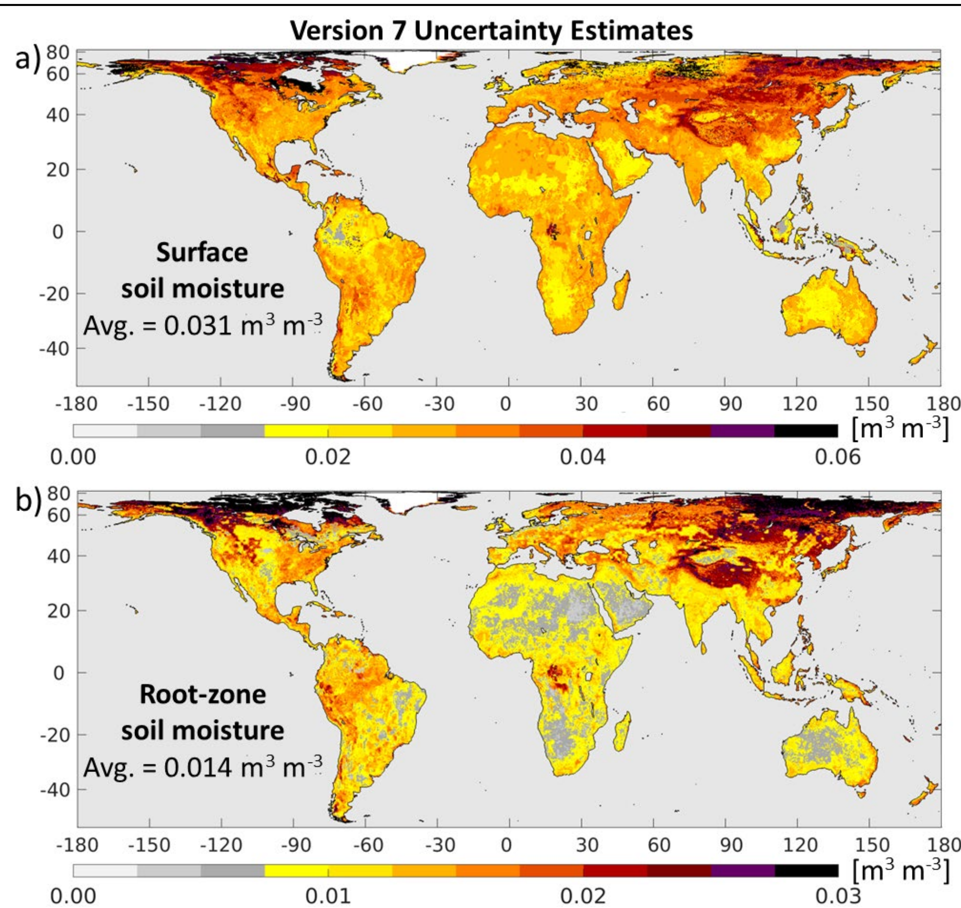

Figure 31. Time-average of Version 7 L4_SM uncertainty estimates for (a) surface and (b) root zone soil moisture for April 2015 – March 2022. Uncertainty estimates are computed as the standard deviation across the (instantaneous) model ensemble that is used in the L4_SM assimilation algorithm. White shading indicates no-data-values.

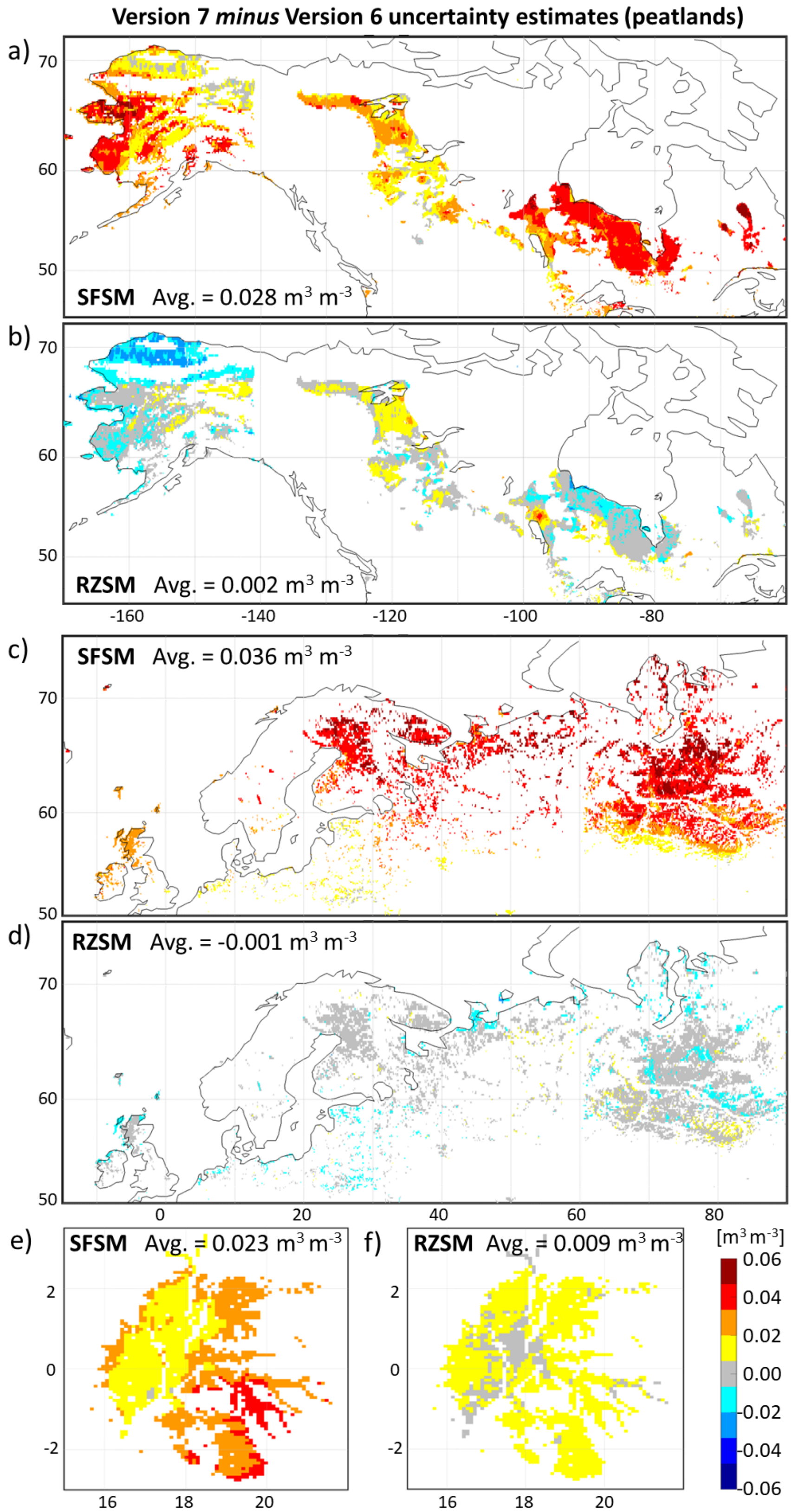

Figure 32. Time-average (April 2015 – March 2022) of Version 7 minus Version 6 differences in L4_SM uncertainty estimates for (a,c,e) surface soil moisture (SFSM) and (b,d,f) root zone soil moisture (RZSM) in the peatlands of (a,b) high-latitude North America, (c,d) high-latitude western Eurasia, and (e,f) the Cuvette Centrale (Congo) using the Version 7 peatland mask.

7 LIMITATIONS AND PLAN FOR FUTURE IMPROVEMENTS

Several limitations and avenues for future development of the L4_SM product are revealed by the Version 7 assessment presented above and by earlier validation results (Reichle et al. 2021b, 2022a) that still apply to Version 7.

7.1 L4_SM Algorithm Calibration and Temporal Homogeneity

Compared to earlier versions, the calibration of the Version 7 L4_SM algorithm utilized longer records of model-only Tb data and SMAP Tb observations. There are, however, still regions with a residual bias in the O-F Tb residuals (Figure 23a), which in turn leads to non-zero long-term mean soil moisture analysis increments (Figure 28a and c). Further improvements in the L4_SM algorithm calibration will be facilitated by an even longer record of SMAP observations and matching model-only Tb estimates. By themselves, however, longer SMAP records for the computation of the Tb scaling parameters are not sufficient.

Version changes in the GEOS FP system (Lucchesi 2018) during the SMAP period adversely impact the homogeneity of the surface meteorological forcing data that are needed to calibrate the L4_SM algorithm and to generate the L4_SM data product. A forthcoming GEOS reanalysis product for the 21st century (R21C) is expected to be available in 2024. This new reanalysis dataset will provide a more homogeneous record of surface meteorological forcing data during the SMAP period and will also be more consistent with the future operational FP version that will provide the surface meteorological forcing data for L4_SM forward processing. We plan to use the R21C data (once they are available) in future L4_SM versions for both calibration and retrospective L4_SM processing.

7.2 Precipitation Data

The daily precipitation corrections in the Version 7 L4_SM algorithm are primarily based on IMERG data, with the CPCU product used only in North America and for spin-up (Reichle et al. 2022a). This approach is nearly identical to that of Version 6 (section 5.3). Specifically, the satellite-gauge IMERG-Final data are used if they are available (through 30 September 2021 in Vv7032). Beginning on 1 October 2021, the daily precipitation corrections in Vv7030 are based on satellite-only IMERG-Late data, which are presumably of somewhat lesser quality than IMERG-Final data. Additional research is needed to determine the impact of switching from IMERG-Final to IMERG-Late inputs on the L4_SM soil moisture skill.

Moreover, the GPM project plans to change the IMERG processing algorithm from Version 06B to a new major version in 2023. Additional research will be needed to assess the impact of the upcoming IMERG version change on the quality of the L4_SM product.

7.3 Peatland and Permafrost Modeling

The version of the peatland hydrology module (PEATCLSM) implemented in the Version 7 L4_SM algorithm was developed for high-latitude natural peatlands (Bechtold et al. 2019). The hydrological functioning of tropical peatlands, however, differs from that of northern peatlands. Moreover, many peatlands in the tropics and in Europe are drained artificially, which changes their hydrological regime. Recently, Apers et al. (2022) further developed PEATCLSM with a focus on improving the simulation of hydrological processes in natural and drained tropical peatlands. Moreover, ongoing development addresses drained high-latitude peatlands. Future L4_SM versions should adopt the newer PEATCLSM version.

Research suggests that relatively simple model revisions can improve the Catchment model skill in permafrost regions (Tao et al. 2017, 2019). Implementing these model advances in the L4_SM algorithm should improve the skill of the L4_SM product in the high latitudes, where the coupling with the carbon cycle is of particular interest in the context of the SMAP science objectives (Entekhabi et al. 2010).

8 SUMMARY AND CONCLUSIONS

The present report assesses Version 7 of the SMAP L4_SM product for the period from 1 April 2015, 0z to 1 April 2022, 0z. The most important changes in the Version 7 algorithm are the **revised global peatland mask** (Figure 5) and the **new peatland hydrology module (PEATCLSM)**, including new, peatland-specific water level output. Moreover, the Version 7 algorithm uses climatological parameters for the **L-band soil roughness, scattering albedo, and (seasonally varying) vegetation opacity** that were **derived from the SMAP L2 soil moisture retrieval product**, replacing the values that were calibrated to the SMOS L-band Tb climatology in previous L4_SM versions (Figures 13-15). Additional updates in the Version 7 algorithm include (i) the recalibration of the Tb scaling parameters over a longer, 7-year period, (ii) the use of a longer, 21-year period in the derivation of the soil moisture climatology underpinning the root zone and profile soil moisture percentile output, (iii) the use of the gauge-based IMERG-Final precipitation data through September 2021 before switching to the satellite-only IMERG-Late precipitation data, and (iv) the use of only lossless compression of the aup output to facilitate the post-processing of analysis increments (section 5.3).

The Version 7 L4_SM product was validated using in situ soil moisture measurements from SMAP core validation sites and sparse networks. Peatland water level was validated for the Nature Run simulation using in situ measurements mostly taken before the SMAP launch. Additionally, independent soil moisture retrievals from ASCAT were used to determine anomaly correlation skill differences between the Version 6 and Version 7 soil moisture estimates. The product was further evaluated through an assessment of the data assimilation diagnostics generated by the L4_SM algorithm, such as the O-F Tb residuals and the soil moisture analysis increments.

The global pattern of arid and humid regions is well captured by the Version 7 L4_SM soil moisture estimates (Figure 3). Outside of peatlands, there are only small changes in the time-average soil moisture between Version 6 and Version 7 (Figure 4). Across peatlands, surface soil moisture is typically wetter by 0.1-0.3 $m^3 m^{-3}$ in Version 7 than in Version 6, but a few small regions are drier by ~0.1 $m^3 m^{-3}$ in Version 7. Root zone soil moisture is considerably wetter in Version 7 compared to Version 6 (Figure 7). In regions simulated as mineral soil in Version 6 but as peatlands in Version 7, the time-average root zone soil moisture increases by up to 0.6 $m^3 m^{-3}$ (Figure 7). Moreover, the time series variability of surface soil moisture in peatlands is considerably larger in Version 7 than in Version 6 (Figure 9), which more realistically reflects the typical swings between very wet and very dry surface conditions seen in peatlands. The latent heat flux in peatlands is generally smaller by a few W m^{-2} in Version 7 than in Version 6, with the reverse being true for the sensible heat flux (Figure 10). Compared to Version 6, total runoff (including surface runoff and baseflow) increases by ~0.5-1 mm d^{-1} in Version 7 across high-latitude peatlands but decreases by ~0.5 mm d^{-1} in tropical peatlands (Figure 10). Finally, peatland water level estimates are much shallower and less variable in Version 7 than in Version 6 and reflect the hydrological conditions in peatlands much more realistically (Figures 11 and 12).

Because of these climatological differences, **the Version 6 and Version 7 products should *not* be combined into a single dataset for use in applications that include peatlands** (defined as the union of the Version 6 and Version 7 peatland masks; see Figure 5).

When compared to in situ measurements from the SMAP core validation sites, the Version 7 surface soil moisture ubRMSD is 0.041 $m^3 m^{-3}$ at the 9 km scale and 0.038 $m^3 m^{-3}$ at the 33 km scale, which is slightly worse than in Version 6 (Figure 16a, Table A1). For root zone soil moisture, the ubRMSD is 0.026 $m^3 m^{-3}$ at the 9 km scale and 0.023 $m^3 m^{-3}$ at the 33 km scale, which is slightly better than in Version 6 (Figure 16a, Table A3). On balance, the Version 7 ubRMSD metrics are thus unchanged from those of the Version 6 product. When factoring in the measurement error of the in situ measurements (conservatively estimated to be ~0.01-0.02 $m^3 m^{-3}$), the **Version 7 L4_SM surface and root zone soil moisture clearly meet the product accuracy requirement** (ubRMSE $\leq$ 0.04 $m^3 m^{-3}$). Furthermore, it is important to keep in mind that, whereas the surface soil moisture in situ measurements are typically at ~5 cm depth, the L4_SM estimates are for the 0-5 cm soil layer. As with the error in the in situ measurements themselves, this mismatch in layer depths adversely impacts all of our validation metrics.

The Version 7 product has slightly but consistently better correlation skill for both surface and root zone soil moisture than the Version 6 product (Figure 17a). For the anomaly correlation skill, results are neutral on balance. The small increase in correlation (but not anomaly correlation) skill is consistent with the introduction in Version 7 of the seasonally varying climatology of vegetation opacity derived from the SMAP L2 radiometer retrieval product. In Version 7, this climatology is based on L-band observations and thus better represents the required microwave vegetation opacity than the vegetation opacity climatology that was derived from optical data in previous L4_SM versions.

The assimilation of SMAP Tb observations is beneficial for the Version 7 L4_SM surface and root zone soil moisture estimates, with improvements over the model-only Open Loop (OL7000) estimates that are consistent across the 9 km and 33 km scales and across the ubRMSD and correlation metrics (Figures 16 and 17). For surface soil moisture, the correlation improvements are statistically significant at the 5% level. The improvement from SMAP Tb assimilation is essentially the same in Versions 6 and 7. The comparison with in situ measurements from a global set of sparse networks (Figure 18) corroborates the results obtained with the core site measurements. Moreover, the anomaly correlation skill obtained using the independent ASCAT soil moisture retrievals remains essentially unchanged between Versions 6 and 7, with the largest improvements from the SMAP Tb assimilation seen in otherwise data-sparse regions across much of South America and Africa (Figure 21).

The soil moisture performance metrics vs. in situ measurements for Versions 6 and 7 are expected to be close, given that (i) none of the soil moisture in situ sites are in peatlands, (ii) ASCAT retrievals are unreliable and thus not used in peatlands, and (iii) both versions only use climatological microwave radiative transfer model parameters.

Peatland water levels were validated against in situ measurements for the Nature Run simulations of the Version 6 (NRv9.1) and Version 7 (NRv10.0) systems (Figures 19 and 20). The average ubRMSD decreased from 0.22 m for Version 6 to 0.06 m for Version 7, and the average MD improved from -1.5 m for Version 6 to -0.07 m for Version 7. The average correlation increased from 0.20 for Version 6 to 0.42 for Version 7, and the average anomaly correlation increased from 0.15 for Version 6 to 0.44 for Version 7. These results indicate that the Version 7 L4_SM product provides improved estimates of peatland water levels.

The data assimilation diagnostics further broaden the validation results to the global domain. The global average number of Tb observations assimilated in the Version 7 system is nearly identical to that in Version 6 (Figures 22), and the same is true for the number of analysis increments (Figure 27). The time-mean, globally averaged increments for surface and root zone soil moisture remain very small in Version 7; regionally, however, time-mean increments can still be as large as 0.5 mm d^{-1} (Figure 28a,c). These biases in the increments are caused by modest biases in the O-F Tb residuals that can be up to ±3 K in small regions (Figure 23). The assimilation diagnostics further reveal that, on a regional basis, the errors in Tb are over- or underestimated considerably in the Version 7 L4_SM system (Figure 26). For the most part, these diagnostics are unchanged from those of Version 6.

The time series standard deviation of the O-F Tb residuals is reduced from 5.1 K in Version 6 to 5.0 K in Version 7 (Figure 24). This improvement in the Tb simulation skill in the Version 7 system is strongest and most consistent across peatlands, where the typical O-F Tb misfits are reduced by more than 1 K in high-latitude peatlands and by ~0.5 K in tropical peatlands (Figure 25). Outside of peatlands, typical O-F Tb misfits are reduced in much of eastern North America, Africa, China, and the high latitudes but increased in parts of South America, the Arabian Peninsula, the Middle East, and parts of Central Asia (Figure 24b).

On average, the typical magnitude of the soil moisture increments remains unchanged between Versions 6 and 7 (Figure 29). In peatlands, however, the typical magnitude of the root zone soil moisture increments is considerably larger in Version 7 than in Version 6 (Figure 30), owing to the addition of the catchment deficit model variable to the EnKF state vector for peatlands.

Ensemble-based uncertainty estimates for the analyzed soil moisture and temperature fields are also provided with the product. These uncertainty estimates are designed to reflect the random error in the geophysical product fields. On average, the uncertainty is estimated to be 0.031 $m^3 m^{-3}$ for surface soil moisture and 0.014 $m^3 m^{-3}$ for root zone soil moisture (Figure 31). Outside of peatlands, the uncertainty estimates are essentially the same for Versions 6 and 7. Across peatlands, surface soil moisture uncertainty in Version 7 increased from Version 6 (Figure 32), which primarily reflects the increased variability in peatland surface soil moisture in Version 7 (Figure 9).

Based on the results presented in this report, the public release of Version 7 of the L4_SM data product is recommended. Looking ahead, the IMERG version upgrade, now planned for 2023, will necessitate an investigation of its impact on the L4_SM product skill (section 7.2). Possible avenues for future development include the use of the forthcoming GEOS R21C reanalysis that will provide a more temporally homogeneous record of surface meteorological forcing data (section 7.1) and the use of improved Catchment model physics for tropical peatlands and permafrost (section 7.3). These developments will be addressed in future work. Finally, efforts are underway to construct a weakly-coupled land-atmosphere assimilation system by introducing the L4_SM algorithm into the GEOS weather analysis system (Reichle et al. 2021f).

ACKNOWLEDGEMENTS

This report was made possible by the contributions of many individuals from the SMAP Project, the SMAP Science Team, the SMAP Cal/Val Partner Program, and the NASA Global Modeling and Assimilation Office. The NASA SMAP mission and the NASA Modeling, Analysis, and Prediction program supported the research. Computational resources were provided by the NASA High-End Computing Program through the NASA Center for Climate Simulation at the Goddard Space Flight Center. This research was also supported by the U.S. Department of Agriculture (USDA) Agricultural Research Service (ARS). USDA is an equal opportunity provider and employer.

For the soil moisture validation data we thank A. Berg, S. Bircher, D. Bosch, T. G. Caldwell, A. Colliander, M. Cosh, Á. González-Zamora, C. D. Holifield Collins, T. Jackson, K. H. Jensen, S. Livingston, E. Lopez-Baeza, J. Martínez-Fernández, H. McNairn, M. Moghaddam, A. Pacheco, T. Pellarin, J. Prueger, T. Rowlandson, M. Seyfried, P. Starks, Z. Su, E. Tetlock, M. Thibeault, R. van der Velde, J. P. Walker, X. Wu, Y. Zeng, staff at USGS, USDA-ARS, and the University of Valencia, and the USDA Long-Term Agroecosystem Research (LTAR) network. Funding for the Kenaston network was provided by the Canadian Space Agency and by Environment and Climate Change Canada.

For the peatland water level validation data we thank M. Aurela, N. Balliston, K. Devito, M. Grygoruk, A. Lohila, J. Price, Biebrza National Park, the Estonian Environmental Agency, Mukhrino Field Station, and Utikuma Research Study Area Observatory.

APPENDIX

Performance Metrics at Core Validation Site Reference Pixels

Tables A1-A8 in this Appendix provide a complete listing of the performance metrics, including ubRMSD, MD, R, and anomaly R, for all 9 km and 33 km SMAP core site reference pixels. Metrics are provided for surface soil moisture, root zone soil moisture, surface soil temperature at 6am local time, and surface soil temperature at 6pm local time for the L4_SM Vv7032 and Vv6032 product versions as well as for the model-only OL7000 and OL6000 estimates. Table A9 provides the L4_SM Vv7032 performance metrics for the 9 km reference pixels categorized by land cover.

Table A1. Surface soil moisture ubRMSD and MD at individual core site reference pixels and averaged over 33 km and 9 km reference pixels, including average and average absolute metrics across all sites (bottom rows labeled "All"). Information for 33 km reference pixels is shown in bold font. Italics indicate Version 7 L4_SM metrics.

			Surface soil moisture								
	Reference pixel		ubRMSD (m3 m-3)					MD (m3 m-3)			
Site name	ID	Horiz. scale (km)	OL7000	*Vv7032*	OL6000	Vv6032	95% conf. interval	OL7000	*Vv7032*	OL6000	Vv6032
RM	**03013302**	**33**	**0.029**	***0.038***	**0.029**	**0.037**	**0.005**	**0.049**	***0.053***	**0.049**	**0.051**
	03010903	9	0.028	*0.036*	0.028	0.036	0.003	0.122	*0.141*	0.122	0.136
	03010908	9	0.040	*0.045*	0.040	0.047	0.007	-0.013	*-0.009*	-0.013	-0.011
RC	**04013302**	**33**	**0.042**	***0.039***	**0.042**	**0.040**	**0.010**	**-0.002**	***0.005***	**-0.002**	**0.004**
	04010907	9	0.041	*0.038*	0.041	0.040	0.008	-0.013	*-0.008*	-0.013	-0.010
	04010910	9	0.048	*0.046*	0.048	0.047	0.013	-0.033	*-0.032*	-0.033	-0.033
YC	**07013301**	**33**	**0.045**	***0.039***	**0.045**	**0.033**	**0.007**	**-0.006**	***-0.013***	**-0.007**	**-0.012**
	07010902	9	0.073	*0.051*	0.072	0.058	0.012	-0.047	*-0.039*	-0.047	-0.044
	07010916	9	0.051	*0.050*	0.051	0.043	0.009	-0.002	*-0.011*	-0.002	-0.011
CR	**09013301**	**33**	**0.036**	***0.052***	**0.036**	**0.052**	**0.007**	**-0.030**	***-0.028***	**-0.030**	**-0.030**
	09010906	9	0.030	*0.053*	0.030	0.051	0.005	0.026	*0.026*	0.025	0.024
NG	**12033301**	**33**	**0.020**	***0.020***	**0.020**	**0.020**	**0.004**	**-0.032**	***-0.032***	**-0.032**	**-0.033**
WG	**16013302**	**33**	**0.026**	***0.028***	**0.026**	**0.029**	**0.002**	**0.025**	***0.032***	**0.025**	**0.033**
	16010906	9	0.026	*0.027*	0.027	0.028	0.002	-0.004	*0.006*	-0.004	0.008
	16010907	9	0.027	*0.030*	0.027	0.031	0.002	0.022	*0.031*	0.022	0.033
	16010913	9	0.033	*0.038*	0.033	0.038	0.003	0.100	*0.105*	0.100	0.104
LW	**16023302**	**33**	**0.037**	***0.031***	**0.037**	**0.030**	**0.003**	**-0.041**	***-0.040***	**-0.041**	**-0.042**
	16020905	9	0.048	*0.043*	0.048	0.042	0.004	-0.001	*0.005*	0.000	0.002
	16020906	9	0.044	*0.037*	0.044	0.037	0.004	-0.012	*-0.013*	-0.011	-0.014
	16020907	9	0.041	*0.035*	0.041	0.035	0.005	-0.043	*-0.044*	-0.042	-0.045
FC	**16033302**	**33**	**0.038**	***0.036***	**0.038**	**0.036**	**0.003**	**-0.024**	***-0.020***	**-0.024**	**-0.022**
	16030911	9	0.050	*0.038*	0.050	0.040	0.004	-0.046	*-0.039*	-0.046	-0.040
	16030916	9	0.037	*0.034*	0.037	0.034	0.003	-0.026	*-0.022*	-0.026	-0.024
LR	**16043302**	**33**	**0.041**	***0.040***	**0.041**	**0.039**	**0.003**	**0.003**	***0.003***	**0.003**	**0.003**
	16040901	9	0.034	*0.033*	0.034	0.032	0.003	0.076	*0.085*	0.076	0.084
SJ	**16063302**	**33**	**0.051**	***0.050***	**0.044**	**0.041**	**0.007**	**0.197**	***0.192***	**0.136**	**0.132**
	16060907	9	0.045	*0.040*	0.045	0.042	0.013	0.064	*0.054*	0.067	0.061
SF	**16073302**	**33**	**0.055**	***0.048***	**0.055**	**0.047**	**0.007**	**0.028**	***0.023***	**0.027**	**0.025**
	16070909	9	0.060	*0.050*	0.060	0.053	0.006	-0.013	*-0.012*	-0.013	-0.012
	16070910	9	0.061	*0.053*	0.061	0.054	0.006	0.031	*0.027*	0.031	0.030
	16070911	9	0.064	*0.057*	0.064	0.056	0.007	0.044	*0.040*	0.044	0.042
MB	**19023301**	**33**	**0.040**	***0.043***	**0.040**	**0.037**	**0.007**	**-0.056**	***-0.047***	**-0.056**	**-0.055**
	19020902	9	0.040	*0.042*	0.040	0.035	0.009	-0.047	*-0.046*	-0.047	-0.055
TZ	**25013301**	**33**	**0.045**	***0.045***	**0.045**	**0.040**	**0.013**	**0.027**	***0.029***	**0.027**	**0.025**
	25010911	9	0.050	*0.050*	0.050	0.046	0.011	0.025	*0.028*	0.025	0.021
KN	**27013301**	**33**	**0.042**	***0.043***	**0.042**	**0.039**	**0.008**	**-0.004**	***0.004***	**-0.005**	**-0.004**
	27010910	9	0.032	*0.031*	0.032	0.029	0.006	-0.039	*-0.019*	-0.039	-0.029
	27010911	9	0.040	*0.038*	0.040	0.035	0.007	-0.065	*-0.050*	-0.065	-0.060
VA	41010906	9	0.028	*0.028*	0.028	0.026	0.006	0.066	*0.060*	0.066	0.064
NI	**45013301**	**33**	**0.039**	***0.036***	**0.039**	**0.036**	**0.006**	**0.061**	***0.073***	**0.063**	**0.081**
	45010902	9	0.039	*0.036*	0.039	0.036	0.005	0.070	*0.081*	0.072	0.088
BN	**45023301**	**33**	**0.048**	***0.046***	**0.048**	**0.047**	**0.008**	**0.120**	***0.120***	**0.119**	**0.120**
	45020902	9	0.048	*0.045*	0.048	0.046	0.007	0.118	*0.119*	0.118	0.120
TX	**48013301**	**33**	**0.034**	***0.030***	**0.034**	**0.028**	**0.004**	**0.031**	***0.033***	**0.031**	**0.030**
	48010902	9	0.040	*0.039*	0.040	0.036	0.004	0.068	*0.071*	0.068	0.067
	48010911	9	0.038	*0.034*	0.038	0.032	0.004	0.075	*0.078*	0.075	0.074
HB	**67013301**	**33**	**0.033**	***0.029***	**0.033**	**0.031**	**0.007**	**-0.014**	***-0.015***	**-0.014**	**-0.015**
	67010901	9	0.046	*0.044*	0.046	0.046	0.021	-0.018	*-0.013*	-0.018	-0.016
All	**Average**	**33**	**0.039**	***0.038***	**0.039**	**0.037**	**0.001**	**0.018**	***0.021***	**0.015**	**0.016**
	Average	9	0.042	*0.041*	0.042	0.040	0.002	0.023	*0.026*	0.023	0.025
	Avg. Abs.	**33**	n/a	*n/a*	n/a	n/a	n/a	**0.042**	***0.042***	**0.038**	**0.040**
	Avg. Abs.	9	Same as average.					0.048	*0.048*	0.049	0.050

Table A2. As in Table A1, but for R and anomaly R.

			Surface soil moisture									
	Reference pixel		R (dimensionless)					anomaly R (dimensionless)				
Site name	ID	Horiz. scale (km)	OL7000	Vv7032	OL6000	Vv6032	95% conf. interval	OL7000	Vv7032	OL6000	Vv6032	95% conf. interval
RM	03013302	33	0.80	0.83	0.80	0.82	0.05	0.64	0.73	0.64	0.73	0.05
	03010903	9	0.61	0.62	0.61	0.63	0.07	0.58	0.64	0.58	0.65	0.06
	03010908	9	0.71	0.72	0.71	0.69	0.07	0.49	0.61	0.49	0.59	0.07
RC	04013302	33	0.62	0.71	0.63	0.70	0.15	0.61	0.69	0.61	0.70	0.19
	04010907	9	0.64	0.71	0.64	0.69	0.13	0.60	0.70	0.60	0.71	0.14
	04010910	9	0.70	0.74	0.70	0.72	0.12	0.53	0.68	0.53	0.68	0.14
YC	07013301	33	0.86	0.91	0.86	0.92	0.04	0.80	0.90	0.80	0.90	0.04
	07010902	9	0.85	0.90	0.85	0.90	0.05	0.74	0.86	0.74	0.84	0.05
	07010916	9	0.82	0.87	0.82	0.88	0.05	0.78	0.86	0.78	0.85	0.05
CR	09013301	33	0.70	0.66	0.70	0.62	0.07	0.67	0.66	0.66	0.66	0.07
	09010906	9	0.71	0.71	0.71	0.68	0.07	0.64	0.70	0.64	0.71	0.06
NG	12033301	33	0.66	0.68	0.67	0.68	0.14	0.47	0.51	0.48	0.51	0.15
WG	16013302	33	0.75	0.80	0.75	0.80	0.04	0.72	0.79	0.71	0.78	0.04
	16010906	9	0.67	0.72	0.67	0.72	0.05	0.64	0.70	0.64	0.70	0.05
	16010907	9	0.68	0.72	0.68	0.72	0.05	0.64	0.71	0.64	0.70	0.05
	16010913	9	0.74	0.80	0.74	0.80	0.05	0.74	0.81	0.73	0.81	0.04
LW	16023302	33	0.72	0.86	0.72	0.85	0.03	0.70	0.85	0.70	0.85	0.03
	16020905	9	0.65	0.75	0.65	0.75	0.05	0.60	0.72	0.60	0.72	0.05
	16020906	9	0.68	0.80	0.67	0.79	0.04	0.65	0.81	0.65	0.80	0.04
	16020907	9	0.68	0.81	0.68	0.80	0.06	0.68	0.79	0.68	0.78	0.05
FC	16033302	33	0.70	0.84	0.70	0.84	0.04	0.67	0.84	0.67	0.84	0.03
	16030911	9	0.67	0.83	0.67	0.81	0.04	0.63	0.84	0.63	0.83	0.04
	16030916	9	0.70	0.83	0.70	0.82	0.03	0.69	0.82	0.69	0.82	0.03
LR	16043302	33	0.70	0.74	0.70	0.74	0.05	0.67	0.71	0.67	0.72	0.05
	16040901	9	0.78	0.80	0.79	0.81	0.05	0.77	0.79	0.77	0.79	0.04
SJ	16063302	33	0.66	0.75	0.64	0.71	0.11	0.51	0.74	0.47	0.67	0.10
	16060907	9	0.66	0.76	0.66	0.72	0.15	0.46	0.67	0.45	0.66	0.12
SF	16073302	33	0.63	0.77	0.63	0.74	0.07	0.67	0.80	0.67	0.80	0.05
	16070909	9	0.58	0.74	0.58	0.69	0.07	0.65	0.80	0.65	0.79	0.05
	16070910	9	0.54	0.72	0.54	0.67	0.08	0.59	0.76	0.59	0.75	0.06
	16070911	9	0.51	0.68	0.51	0.64	0.08	0.52	0.70	0.53	0.70	0.06
MB	19023301	33	0.57	0.77	0.57	0.75	0.06	0.59	0.78	0.60	0.75	0.05
	19020902	9	0.58	0.81	0.58	0.78	0.08	0.62	0.81	0.63	0.79	0.08
TZ	25013301	33	0.93	0.95	0.93	0.94	0.04	0.69	0.76	0.69	0.72	0.07
	25010911	9	0.92	0.94	0.92	0.92	0.04	0.67	0.75	0.67	0.69	0.07
KN	27013301	33	0.57	0.71	0.57	0.71	0.10	0.67	0.74	0.67	0.76	0.08
	27010910	9	0.61	0.76	0.61	0.75	0.09	0.67	0.77	0.67	0.76	0.08
	27010911	9	0.64	0.77	0.64	0.77	0.08	0.67	0.75	0.67	0.75	0.08
VA	41010906	9	0.56	0.69	0.56	0.67	0.15	0.65	0.74	0.65	0.73	0.16
NI	45013301	33	0.59	0.71	0.61	0.73	0.13	n/a	n/a	n/a	n/a	n/a
	45010902	9	0.55	0.67	0.58	0.70	0.12	0.57	0.65	0.56	0.65	0.11
BN	45023301	33	0.71	0.74	0.71	0.74	0.09	0.57	0.69	0.57	0.69	0.07
	45020902	9	0.77	0.80	0.77	0.80	0.07	0.54	0.66	0.54	0.66	0.06
TX	48013301	33	0.83	0.90	0.83	0.91	0.03	0.78	0.87	0.78	0.88	0.04
	48010902	9	0.74	0.82	0.74	0.83	0.05	0.67	0.77	0.67	0.78	0.05
	48010911	9	0.78	0.86	0.78	0.87	0.04	0.72	0.82	0.72	0.83	0.05
HB	67013301	33	0.78	0.83	0.78	0.82	0.05	0.67	0.77	0.67	0.76	0.06
	67010901	9	0.80	0.84	0.80	0.82	0.11	0.39	0.62	0.39	0.59	0.18
All	Average	33	0.71	0.79	0.71	0.78	0.02	0.65	0.76	0.65	0.75	0.02
	Average	9	0.69	0.78	0.69	0.76	0.02	0.62	0.73	0.61	0.73	0.02

Table A3. As in Table A1, but for root zone soil moisture.

	Reference pixel		Root zone soil moisture								
			ubRMSD (m3 m-3)					MD (m3 m-3)			
Site name	ID	Horiz. scale (km)	OL7000	Vv7032	OL6000	Vv6032	95% conf. interval	OL7000	Vv7032	OL6000	Vv6032
RM	03013302	33	n/a	n/a	n/a	n/a	n/a	n/a	n/a	n/a	n/a
	03010903	9	n/a	n/a	n/a	n/a	n/a	n/a	n/a	n/a	n/a
	03010908	9	n/a	n/a	n/a	n/a	n/a	n/a	n/a	n/a	n/a
RC	04013302	33	n/a	n/a	n/a	n/a	n/a	n/a	n/a	n/a	n/a
	04010907	9	n/a	n/a	n/a	n/a	n/a	n/a	n/a	n/a	n/a
	04010910	9	n/a	n/a	n/a	n/a	n/a	n/a	n/a	n/a	n/a
YC	07013301	33	0.012	0.017	0.012	0.011	0.008	-0.110	-0.090	-0.110	-0.098
	07010902	9	n/a	n/a	n/a	n/a	n/a	n/a	n/a	n/a	n/a
	07010916	9	n/a	n/a	n/a	n/a	n/a	n/a	n/a	n/a	n/a
CR	09013301	33	n/a	n/a	n/a	n/a	n/a	n/a	n/a	n/a	n/a
	09010906	9	n/a	n/a	n/a	n/a	n/a	n/a	n/a	n/a	n/a
NG	12033301	33	n/a	n/a	n/a	n/a	n/a	n/a	n/a	n/a	n/a
WG	16013302	33	n/a	n/a	n/a	n/a	n/a	n/a	n/a	n/a	n/a
	16010906	9	n/a	n/a	n/a	n/a	n/a	n/a	n/a	n/a	n/a
	16010907	9	n/a	n/a	n/a	n/a	n/a	n/a	n/a	n/a	n/a
	16010913	9	n/a	n/a	n/a	n/a	n/a	n/a	n/a	n/a	n/a
LW	16023302	33	0.030	0.025	0.030	0.027	0.004	-0.033	-0.029	-0.033	-0.033
	16020905	9	n/a	n/a	n/a	n/a	n/a	n/a	n/a	n/a	n/a
	16020906	9	0.030	0.026	0.030	0.027	0.005	-0.008	-0.004	-0.008	-0.008
	16020907	9	0.035	0.030	0.035	0.032	0.008	-0.029	-0.027	-0.029	-0.031
FC	16033302	33	0.028	0.022	0.028	0.022	0.003	0.036	0.051	0.036	0.049
	16030911	9	0.033	0.027	0.033	0.028	0.005	-0.003	0.013	-0.003	0.011
	16030916	9	0.025	0.022	0.025	0.023	0.003	-0.004	0.007	-0.004	0.005
LR	16043302	33	0.029	0.029	0.029	0.029	0.003	0.067	0.068	0.066	0.067
	16040901	9	0.027	0.028	0.027	0.028	0.003	0.096	0.102	0.095	0.100
SJ	16063302	33	n/a	n/a	n/a	n/a	n/a	n/a	n/a	n/a	n/a
	16060907	9	n/a	n/a	n/a	n/a	n/a	n/a	n/a	n/a	n/a
SF	16073302	33	0.034	0.031	0.034	0.034	0.006	0.009	0.012	0.009	0.009
	16070909	9	0.037	0.034	0.037	0.037	0.006	-0.045	-0.040	-0.046	-0.044
	16070910	9	0.038	0.034	0.038	0.037	0.005	0.031	0.035	0.031	0.031
	16070911	9	0.036	0.034	0.036	0.036	0.005	0.022	0.025	0.022	0.021
MB	19023301	33	n/a	n/a	n/a	n/a	n/a	n/a	n/a	n/a	n/a
	19020902	9	n/a	n/a	n/a	n/a	n/a	n/a	n/a	n/a	n/a
TZ	25013301	33	0.023	0.021	0.023	0.025	0.013	0.044	0.046	0.044	0.041
	25010911	9	0.027	0.025	0.027	0.028	0.013	0.048	0.051	0.048	0.045
KN	27013301	33	0.026	0.023	0.026	0.022	0.011	-0.040	-0.024	-0.041	-0.035
	27010910	9	n/a	n/a	n/a	n/a	n/a	n/a	n/a	n/a	n/a
	27010911	9	0.028	0.023	0.028	0.023	0.008	-0.063	-0.043	-0.064	-0.055
VA	41010906	9	n/a	n/a	n/a	n/a	n/a	n/a	n/a	n/a	n/a
NI	45013301	33	n/a	n/a	n/a	n/a	n/a	n/a	n/a	n/a	n/a
	45010902	9	n/a	n/a	n/a	n/a	n/a	n/a	n/a	n/a	n/a
BN	45023301	33	n/a	n/a	n/a	n/a	n/a	n/a	n/a	n/a	n/a
	45020902	9	n/a	n/a	n/a	n/a	n/a	n/a	n/a	n/a	n/a
TX	48013301	33	0.023	0.020	0.023	0.020	0.005	0.046	0.052	0.046	0.048
	48010902	9	0.026	0.025	0.026	0.022	0.005	0.112	0.117	0.112	0.113
	48010911	9	0.021	0.018	0.021	0.018	0.004	0.106	0.111	0.106	0.107
HB	67013301	33	n/a	n/a	n/a	n/a	n/a	n/a	n/a	n/a	n/a
	67010901	9	n/a	n/a	n/a	n/a	n/a	n/a	n/a	n/a	n/a
All	Average	33	0.026	0.023	0.026	0.024	0.002	0.002	0.011	0.002	0.006
	Average	9	0.029	0.026	0.029	0.027	0.002	0.024	0.032	0.024	0.027
	Avg. Abs.	33	n/a	n/a	n/a	n/a	n/a	0.048	0.047	0.048	0.047
	Avg. Abs.	9	Same as average.					0.053	0.053	0.053	0.053

Table A4. As in Table A1, but for root zone soil moisture R and anomaly R.

			Root zone soil moisture									
	Reference pixel		R (dimensionless)					anomaly R (dimensionless)				
Site name	ID	Horiz. scale (km)	OL7000	Vv7032	OL6000	Vv6032	95% conf. interval	OL7000	Vv7032	OL6000	Vv6032	95% conf. interval
RM	03013302	33	n/a	n/a	n/a	n/a	n/a	n/a	n/a	n/a	n/a	n/a
	03010903	9	n/a	n/a	n/a	n/a	n/a	n/a	n/a	n/a	n/a	n/a
	03010908	9	n/a	n/a	n/a	n/a	n/a	n/a	n/a	n/a	n/a	n/a
RC	04013302	33	n/a	n/a	n/a	n/a	n/a	n/a	n/a	n/a	n/a	n/a
	04010907	9	n/a	n/a	n/a	n/a	n/a	n/a	n/a	n/a	n/a	n/a
	04010910	9	n/a	n/a	n/a	n/a	n/a	n/a	n/a	n/a	n/a	n/a
YC	07013301	33	0.87	0.90	0.87	0.93	0.26	n/a	n/a	n/a	n/a	n/a
	07010902	9	n/a	n/a	n/a	n/a	n/a	n/a	n/a	n/a	n/a	n/a
	07010916	9	n/a	n/a	n/a	n/a	n/a	n/a	n/a	n/a	n/a	n/a
CR	09013301	33	n/a	n/a	n/a	n/a	n/a	n/a	n/a	n/a	n/a	n/a
	09010906	9	n/a	n/a	n/a	n/a	n/a	n/a	n/a	n/a	n/a	n/a
NG	12033301	33	n/a	n/a	n/a	n/a	n/a	n/a	n/a	n/a	n/a	n/a
WG	16013302	33	n/a	n/a	n/a	n/a	n/a	n/a	n/a	n/a	n/a	n/a
	16010906	9	n/a	n/a	n/a	n/a	n/a	n/a	n/a	n/a	n/a	n/a
	16010907	9	n/a	n/a	n/a	n/a	n/a	n/a	n/a	n/a	n/a	n/a
	16010913	9	n/a	n/a	n/a	n/a	n/a	n/a	n/a	n/a	n/a	n/a
LW	16023302	33	0.72	0.83	0.72	0.80	0.10	0.68	0.83	0.68	0.82	0.09
	16020905	9	n/a	n/a	n/a	n/a	n/a	n/a	n/a	n/a	n/a	n/a
	16020906	9	0.62	0.75	0.62	0.73	0.13	0.59	0.76	0.59	0.74	0.13
	16020907	9	0.68	0.79	0.68	0.75	0.16	n/a	n/a	n/a	n/a	n/a
FC	16033302	33	0.73	0.84	0.72	0.83	0.09	0.67	0.83	0.67	0.82	0.08
	16030911	9	0.73	0.84	0.73	0.83	0.09	0.65	0.83	0.65	0.82	0.09
	16030916	9	0.72	0.80	0.72	0.79	0.09	0.64	0.76	0.64	0.76	0.09
LR	16043302	33	0.66	0.67	0.66	0.66	0.11	0.61	0.62	0.60	0.63	0.11
	16040901	9	0.60	0.60	0.61	0.60	0.15	0.66	0.64	0.66	0.66	0.13
SJ	16063302	33	n/a	n/a	n/a	n/a	n/a	n/a	n/a	n/a	n/a	n/a
	16060907	9	n/a	n/a	n/a	n/a	n/a	n/a	n/a	n/a	n/a	n/a
SF	16073302	33	0.63	0.70	0.62	0.63	0.18	0.74	0.83	0.74	0.86	0.10
	16070909	9	0.58	0.67	0.58	0.60	0.18	0.72	0.82	0.73	0.86	0.10
	16070910	9	0.44	0.57	0.44	0.46	0.20	0.60	0.77	0.60	0.81	0.12
	16070911	9	0.44	0.54	0.44	0.46	0.19	0.55	0.70	0.55	0.74	0.13
MB	19023301	33	n/a	n/a	n/a	n/a	n/a	n/a	n/a	n/a	n/a	n/a
	19020902	9	n/a	n/a	n/a	n/a	n/a	n/a	n/a	n/a	n/a	n/a
TZ	25013301	33	0.94	0.95	0.94	0.93	0.10	0.82	0.84	0.82	0.78	0.17
	25010911	9	0.94	0.95	0.94	0.92	0.11	0.83	0.86	0.83	0.79	0.14
KN	27013301	33	0.84	0.81	0.84	0.85	0.23	0.89	0.85	0.89	0.91	0.15
	27010910	9	n/a	n/a	n/a	n/a	n/a	n/a	n/a	n/a	n/a	n/a
	27010911	9	0.89	0.85	0.89	0.89	0.13	0.90	0.86	0.90	0.91	0.10
VA	41010906	9	n/a	n/a	n/a	n/a	n/a	n/a	n/a	n/a	n/a	n/a
NI	45013301	33	n/a	n/a	n/a	n/a	n/a	n/a	n/a	n/a	n/a	n/a
	45010902	9	n/a	n/a	n/a	n/a	n/a	n/a	n/a	n/a	n/a	n/a
BN	45023301	33	n/a	n/a	n/a	n/a	n/a	n/a	n/a	n/a	n/a	n/a
	45020902	9	n/a	n/a	n/a	n/a	n/a	n/a	n/a	n/a	n/a	n/a
TX	48013301	33	0.91	0.93	0.91	0.94	0.07	0.89	0.91	0.89	0.93	0.07
	48010902	9	0.79	0.83	0.79	0.85	0.12	0.72	0.77	0.72	0.80	0.12
	48010911	9	0.89	0.92	0.89	0.92	0.07	0.88	0.92	0.88	0.92	0.06
HB	67013301	33	n/a	n/a	n/a	n/a	n/a	n/a	n/a	n/a	n/a	n/a
	67010901	9	n/a	n/a	n/a	n/a	n/a	n/a	n/a	n/a	n/a	n/a
All	Average	33	0.79	0.83	0.79	0.82	0.05	0.76	0.82	0.75	0.82	0.04
	Average	9	0.73	0.78	0.73	0.76	0.05	0.72	0.79	0.72	0.79	0.04

Table A5. As in Table A1, but for surface soil temperature at 6am local time.

			Surface Soil Temperature (6am)								
	Reference pixel		ubRMSD (K)					MD (K)			
Site name	ID	Horiz. scale (km)	OL7000	Vv7032	OL6000	Vv6032	95% conf. interval	OL7000	Vv7032	OL6000	Vv6032
RM	03013302	33	1.8	1.8	1.8	1.8	0.5	-3.5	-3.6	-3.5	-3.6
	03010903	9	1.9	1.9	1.9	1.9	0.5	-4.1	-4.1	-4.1	-4.1
	03010908	9	1.5	1.5	1.5	1.5	0.4	-3.1	-3.2	-3.1	-3.1
RC	04013302	33	2.4	2.3	2.4	2.3	0.7	0.9	0.9	0.9	0.9
	04010907	9	1.5	1.5	1.5	1.5	0.6	0.9	0.9	0.9	0.9
	04010910	9	2.0	2.0	2.0	2.0	0.8	-0.5	-0.5	-0.5	-0.5
YC	07013301	33	2.4	2.3	2.4	2.4	0.5	-3.8	-3.8	-3.8	-3.8
	07010902	9	1.9	1.8	1.9	1.8	0.4	-2.5	-2.6	-2.5	-2.6
	07010916	9	2.3	2.3	2.3	2.3	0.5	-3.2	-3.2	-3.2	-3.2
CR	09013301	33	1.2	1.2	1.2	1.2	0.3	-0.8	-0.9	-0.8	-0.8
	09010906	9	1.2	1.2	1.2	1.2	0.3	-0.9	-0.9	-0.9	-0.9
NG	12033301	33	2.1	2.1	2.1	2.1	0.7	-4.8	-4.8	-4.8	-4.8
WG	16013302	33	1.5	1.5	1.5	1.5	0.4	-2.1	-2.2	-2.1	-2.2
	16010906	9	1.9	1.9	1.9	1.9	0.4	-1.5	-1.7	-1.5	-1.7
	16010907	9	1.5	1.5	1.5	1.5	0.3	-3.1	-3.2	-3.1	-3.2
	16010913	9	2.0	1.9	2.0	1.9	0.5	-2.2	-2.2	-2.2	-2.2
LW	16023302	33	1.8	1.8	1.8	1.8	0.5	-1.7	-1.8	-1.7	-1.8
	16020905	9	2.0	2.0	2.0	2.0	0.6	-1.8	-1.8	-1.8	-1.8
	16020906	9	1.9	1.9	1.9	1.9	0.5	-1.7	-1.8	-1.7	-1.7
	16020907	9	1.7	1.7	1.7	1.7	0.7	-1.6	-1.7	-1.6	-1.6
FC	16033302	33	1.7	1.7	1.7	1.7	0.5	-1.8	-1.9	-1.8	-1.8
	16030911	9	1.5	1.5	1.5	1.5	0.6	-1.6	-1.6	-1.6	-1.6
	16030916	9	1.4	1.4	1.4	1.4	1.4	-1.3	-1.3	-1.3	-1.3
LR	16043302	33	1.8	1.8	1.8	1.8	0.4	-2.3	-2.3	-2.3	-2.3
	16040901	9	1.5	1.5	1.5	1.5	0.4	-2.2	-2.2	-2.2	-2.2
SJ	16063302	33	1.6	1.6	1.7	1.7	0.6	-1.3	-1.3	-1.3	-1.3
	16060907	9	1.7	1.6	1.7	1.6	0.9	-1.5	-1.5	-1.5	-1.5
SF	16073302	33	1.6	1.6	1.6	1.6	0.5	-1.7	-1.7	-1.7	-1.7
	16070909	9	1.5	1.5	1.5	1.5	0.5	-1.4	-1.4	-1.4	-1.4
	16070910	9	1.5	1.6	1.5	1.6	0.5	-1.8	-1.8	-1.8	-1.8
	16070911	9	1.5	1.5	1.5	1.5	0.4	-1.9	-1.9	-1.9	-1.9
MB	19023301	33	1.5	1.6	1.5	1.6	0.3	-1.6	-1.8	-1.6	-1.7
	19020902	9	n/a	n/a	n/a	n/a	n/a	n/a	n/a	n/a	n/a
TZ	25013301	33	n/a	n/a	n/a	n/a	n/a	n/a	n/a	n/a	n/a
	25010911	9	n/a	n/a	n/a	n/a	n/a	n/a	n/a	n/a	n/a
KN	27013301	33	1.5	1.5	1.5	1.5	0.5	-0.6	-0.7	-0.6	-0.6
	27010910	9	1.2	1.1	1.2	1.2	0.4	-0.9	-1.1	-0.9	-1.0
	27010911	9	1.5	1.4	1.5	1.5	0.5	-0.9	-1.1	-0.9	-1.0
VA	41010906	9	n/a	n/a	n/a	n/a	n/a	n/a	n/a	n/a	n/a
NI	45013301	33	n/a	n/a	n/a	n/a	n/a	n/a	n/a	n/a	n/a
	45010902	9	n/a	n/a	n/a	n/a	n/a	n/a	n/a	n/a	n/a
BN	45023301	33	n/a	n/a	n/a	n/a	n/a	n/a	n/a	n/a	n/a
	45020902	9	n/a	n/a	n/a	n/a	n/a	n/a	n/a	n/a	n/a
TX	48013301	33	1.3	1.3	1.3	1.3	0.2	-2.0	-2.0	-2.0	-2.0
	48010902	9	1.4	1.4	1.4	1.4	0.3	-2.5	-2.5	-2.5	-2.5
	48010911	9	1.6	1.5	1.6	1.5	0.3	-2.1	-2.1	-2.1	-2.1
HB	67013301	33	1.1	1.1	1.1	1.1	0.3	-0.6	-0.6	-0.6	-0.6
	67010901	9	1.0	1.0	1.0	1.0	0.5	-0.5	-0.5	-0.5	-0.5
All	Average	33	1.7	1.7	1.7	1.7	0.1	-1.8	-1.9	-1.8	-1.9
	Average	9	1.6	1.6	1.6	1.6	0.1	-1.7	-1.7	-1.7	-1.7
	Average Abs	33	n/a	n/a	n/a	n/a	n/a	2.0	2.0	2.0	2.0
	Average Abs	9	n/a	n/a	n/a	n/a	n/a	1.7	1.8	1.7	1.8

Table A6. As in Table A1, but for 6am surface soil temperature R and anomaly R.

Site name	Reference pixel		Surface Soil Temperature (6am)									
			R (dimensionless)					anomaly R (dimensionless)				
	ID	Horiz. scale (km)	OL7000	Vv7032	OL6000	Vv6032	95% conf. interval	OL7000	Vv7032	OL6000	Vv6032	95% conf. interval
RM	03013302	33	0.98	0.98	0.98	0.98	0.01	0.89	0.90	0.89	0.90	0.02
	03010903	9	0.98	0.98	0.98	0.98	0.01	0.87	0.88	0.87	0.88	0.02
	03010908	9	0.98	0.98	0.98	0.98	0.01	0.89	0.90	0.89	0.90	0.02
RC	04013302	33	0.96	0.96	0.96	0.96	0.03	n/a	n/a	n/a	n/a	n/a
	04010907	9	0.98	0.98	0.98	0.98	0.01	n/a	n/a	n/a	n/a	n/a
	04010910	9	0.97	0.97	0.97	0.97	0.03	n/a	n/a	n/a	n/a	n/a
YC	07013301	33	0.95	0.96	0.95	0.95	0.02	0.74	0.76	0.74	0.75	0.04
	07010902	9	0.97	0.97	0.97	0.97	0.01	0.85	0.86	0.85	0.86	0.02
	07010916	9	0.97	0.98	0.97	0.98	0.01	0.85	0.87	0.85	0.86	0.02
CR	09013301	33	0.98	0.98	0.98	0.98	0.01	0.94	0.94	0.94	0.94	0.01
	09010906	9	0.98	0.98	0.98	0.98	0.01	0.94	0.94	0.94	0.94	0.01
NG	12033301	33	0.91	0.91	0.91	0.91	0.11	n/a	n/a	n/a	n/a	n/a
WG	16013302	33	0.98	0.98	0.98	0.98	0.01	0.89	0.90	0.89	0.90	0.02
	16010906	9	0.97	0.97	0.97	0.97	0.02	0.84	0.85	0.84	0.85	0.02
	16010907	9	0.98	0.98	0.98	0.98	0.01	0.89	0.89	0.89	0.90	0.02
	16010913	9	0.98	0.98	0.98	0.98	0.01	n/a	n/a	n/a	n/a	n/a
LW	16023302	33	0.98	0.98	0.98	0.98	0.01	0.91	0.92	0.91	0.92	0.01
	16020905	9	0.98	0.98	0.98	0.98	0.01	0.91	0.91	0.91	0.91	0.01
	16020906	9	0.98	0.98	0.98	0.98	0.01	0.91	0.91	0.91	0.91	0.01
	16020907	9	0.98	0.99	0.98	0.99	0.01	n/a	n/a	n/a	n/a	n/a
FC	16033302	33	0.99	0.99	0.99	0.99	0.01	0.91	0.92	0.91	0.92	0.01
	16030911	9	0.99	0.99	0.99	0.99	0.01	n/a	n/a	n/a	n/a	n/a
	16030916	9	0.98	0.98	0.98	0.98	0.05	n/a	n/a	n/a	n/a	n/a
LR	16043302	33	0.97	0.97	0.97	0.97	0.01	0.90	0.90	0.90	0.90	0.02
	16040901	9	0.98	0.98	0.98	0.98	0.01	0.94	0.94	0.94	0.94	0.02
SJ	16063302	33	0.98	0.98	0.97	0.97	0.02	0.91	0.91	0.91	0.91	0.03
	16060907	9	0.97	0.97	0.97	0.97	0.03	n/a	n/a	n/a	n/a	n/a
SF	16073302	33	0.98	0.98	0.98	0.98	0.01	0.92	0.92	0.92	0.92	0.01
	16070909	9	0.98	0.98	0.98	0.98	0.01	0.93	0.93	0.93	0.93	0.02
	16070910	9	0.98	0.98	0.98	0.98	0.01	0.92	0.92	0.92	0.92	0.02
	16070911	9	0.98	0.98	0.98	0.98	0.01	0.92	0.92	0.92	0.92	0.02
MB	19023301	33	0.96	0.96	0.96	0.96	0.02	0.89	0.88	0.89	0.88	0.02
	19020902	9	n/a	n/a	n/a	n/a	n/a	n/a	n/a	n/a	n/a	n/a
TZ	25013301	33	n/a	n/a	n/a	n/a	n/a	n/a	n/a	n/a	n/a	n/a
	25010911	9	n/a	n/a	n/a	n/a	n/a	n/a	n/a	n/a	n/a	n/a
KN	27013301	33	0.97	0.97	0.97	0.97	0.02	0.89	0.89	0.89	0.89	0.03
	27010910	9	0.98	0.98	0.98	0.98	0.01	0.93	0.93	0.93	0.93	0.02
	27010911	9	0.97	0.97	0.97	0.97	0.02	0.89	0.89	0.89	0.89	0.03
VA	41010906	9	n/a	n/a	n/a	n/a	n/a	n/a	n/a	n/a	n/a	n/a
NI	45013301	33	n/a	n/a	n/a	n/a	n/a	n/a	n/a	n/a	n/a	n/a
	45010902	9	n/a	n/a	n/a	n/a	n/a	n/a	n/a	n/a	n/a	n/a
BN	45023301	33	n/a	n/a	n/a	n/a	n/a	n/a	n/a	n/a	n/a	n/a
	45020902	9	n/a	n/a	n/a	n/a	n/a	n/a	n/a	n/a	n/a	n/a
TX	48013301	33	0.98	0.99	0.98	0.99	0.01	0.93	0.93	0.93	0.93	0.01
	48010902	9	0.98	0.98	0.98	0.98	0.01	0.90	0.91	0.90	0.91	0.01
	48010911	9	0.98	0.98	0.98	0.98	0.01	0.90	0.90	0.90	0.90	0.01
HB	67013301	33	0.98	0.98	0.98	0.98	0.01	n/a	n/a	n/a	n/a	n/a
	67010901	9	0.98	0.98	0.98	0.98	0.03	n/a	n/a	n/a	n/a	n/a
All	Average	33	0.97	0.97	0.97	0.97	0.01	0.89	0.90	0.89	0.90	0.01
	Average	9	0.98	0.98	0.98	0.98	0.00	0.90	0.91	0.90	0.91	0.01

Table A7. As in Table A1, but for surface soil temperature at 6pm local time.

	Reference pixel		Surface Soil Temperature (6pm)								
			ubRMSD (K)					MD (K)			
Site name	ID	Horiz. scale (km)	OL7000	Vv7032	OL6000	Vv6032	95% conf. interval	OL7000	Vv7032	OL6000	Vv6032
RM	03013302	33	1.7	1.7	1.7	1.7	0.5	-1.5	-1.6	-1.5	-1.6
	03010903	9	2.1	2.1	2.1	2.1	0.6	-2.6	-2.7	-2.6	-2.7
	03010908	9	1.5	1.6	1.5	1.6	0.5	-1.0	-1.1	-1.0	-1.1
RC	04013302	33	2.2	2.2	2.2	2.2	0.7	1.5	1.4	1.5	1.4
	04010907	9	1.5	1.5	1.5	1.5	0.6	0.9	0.9	0.9	0.9
	04010910	9	2.0	1.9	2.0	2.0	0.8	0.3	0.3	0.3	0.3
YC	07013301	33	2.1	2.2	2.1	2.1	0.4	-0.6	-0.7	-0.6	-0.7
	07010902	9	1.5	1.5	1.5	1.5	0.3	0.3	0.2	0.3	0.2
	07010916	9	1.6	1.6	1.6	1.6	0.3	-0.1	-0.1	-0.1	-0.1
CR	09013301	33	1.7	1.7	1.7	1.7	0.4	-0.5	-0.7	-0.5	-0.7
	09010906	9	1.7	1.7	1.7	1.7	0.3	-0.6	-0.8	-0.6	-0.7
NG	12033301	33	4.1	4.1	4.1	4.1	1.0	-8.9	-8.9	-8.9	-8.9
WG	16013302	33	2.0	1.9	2.0	1.9	0.4	-0.7	-0.8	-0.7	-0.9
	16010906	9	2.4	2.4	2.4	2.4	0.5	-0.4	-0.6	-0.4	-0.7
	16010907	9	1.9	1.9	1.9	1.9	0.4	-1.3	-1.5	-1.3	-1.6
	16010913	9	2.7	2.5	2.7	2.6	0.6	-1.5	-1.6	-1.5	-1.6
LW	16023302	33	1.9	1.9	1.9	1.9	0.6	-0.3	-0.4	-0.3	-0.3
	16020905	9	2.1	2.1	2.1	2.1	0.7	-0.2	-0.3	-0.2	-0.2
	16020906	9	2.0	2.0	2.0	2.0	0.6	-0.2	-0.3	-0.2	-0.2
	16020907	9	1.8	1.7	1.8	1.7	0.8	-0.5	-0.5	-0.5	-0.4
FC	16033302	33	1.8	1.8	1.8	1.8	0.6	-0.1	-0.2	-0.1	-0.2
	16030911	9	1.6	1.6	1.6	1.6	0.7	-0.1	-0.3	-0.1	-0.2
	16030916	9	1.4	1.4	1.4	1.4	1.4	-0.1	-0.2	-0.1	-0.2
LR	16043302	33	1.8	1.7	1.8	1.7	0.4	-1.5	-1.5	-1.5	-1.5
	16040901	9	1.6	1.6	1.6	1.6	0.5	-1.4	-1.5	-1.4	-1.5
SJ	16063302	33	1.7	1.7	1.8	1.8	0.7	-0.5	-0.5	-0.4	-0.4
	16060907	9	1.7	1.7	1.7	1.6	1.0	-0.7	-0.6	-0.7	-0.6
SF	16073302	33	1.7	1.8	1.7	1.7	0.6	-0.5	-0.5	-0.5	-0.5
	16070909	9	1.7	1.7	1.7	1.6	0.5	-0.6	-0.6	-0.6	-0.6
	16070910	9	1.8	1.8	1.8	1.8	0.6	-1.0	-1.0	-1.0	-1.0
	16070911	9	1.7	1.8	1.7	1.7	0.5	-1.1	-1.1	-1.1	-1.1
MB	19023301	33	2.1	2.4	2.1	2.3	0.5	0.6	0.3	0.6	0.5
	19020902	9	1.6	1.8	1.6	1.7	0.5	-0.7	-0.8	-0.7	-0.6
TZ	25013301	33	n/a	n/a	n/a	n/a	n/a	n/a	n/a	n/a	n/a
	25010911	9	n/a	n/a	n/a	n/a	n/a	n/a	n/a	n/a	n/a
KN	27013301	33	2.1	2.1	2.1	2.1	0.7	1.2	1.0	1.2	1.1
	27010910	9	1.8	1.7	1.8	1.8	0.5	0.4	0.1	0.4	0.3
	27010911	9	2.1	2.0	2.1	2.1	0.6	0.5	0.2	0.5	0.3
VA	41010906	9	n/a	n/a	n/a	n/a	n/a	n/a	n/a	n/a	n/a
NI	45013301	33	n/a	n/a	n/a	n/a	n/a	n/a	n/a	n/a	n/a
	45010902	9	n/a	n/a	n/a	n/a	n/a	n/a	n/a	n/a	n/a
BN	45023301	33	n/a	n/a	n/a	n/a	n/a	n/a	n/a	n/a	n/a
	45020902	9	n/a	n/a	n/a	n/a	n/a	n/a	n/a	n/a	n/a
TX	48013301	33	1.7	1.6	1.7	1.6	0.3	-1.7	-1.8	-1.7	-1.7
	48010902	9	1.8	1.8	1.8	1.8	0.4	-1.8	-1.8	-1.8	-1.8
	48010911	9	2.0	1.9	2.0	1.9	0.4	-2.0	-2.1	-2.0	-2.0
HB	67013301	33	1.1	1.1	1.1	1.1	0.4	-1.5	-1.5	-1.5	-1.5
	67010901	9	1.4	1.4	1.4	1.4	0.7	-1.7	-1.7	-1.7	-1.7
All	Average	33	2.0	2.0	2.0	2.0	0.1	-1.0	-1.1	-1.0	-1.1
	Average	9	1.7	1.7	1.7	1.7	0.2	-0.7	-0.8	-0.7	-0.8
	Average Abs	33	n/a	n/a	n/a	n/a	n/a	1.4	1.5	1.4	1.5
	Average Abs	9	n/a	n/a	n/a	n/a	n/a	0.9	0.9	0.9	0.9

Table A8. As in Table A1, but for 6pm surface soil temperature R and anomaly R.

			Surface Soil Temperature (6pm)									
	Reference pixel		R (dimensionless)					anomaly R (dimensionless)				
Site name	ID	Horiz. scale (km)	OL7000	Vv7032	OL6000	Vv6032	95% conf. interval	OL7000	Vv7032	OL6000	Vv6032	95% conf. interval
RM	03013302	33	0.99	0.99	0.99	0.99	0.01	0.91	0.92	0.91	0.92	0.02
	03010903	9	0.99	0.99	0.99	0.99	0.01	0.90	0.92	0.90	0.92	0.02
	03010908	9	0.98	0.98	0.98	0.98	0.01	0.87	0.88	0.87	0.88	0.02
RC	04013302	33	0.96	0.96	0.96	0.96	0.03	n/a	n/a	n/a	n/a	n/a
	04010907	9	0.98	0.98	0.98	0.98	0.01	n/a	n/a	n/a	n/a	n/a
	04010910	9	0.97	0.97	0.97	0.97	0.02	n/a	n/a	n/a	n/a	n/a
YC	07013301	33	0.96	0.96	0.96	0.96	0.02	0.78	0.79	0.78	0.79	0.03
	07010902	9	0.98	0.98	0.98	0.98	0.01	0.90	0.90	0.90	0.90	0.02
	07010916	9	0.98	0.98	0.98	0.98	0.01	0.89	0.90	0.89	0.91	0.02
CR	09013301	33	0.97	0.97	0.97	0.97	0.01	0.92	0.93	0.92	0.93	0.02
	09010906	9	0.98	0.98	0.98	0.97	0.01	0.92	0.93	0.92	0.93	0.01
NG	12033301	33	0.83	0.83	0.83	0.83	0.14	n/a	n/a	n/a	n/a	n/a
WG	16013302	33	0.98	0.98	0.98	0.98	0.01	0.88	0.90	0.88	0.90	0.02
	16010906	9	0.97	0.97	0.97	0.97	0.01	0.85	0.86	0.85	0.87	0.02
	16010907	9	0.98	0.98	0.98	0.98	0.01	0.87	0.89	0.87	0.89	0.02
	16010913	9	0.98	0.98	0.98	0.98	0.01	n/a	n/a	n/a	n/a	n/a
LW	16023302	33	0.98	0.98	0.98	0.98	0.01	0.90	0.91	0.90	0.91	0.02
	16020905	9	0.98	0.98	0.98	0.98	0.01	0.88	0.89	0.88	0.89	0.02
	16020906	9	0.98	0.98	0.98	0.98	0.01	0.89	0.89	0.89	0.89	0.02
	16020907	9	0.98	0.98	0.98	0.98	0.02	n/a	n/a	n/a	n/a	n/a
FC	16033302	33	0.98	0.98	0.98	0.98	0.01	0.90	0.91	0.90	0.91	0.02
	16030911	9	0.98	0.98	0.98	0.98	0.01	n/a	n/a	n/a	n/a	n/a
	16030916	9	0.98	0.98	0.98	0.98	0.05	n/a	n/a	n/a	n/a	n/a
LR	16043302	33	0.97	0.97	0.97	0.97	0.02	0.88	0.88	0.88	0.89	0.02
	16040901	9	0.97	0.97	0.97	0.97	0.02	0.90	0.91	0.90	0.91	0.03
SJ	16063302	33	0.98	0.98	0.98	0.98	0.02	0.92	0.92	0.91	0.91	0.03
	16060907	9	0.98	0.98	0.98	0.98	0.03	n/a	n/a	n/a	n/a	n/a
SF	16073302	33	0.98	0.98	0.98	0.98	0.01	0.92	0.92	0.92	0.92	0.02
	16070909	9	0.98	0.98	0.98	0.98	0.01	0.93	0.92	0.93	0.93	0.02
	16070910	9	0.98	0.97	0.98	0.98	0.02	0.91	0.91	0.91	0.91	0.02
	16070911	9	0.98	0.98	0.98	0.98	0.01	0.91	0.91	0.91	0.91	0.02
MB	19023301	33	0.93	0.92	0.93	0.93	0.03	0.72	0.68	0.72	0.70	0.05
	19020902	9	0.97	0.96	0.97	0.96	0.03	n/a	n/a	n/a	n/a	n/a
TZ	25013301	33	n/a	n/a	n/a	n/a	n/a	n/a	n/a	n/a	n/a	n/a
	25010911	9	n/a	n/a	n/a	n/a	n/a	n/a	n/a	n/a	n/a	n/a
KN	27013301	33	0.95	0.95	0.95	0.95	0.03	0.88	0.89	0.88	0.88	0.03
	27010910	9	0.97	0.97	0.97	0.97	0.02	0.91	0.92	0.91	0.91	0.02
	27010911	9	0.95	0.96	0.95	0.95	0.03	0.88	0.89	0.88	0.88	0.03
VA	41010906	9	n/a	n/a	n/a	n/a	n/a	n/a	n/a	n/a	n/a	n/a
NI	45013301	33	n/a	n/a	n/a	n/a	n/a	n/a	n/a	n/a	n/a	n/a
	45010902	9	n/a	n/a	n/a	n/a	n/a	n/a	n/a	n/a	n/a	n/a
BN	45023301	33	n/a	n/a	n/a	n/a	n/a	n/a	n/a	n/a	n/a	n/a
	45020902	9	n/a	n/a	n/a	n/a	n/a	n/a	n/a	n/a	n/a	n/a
TX	48013301	33	0.98	0.98	0.98	0.98	0.01	0.91	0.92	0.91	0.92	0.01
	48010902	9	0.98	0.98	0.98	0.98	0.01	0.88	0.89	0.88	0.89	0.02
	48010911	9	0.97	0.97	0.97	0.98	0.01	0.87	0.89	0.87	0.89	0.02
HB	67013301	33	0.98	0.98	0.98	0.98	0.01	n/a	n/a	n/a	n/a	n/a
	67010901	9	0.98	0.98	0.98	0.98	0.03	n/a	n/a	n/a	n/a	n/a
All	Average	33	0.96	0.96	0.96	0.96	0.01	0.88	0.88	0.88	0.88	0.01
	Average	9	0.98	0.98	0.98	0.98	0.01	0.89	0.90	0.89	0.90	0.01

Table A9. Metrics for Version 7 (Vv7032) L4_SM surface (SF) and root zone (RZ) soil moisture at the 9 km scale categorized based on land cover.

L4 (9-km, 3-hourly)		ubRMSD (m3/m3)		MD (m3/m3)		RMSD (m3/m3)		R (-)		Anomaly R (-)		No. of 9-km ref. pixels		Avg. no. of 3-hr data per ref. pix.	
Land Cover	**Site Name**	**SF**	**RZ**	**SF**	**RZ**	**SF**	**RZ**	**SF**	**RZ**	**SF**	**RZ**	**SF**	**RZ**	**SF**	**RZ**
Grasslands	Reynolds Creek	0.042	n/a	-0.020	n/a	0.048	n/a	0.72	n/a	0.69	n/a	2	n/a	3,220	n/a
	TxSON	0.037	0.021	0.075	0.114	0.083	0.116	0.84	0.87	0.80	0.84	2	2	17,218	15,268
	Fort Cobb	0.036	0.025	-0.030	0.010	0.047	0.042	0.83	0.82	0.83	0.80	2	2	12,097	8,624
	Little Washita	0.038	0.028	-0.017	-0.016	0.046	0.033	0.79	0.77	0.77	0.76	3	2	9,113	3,844
	Niger	0.036	n/a	0.081	n/a	0.088	n/a	0.67	n/a	0.65	n/a	1	n/a	999	n/a
	Yanco	0.050	n/a	-0.025	n/a	0.057	n/a	0.88	n/a	0.86	n/a	2	n/a	10,155	n/a
	Average	***0.040***	***0.025***	***0.010***	***0.036***	***0.062***	***0.064***	***0.79***	***0.82***	***0.77***	***0.80***				
Croplands	South Fork	0.053	0.034	0.019	0.007	0.060	0.048	0.71	0.60	0.75	0.76	3	3	9,250	4,882
	Kenaston	0.035	0.023	-0.035	-0.043	0.050	0.048	0.77	0.85	0.76	0.86	2	1	5,149	2,890
	Carman	0.053	n/a	0.026	n/a	0.059	n/a	0.71	n/a	0.70	n/a	1	n/a	8,216	n/a
	Monte Buey	0.042	n/a	-0.046	n/a	0.063	n/a	0.81	n/a	0.81	n/a	1	n/a	3,723	n/a
	REMEDHUS	0.041	n/a	0.066	n/a	0.096	n/a	0.67	n/a	0.62	n/a	2	n/a	9,658	n/a
	HOBE	0.044	n/a	-0.013	n/a	0.046	n/a	0.84	n/a	0.62	n/a	1	n/a	1,067	n/a
	St Josephs	0.040	n/a	0.054	n/a	0.067	n/a	0.76	n/a	0.67	n/a	1	n/a	2,398	n/a
	Average	***0.044***	***0.028***	***0.010***	***-0.018***	***0.063***	***0.048***	***0.75***	***0.72***	***0.71***	***0.81***				
Crops/natural	Little River	0.033	0.028	0.085	0.102	0.091	0.106	0.80	0.60	0.79	0.64	1	1	4,244	3,437
Open shrubs	Walnut Gulch	0.032	n/a	0.047	n/a	0.061	n/a	0.75	n/a	0.74	n/a	3	n/a	12,281	n/a
Woody savannas	Tonzi Ranch	0.050	0.025	0.028	0.051	0.058	0.045	0.94	0.95	0.75	0.86	1	1	10,259	3,637
	Valencia	0.028	n/a	0.060	n/a	0.066	n/a	0.69	n/a	0.74	n/a	1	n/a	1,766	n/a
Savannas	Benin	0.045	n/a	0.119	n/a	0.128	n/a	0.80	n/a	0.66	n/a	1	n/a	6,620	n/a

REFERENCES

Apers, S., G. J. M. De Lannoy, A. J. Baird, A. R. Cobb, G. C. Dargie, J. del Aguila Pasquel, A. Gruber, A. Hastie, H. Hidayat, T. Hirano, A. M. Hoyt, A. J. Jovani-Sancho, A. Katimon, A. Kurnain, R. D. Koster, M. Lampela, S. P. P. Mahanama, L. Melling, S. E. Page, R. H. Reichle, M. Taufik, J. Vanderborght, and M. Bechtold (2022), Tropical peatland hydrology simulated with a global land surface model, *Journal of Advances in Modeling Earth Systems, 14*, e2021MS002784, doi:10.1029/2021MS002784.

Bechtold, M., G. J. M. De Lannoy, R. D. Koster, R. H. Reichle, S. P. Mahanama, et al. (2019), PEAT-CLSM: A Specific Treatment of Peatland Hydrology in the NASA Catchment Land Surface Model, *Journal of Advances in Modeling Earth Systems, 11*, 2130-2162, doi:10.1029/2018MS001574.

Bechtold, M., G. J. M. De Lannoy, R. H. Reichle, D. Roose, N. Balliston, I. Burdun, K. Devito, J. Kurbatova, M. Strack, and E. A. Zarov (2020), Improved Groundwater Table and L-band Brightness Temperature Estimates for Northern Hemisphere Peatlands Using New Model Physics and SMOS Observations in a Global Data Assimilation Framework, *Remote Sensing of Environment, 246*, 111805, doi:10.1016/j.rse.2020.111805.

Bell, J. E., Palecki, M. A., Baker, C. B., Collins, W. G., Lawrimore, J. H., Leeper, R. D., Hall, M. E., Kochendorfer, J., Meyers, T. P., Wilson, T., & Diamond, H. J. (2013), U.S. Climate Reference Network soil moisture and temperature observations, *Journal of Hydrometeorology, 14*, 977–988, doi:10.1175/jhm-d-12-0146.1.

Bircher, S., N. Skou, K. H. Jensen, J. P. Walker, and L. Rasmussen (2012), A soil moisture and temperature network for SMOS validation in Western Denmark, *Hydrology and Earth System Sciences, 16*, 1445–1463, doi:10.5194/hess-16-1445-2012.

Bosch, D. D., J. M. Sheridan, and L. K. Marshall (2007), Precipitation, soil moisture, and climate database, Little River Experimental Watershed, Georgia, United States, *Water Resources Research*, 43, doi:10.1029/2006wr005834.

Brodzik, M. J., B. Billingsley, T. Haran, B. Raup, and M. H. Savoie (2012), EASE-Grid 2.0: Incremental but significant improvements for Earth-gridded data sets, *ISPRS Int. J. Geoinf., 1*, 32–45, doi:10.3390/ijgi1010032.

Caldwell, T. G., T. Bongiovanni, M. H. Cosh, C. Halley, and M. H. Young (2018), Field and Laboratory Evaluation of the CS655 Soil Water Content Sensor, *Vadose Zone Journal, 17*, 170214, doi:10.2136/vzj2017.12.0214.

Calvet, J.-C., N. Fritz, F. Froissard, D. Suquia, A. Petitpa, and B. Piguet (2007), In situ soil moisture observations for the CAL/VAL of SMOS: the SMOSMANIA network, 2007 IEEE International Geoscience and Remote Sensing Symposium, doi:10.1109/igarss.2007.4423019.

CEOS (2015), Committee on Earth Observation Satellites (CEOS) Working Group on Calibration and Validation (WGCV): http://calvalportal.ceos.org, CEOS WGCV Land Products Sub-Group: http://lpvs.gsfc.nasa.gov. Accessed 7 October 2015.

Chan, S., E. G. Njoku, and A. Colliander (2020), *SMAP L1C Radiometer Half-Orbit 36 km EASE-Grid Brightness Temperatures, Version 5*. NASA National Snow and Ice Data Center Distributed Active Archive Center, doi:10.5067/JJ5FL7FRLKJI.

Chaubell, M. J., et al. (2020), Improved SMAP Dual-Channel Algorithm for the Retrieval of Soil Moisture, *IEEE Transactions on Geoscience and Remote Sensing, 58*, 3894-3905, doi:10.1109/TGRS.2019.2959239.

Chen, F., W. T. Crow, A. Colliander, M. Cosh, T. J. Jackson, R. Bindlish, R. H. Reichle, S. K. Chan, D. D. Bosch, P. J. Starks, D. C. Goodrich, M. Seyfried (2017), Application of Triple Collocation in Ground-based Validation of Soil Moisture Active/Passive (SMAP) Level 2 Data Products, *IEEE Journal of Selected Topics in Applied Earth Observations and Remote Sensing*, *10*, 489-502, doi:10.1109/JSTARS.2016.2569998..

Chen, F. et al. (2019), Uncertainty of Reference Pixel Soil Moisture Averages Sampled at SMAP Core Validation Sites, *Journal of Hydrometeorology, 20,* 1553–1569, doi:10.1175/jhm-d-19-0049.1.

Clewley, D., J. B. Whitcomb, R. Akbar, A. R. Silva, A. Berg, J. R. Adams, T. Caldwell, D. Entekhabi, and M. Moghaddam (2017), A Method for Upscaling In Situ Soil Moisture Measurements to Satellite Footprint Scale Using Random Forests, *IEEE Journal of Selected Topics in Applied Earth Observations and Remote Sensing*, 10(6), 2663–2673, doi:10.1109/jstars.2017.2690220.

Colliander, A., S. Chan, N. Das, S. Kim, S. Dunbar, T. Jackson, C. Derksen, K. McDonald, J. Kimball, E. Njoku, R. Reichle, and B. Weiss (2014), SMAP L2-L4 Data Products Calibration and Validation Plan, Soil Moisture Active Passive (SMAP) Mission Science Document. JPL D-79463, Jet Propulsion Laboratory, Pasadena, CA.

Colliander, A., et al. (2017a), SMAP/In Situ Core Validation Site Land Surface Parameters Match-Up Data, Version 1. NASA National Snow and Ice Data Center DAAC, doi:10.5067/DXAVIXLY18KM.

Colliander, A., et al. (2017b), Validation of SMAP surface soil moisture products with core validation sites, *Remote Sensing of Environment, 191*, 215–231, doi:10.1016/j.rse.2017.01.021.

Colliander, A., R. H. Reichle, W. T. Crow, M. H. Cosh, et al. (2022), Validation of Soil Moisture Data Products from the NASA SMAP Mission, *IEEE Journal of Selected Topics in Applied Earth Observations and Remote Sensing, 15,* 364-392, doi: 10.1109/JSTARS.2021.3124743.

Coopersmith, E. J., M. H. Cosh, W. A. Petersen, J. Prueger, and J. J. Niemeier (2015), Soil Moisture Model Calibration and Validation: An ARS Watershed on the South Fork Iowa River, *Journal of Hydrometeorology, 16*, 1087–1101, doi:10.1175/jhm-d-14-0145.1.

Cosh, M. H., T. J. Jackson, P. Starks, and G. Heathman (2006), Temporal stability of surface soil moisture in the Little Washita River watershed and its applications in satellite soil moisture product validation, *Journal of Hydrology, 323*, 168–177, doi:10.1016/j.jhydrol.2005.08.020.

Cosh, M. H., P. J. Starks, J. A. Guzman, and D. N. Moriasi (2014), Upper Washita River Experimental Watersheds: Multiyear Stability of Soil Water Content Profiles, *Journal of Environmental Quality, 43*, 1328–1333, doi:10.2134/jeq2013.08.0318.

Dargie, G. C., S. L. Lewis, I. T. Lawson, et al. (2017), Age, extent and carbon storage of the central Congo Basin peatland complex, *Nature, 542* (7639), 86-90, doi:10.1038/nature21048.

De Lannoy, G. J. M, R. H. Reichle, and V. R. N. Pauwels (2013), Global Calibration of the GEOS-5 L-band Microwave Radiative Transfer Model over Nonfrozen Land Using SMOS Observations, *Journal of Hydrometeorology, 14*, 765-785, doi:10.1175/JHM-D-12-092.1.

De Lannoy, G. J. M., R. H. Reichle, and J. A. Vrugt (2014a), Uncertainty Quantification of GEOS-5 L-Band Radiative Transfer Model Parameters using Bayesian Inference and SMOS Observations, *Remote Sensing of Environment, 148*, 146-157, doi:10.1016/j.rse.2014.03.030.

De Lannoy, G. J. M., R. D. Koster, R. H. Reichle, S. P. P. Mahanama, and Q. Liu (2014b), An Updated Treatment of Soil Texture and Associated Hydraulic Properties in a Global Land Modeling System, *Journal of Advances in Modeling Earth Systems, 6*, 957-979, doi:10.1002/2014MS000330.

De Lannoy, G. J. M., and R. H. Reichle (2016), Global Assimilation of Multiangle and Multipolarization SMOS Brightness Temperature Observations into the GEOS-5 Catchment Land Surface Model for Soil Moisture Estimation, *Journal of Hydrometeorology, 17*, 669-691, doi:10.1175/JHM-D-15-0037.1.

Diamond, H. J. et al. (2013), U.S. Climate Reference Network after One Decade of Operations: Status and Assessment, *Bulletin of the American Meteorological Society, 94*, 485–498, doi:10.1175/bams-d-12-00170.1.

Dong, J., W. T. Crow, K. J. Tobin, M. H. Cosh, D. D. Bosch, P. J. Starks, M. Seyfried, and C. Holifield-Collins (2020), Comparison of microwave remote sensing and land surface modeling for surface soil moisture climatology estimation, *Remote Sensing of Environment*, *242*, 111756, doi:10.1016/j.rse.2020.111756.

Entekhabi, D., R. H. Reichle, R. D. Koster, and W. T. Crow (2010), Performance Metrics for Soil Moisture Retrievals and Application Requirements, *Journal of Hydrometeorology, 11*, 832-840, doi:10.1175/2010JHM1223.1.

Entekhabi, D., et al. (2014), SMAP Handbook, *JPL Publication, JPL 400-1567*, NASA Jet Propulsion Laboratory, Pasadena, California, USA, 182 pp.

Galle, S. et al. (2018), AMMA-CATCH, a Critical Zone Observatory in West Africa Monitoring a Region in Transition, *Vadose Zone Journal*, 17(1), 0, doi:10.2136/vzj2018.03.0062.

González-Zamora, Á., N. Sánchez, J. Martínez-Fernández, Á. Gumuzzio, M. Piles, and E. Olmedo (2015), Long-term SMOS soil moisture products: A comprehensive evaluation across scales and methods in the Duero Basin (Spain), *Physics and Chemistry of the Earth, Parts A/B/C*, 83-84, 123–136, doi:10.1016/j.pce.2015.05.009.

Gruber, A., C.-H. Su, S. Zwieback, W. Crow, W. Dorigo, and W. Wagner (2016), Recent advances in (soil moisture) triple collocation analysis, *International Journal of Applied Earth Observation and Geoinformation*, *45B*, 200-211, doi: 10.1016/j.jag.2015.09.002.

Gruber, A., et al. (2020), Validation practices for satellite soil moisture retrievals: What are (the) errors?, *Remote Sensing of Environment, 244*, 111806, doi:10.1016/j.rse.2020.111806.

Heathman, G. C., M. H. Cosh, V. Merwade, and E. Han (2012), Multi-scale temporal stability analysis of surface and subsurface soil moisture within the Upper Cedar Creek Watershed, Indiana, *CATENA*, 95, 91–103, doi:10.1016/j.catena.2012.03.008.

Huffman, G. J., E. F. Stocker, D. T. Bolvin, E. J. Nelkin, and J. Tan (2019a), *GPM IMERG Final Precipitation L3 Half Hourly 0.1 degree x 0.1 degree V06*. Goddard Earth Sciences Data and Information Services Center (GES DISC), doi:10.5067/GPM/IMERG/3B-HH/06.

Huffman, G. J., E. F. Stocker, D. T. Bolvin, E. J. Nelkin, and J. Tan (2019b), *GPM IMERG Late Precipitation L3 Half Hourly 0.1 degree x 0.1 degree V06.* Goddard Earth Sciences Data and Information Services Center (GES DISC), doi:10.5067/GPM/IMERG/3B-HH-L/06.

Jackson, T. J., A. Colliander, J. Kimball, R. Reichle, C. Derksen, W. Crow, D. Entekhabi, P. O'Neill, and E. Njoku (2014), SMAP Science Data Calibration and Validation Plan (Revision A), Soil Moisture Active Passive (SMAP) Mission Science Document. JPL D-52544, Jet Propulsion Laboratory, Pasadena, CA.

Jensen, K. H., and J. C. Refsgaard (2018), HOBE: The Danish Hydrological Observatory, *Vadose Zone Journal, 17*, 180059, doi:10.2136/vzj2018.03.0059.

Juglea, S., Y. Kerr, A. Mialon, J.-P. Wigneron, E. Lopez-Baeza, A. Cano, A. Albitar, C. Millan-Scheiding, M. Carmen Antolin, and S. Delwart (2010), Modelling soil moisture at SMOS scale by use of a SVAT model over the Valencia Anchor Station, *Hydrology and Earth System Sciences*, 14(5), 831–846, doi:10.5194/hess-14-831-2010.

Keefer, T. O., M. S. Moran, and G. B. Paige (2008), Long-term meteorological and soil hydrology database, Walnut Gulch Experimental Watershed, Arizona, United States, *Water Resources Research, 44*, doi:10.1029/2006wr005702.

Khodayar, S., A. Coll, and E. Lopez-Baeza (2019), An improved perspective in the spatial representation of soil moisture: potential added value of SMOS disaggregated 1-km resolution "all weather" product, *Hydrology and Earth System Sciences*, 23(1), 255–275, doi:10.5194/hess-23-255-2019.

Koster, R. D., M. J. Suarez, A. Ducharne, M. Stieglitz, and P. Kumar (2000), A catchment-based approach to modeling land surface processes in a general circulation model: 1. Model structure, *J. Geophys. Res., 105*, 24809–24822, doi:10.1029/2000JD900327.

Liu, Q., R. H. Reichle, R. Bindlish, M. H. Cosh, W. T. Crow, R. de Jeu, G. J. M. De Lannoy, G. J. Huffman, and T. J. Jackson (2011), The contributions of precipitation and soil moisture observations to the skill of soil moisture estimates in a land data assimilation system, *Journal of Hydrometeorology, 12*, 750-765, doi:10.1175/JHM-D-10-05000.1.

Lucchesi, R. (2018), File specification for GEOS-5 FP, *NASA GMAO Office Note No. 4 (version 1.2)*, 56 pp., NASA Goddard Space Flight Center, Greenbelt, MD, USA. Available at: https://gmao.gsfc.nasa.gov/pubs

McNairn, H. et al. (2015), The Soil Moisture Active Passive Validation Experiment 2012 (SMAPVEX12): Prelaunch Calibration and Validation of the SMAP Soil Moisture Algorithms, *IEEE Transactions on Geoscience and Remote Sensing, 53*, 2784–2801, doi:10.1109/tgrs.2014.2364913.

McPherson, R. A. et al. (2007), Statewide Monitoring of the Mesoscale Environment: A Technical Update on the Oklahoma Mesonet, *Journal of Atmospheric and Oceanic Technology, 24*, 301–321, doi:10.1175/jtech1976.1.

Moghaddam, M. et al. (2016), *Soil Moisture Profiles and Temperature Data from SoilSCAPE Sites, USA*, ORNL Distributed Active Archive Center, doi:10.3334/ornldaac/1339.

Montzka, C., et al. (2020), Soil Moisture Product Validation Good Practices Protocol Version 1.0., In: *Good Practices for Satellite Derived Land Product Validation, Land Product Validation Subgroup (WGCV/CEOS)*, edited by C. Montzka, M. Cosh, J. Nickeson, F. Camacho, 123 pp, doi:10.5067/doc/ceoswgcv/lpv/sm.001.

O'Neill, P., et al. (2021), Calibration and Validation for the L2/3_SM_P Version 8 and L2/3_SM_P_E Version 5 Data Products, SMAP Project, JPL D-56297, Jet Propulsion Laboratory, Pasadena, CA.

O'Neill, P. E., S. Chan, E. G. Njoku, T. Jackson, R. Bindlish, J. Chaubell, and A. Colliander (2021), *SMAP Enhanced L2 Radiometer Half-Orbit 9 km EASE-Grid Soil Moisture, Version 5*. NASA National Snow and Ice Data Center Distributed Active Archive Center, doi:10.5067/LOT311EZHH8S.

Panciera, R., et al. (2014), The Soil Moisture Active Passive Experiments (SMAPEx): Toward Soil Moisture Retrieval From the SMAP Mission, *IEEE Transactions on Geoscience and Remote Sensing, 52*, 490–507, doi:10.1109/tgrs.2013.2241774.

Reichle, R. H. (2008), Data Assimilation Methods in the Earth Sciences, *Advances in Water Resources, 31*, 1411-1418, doi:10.1016/j.advwatres.2008.01.001.

Reichle, R. H., and Q. Liu (2014), Observation-Corrected Precipitation Estimates in GEOS-5, *NASA Technical Report Series on Global Modeling and Data Assimilation, NASA/TM-2014-104606, Vol. 35*, National Aeronautics and Space Administration, Goddard Space Flight Center, Greenbelt, Maryland, USA, 18pp. Available at: https://gmao.gsfc.nasa.gov/pubs.

Reichle, R. H., and Q. Liu (2021), Observation-Corrected Precipitation for the SMAP Level 4 Soil Moisture (Version 6) Product and the GEOS R21C Reanalysis, *NASA Technical Report Series on Global Modeling and Data Assimilation, NASA/TM-2021-104606, Vol. 59*, National Aeronautics and Space Administration, Goddard Space Flight Center, Greenbelt, Maryland, USA, 28pp.

Reichle, R. H., G. J. M. De Lannoy, B. A. Forman, C. S. Draper, and Q. Liu (2014a), Connecting Satellite Observations with Water Cycle Variables through Land Data Assimilation: Examples Using the NASA GEOS-5 LDAS, *Surveys in Geophysics, 35*, 577-606, doi:10.1007/s10712-013-9220-8.

Reichle, R. H., R. Koster, G. De Lannoy, W. Crow, and J. Kimball (2014b), SMAP Level 4 Surface and Root Zone Soil Moisture Data Product: L4_SM Algorithm Theoretical Basis Document (Revision A), Soil Moisture Active Passive (SMAP) Mission Science Document. JPL D-66483, Jet Propulsion Laboratory, Pasadena, CA.

Reichle, R. H., G. J. M. De Lannoy, Q. Liu, A. Colliander, A. Conaty, T. Jackson, J. Kimball, and R. D. Koster (2015), Soil Moisture Active Passive (SMAP) Project Assessment Report for the Beta-Release L4_SM Data Product, *NASA Technical Report Series on Global Modeling and Data Assimilation, NASA/TM-2015-104606, Vol. 40*, National Aeronautics and Space Administration, Goddard Space Flight Center, Greenbelt, Maryland, USA, 63pp. Available at: https://gmao.gsfc.nasa.gov/pubs.

Reichle, R. H., G. J. M. De Lannoy, Q. Liu, J. V. Ardizzone, F. Chen, A. Colliander, A. Conaty, W. Crow, T. Jackson, J. Kimball, R. D. Koster, and E. B. Smith (2016), Soil Moisture Active Passive Mission L4_SM Data Product Assessment (Version 2 Validated Release), *NASA GMAO Office Note No. 12 (Version 1.0)*, 55pp., NASA Goddard Space Flight Center, Greenbelt, MD, USA. Available at: https://gmao.gsfc.nasa.gov/pubs

Reichle, R. H., et al. (2017a), Assessment of the SMAP Level-4 Surface and Root-Zone Soil Moisture Product Using In Situ Measurements, *Journal of Hydrometeorology, 18*, 2621-2645, doi:10.1175/JHM-D-17-0063.1.

Reichle, R. H., et al. (2017b), Global Assessment of the SMAP Level-4 Surface and Root-Zone Soil Moisture Product Using Assimilation Diagnostics, *Journal of Hydrometeorology, 18*, 3217-3237, doi:10.1175/JHM-D-17-0130.1.

Reichle, R. H., Q. Liu, R. D. Koster, J. V. Ardizzone, A. Colliander, W. T. Crow, G. J. M. De Lannoy, and J. S. Kimball (2018), Soil Moisture Active Passive (SMAP) Project Assessment Report for Version 4 of the L4_SM Data Product, *NASA Technical Report Series on Global Modeling and Data Assimilation, NASA/TM-2018-104606, Vol. 52*, National Aeronautics and Space Administration, Goddard Space Flight Center, Greenbelt, Maryland, USA, 72pp. Available at: https://gmao.gsfc.nasa.gov/pubs.

Reichle, R. H., et al. (2019), Version 4 of the SMAP Level-4 Soil Moisture Algorithm and Data Product, *Journal of Advances in Modeling Earth Systems, 11*, 3106-3130, doi:10.1029/2019MS001729.

Reichle, R. H., Q. Liu, J. V. Ardizzone, W. T. Crow, G. J. M. De Lannoy, J. Dong, J. S. Kimball, and R. D. Koster (2021a), The Contributions of Gauge-Based Precipitation and SMAP Brightness Temperature Observations to the Skill of the SMAP Level-4 Soil Moisture Product, *Journal of Hydrometeorology, 22*, 405-424, doi:10.1175/JHM-D-20-0217.1.

Reichle, R. H., Q. Liu, R. D. Koster, J. V. Ardizzone, A. Colliander, W. T. Crow, G. J. M. De Lannoy, and J. S. Kimball (2021b), Soil Moisture Active Passive (SMAP) Project Assessment Report for Version 5 of the L4_SM Data Product, *NASA Technical Report Series on Global Modeling and Data Assimilation, NASA/TM-2021-104606, Vol. 58*, National Aeronautics and Space Administration, Goddard Space Flight Center, Greenbelt, Maryland, USA, 56pp. Available at: https://gmao.gsfc.nasa.gov/pubs.

Reichle, R., G. De Lannoy, R. D. Koster, W. T. Crow, J. S. Kimball, and Q. Liu (2021c), *SMAP L4 Global 3-hourly 9 km EASE-Grid Surface and Root Zone Soil Moisture Analysis Update, Version 6*. NASA National Snow and Ice Data Center Distributed Active Archive Center, doi:10.5067/6P2EV47VMYPC.

Reichle, R., G. De Lannoy, R. D. Koster, W. T. Crow, J. S. Kimball, and Q. Liu (2021d), *SMAP L4 Global 3-hourly 9 km EASE-Grid Surface and Root Zone Soil Moisture Geophysical Data, Version 6*. NASA National Snow and Ice Data Center Distributed Active Archive Center, doi: 10.5067/08S1A6811J0U.

Reichle, R., G. De Lannoy, R. D. Koster, W. T. Crow, J. S. Kimball, and Q. Liu (2021e), *SMAP L4 Global 3-hourly 9 km EASE-Grid Surface and Root Zone Soil Moisture Land Model Constants, Version 6*. NASA National Snow and Ice Data Center Distributed Active Archive Center, doi:10.5067/MWAFPGI1KMMH.

Reichle, R. H., S. Q. Zhang, Q. Liu, C. S. Draper, J. Kolassa, and R. Todling (2021f), Assimilation of SMAP Brightness Temperature Observations in the GEOS Land-Atmosphere Data Assimilation System, *IEEE Journal of Selected Topics in Applied Earth Observations and Remote Sensing, 14*, 10628-10643, doi:10.1109/JSTARS.2021.3118595.

Reichle, R. H., Q. Liu, R. D. Koster, J. V. Ardizzone, A. Colliander, W. T. Crow, G. J. M. De Lannoy, and J. S. Kimball (2022a), Soil Moisture Active Passive (SMAP) Project Assessment Report for Version 6 of the L4_SM Data Product, *NASA Technical Report Series on Global Modeling and Data Assimilation, NASA/TM-2022-104606, Vol. 60*, National Aeronautics and Space Administration, Goddard Space Flight Center, Greenbelt, Maryland, USA, 72pp. Available at: https://gmao.gsfc.nasa.gov/pubs.

Reichle, R. H., R. A. Lucchesi, J. V. Ardizzone, G.-K. Kim, E. B. Smith, and B. H. Weiss (2022b), Soil Moisture Active Passive (SMAP) Mission Level 4 Surface and Root Zone Soil Moisture (L4_SM) Product Specification Document, *NASA GMAO Office Note No. 10 (Version 1.6)*, 84 pp., NASA Goddard Space Flight Center, Greenbelt, MD, USA. Available at: https://gmao.gsfc.nasa.gov/pubs.

Reichle, R., G. De Lannoy, R. D. Koster, W. T. Crow, J. S. Kimball, Q. Liu, and M. Bechtold (2022c), *SMAP L4 Global 3-hourly 9 km EASE-Grid Surface and Root Zone Soil Moisture Analysis Update, Version 7*. NASA National Snow and Ice Data Center Distributed Active Archive Center, doi:10.5067/ LWJ6TF5SZRG3.

Reichle, R., G. De Lannoy, R. D. Koster, W. T. Crow, J. S. Kimball, Q. Liu, and M. Bechtold (2022d), *SMAP L4 Global 3-hourly 9 km EASE-Grid Surface and Root Zone Soil Moisture Geophysical Data, Version 7*. NASA National Snow and Ice Data Center Distributed Active Archive Center, doi:10.5067/ EVKPQZ4AFC4D.

Reichle, R., G. De Lannoy, R. D. Koster, W. T. Crow, J. S. Kimball, Q. Liu, and M. Bechtold (2022e), *SMAP L4 Global 3-hourly 9 km EASE-Grid Surface and Root Zone Soil Moisture Land Model Constants, Version 7*. NASA National Snow and Ice Data Center Distributed Active Archive Center, doi:10.5067/ KN96XNPZM4EG.

Rowlandson, T., S. Impera, J. Belanger, A. A. Berg, B. Toth, and R. Magagi (2015), Use of in situ soil moisture network for estimating regional-scale soil moisture during high soil moisture conditions, *Canadian Water Resources Journal / Revue canadienne des ressources hydriques, 40*, 343–351, doi:10.1080/07011784.2015.1061948.

Sanchez, N., J. Martinez-Fernandez, A. Scaini, and C. Perez-Gutierrez (2012), Validation of the SMOS L2 Soil Moisture Data in the REMEDHUS Network (Spain), *IEEE Transactions on Geoscience and Remote Sensing, 50*, 1602–1611, doi:10.1109/tgrs.2012.2186971.

Schaefer, G. L., M. H. Cosh, and T. J. Jackson (2007), The USDA Natural Resources Conservation Service Soil Climate Analysis Network (SCAN), *Journal of Atmospheric and Oceanic Technology, 24*, 2073–2077, doi:10.1175/2007jtecha930.1.

Seyfried, M. S., M. D. Murdock, C. L. Hanson, G. N. Flerchinger, and S. Van Vactor (2001), Long-Term Soil Water Content Database, Reynolds Creek Experimental Watershed, Idaho, United States, *Water Resources Research*, 37(11), 2847–2851, doi:10.1029/2001wr000419.

Smith, A. B., J. P. Walker, A. W. Western, R. I. Young, K. M. Ellett, R. C. Pipunic, R. B. Grayson, L. Siriwardena, F. H. S. Chiew, and H. Richter (2012), The Murrumbidgee soil moisture monitoring network data set, *Water Resources Research, 48*, doi:10.1029/2012wr011976.

Tan, J., G. J. Huffman, D. T. Bolvin, and E. J. Nelkin (2019), IMERG V06: Changes to the Morphing Algorithm. *Journal of Atmospheric and Oceanic Technology, 36*, 2471–2482, doi:10.1175/jtech-d-19-0114.1.

Tao, J., R. H. Reichle, R. D. Koster, B. A. Forman, and Y. Xue (2017), Evaluation and enhancement of permafrost modeling with the NASA Catchment Land Surface Model, *Journal of Advances in Modeling Earth Systems, 9*, 2771-2795, doi:10.1002/2017MS001019.

Tao, J., R. D. Koster, R. H. Reichle, B. A. Forman, Y. Xue, R. H. Chen, and M. Moghaddam (2019), Permafrost Variability over the Northern Hemisphere Based on the MERRA-2 Reanalysis, *The Cryosphere, 13*, 2087-2110, doi:10.5194/tc-13-2087-2019.

Tetlock, E., B. Toth, A. Berg, T. Rowlandson, and J. T. Ambadan (2019), An 11-year (2007–2017) soil moisture and precipitation dataset from the Kenaston Network in the Brightwater Creek basin, Saskatchewan, Canada, *Earth System Science Data, 11*, 787–796, doi:10.5194/essd-11-787-2019.

Thibeault, M., J. M. Caceres, D. Dadamia, A. G. Soldano, M. U. Quirno, J. M. Guerrieri, et al. (2015), Spatial and temporal analysis of the Monte Buey SAOCOM and SMAP core site. In 2015 IEEE International Geoscience and Remote Sensing Symposium (IGARSS), IEEE, doi:10.1109/igarss.2015.7325929.

Wagner, W., S. Hahn, R. Kidd, T. Melzer, Z. Bartalis, S. Hasenauer, et al. (2013), The ASCAT Soil Moisture Product: A Review of its Specifications, Validation Results, and Emerging Applications, *Meteorologische Zeitschrift, 22*, 5-33, doi:10.1127/0941-2948/2013/0399.

Wen, X., H. Lu, C. Li, T. Koike, and I, Kaihotsu. (2014), Inter-comparison of soil moisture products from SMOS, AMSR-E, ECWMF and GLDAS over the Mongolia Plateau. In T. J. Jackson, J. M. Chen, P. Gong, and S. Liang (Eds.), *Land Surface Remote Sensing II*, SPIE, doi: 10.1117/12.2068952.

Xu, J., P. Morris, J. Liu, and J. Holden (2018), PEATMAP: Refining estimates of global peatland distribution based on a meta-analysis, *Catena, 160*, 134–140, doi:10.1016/j.catena.2017.09.010.

Previous Volumes in This Series

Volume 1
September 1994

Documentation of the Goddard Earth Observing System (GEOS) general circulation model - Version 1

L.L. Takacs, A. Molod, and T. Wang

Volume 2
October 1994

Direct solution of the implicit formulation of fourth order horizontal diffusion for gridpoint models on the sphere

Y. Li, S. Moorthi, and J.R. Bates

Volume 3
December 1994

An efficient thermal infrared radiation parameterization for use in general circulation models

M.-D. Chou and M.J. Suarez

Volume 4
January 1995

Documentation of the Goddard Earth Observing System (GEOS) Data Assimilation System - Version 1

James Pfaendtner, Stephen Bloom, David Lamich, Michael Seablom, Meta Sienkiewicz, James Stobie, and Arlindo da Silva

Volume 5
April 1995

Documentation of the Aries-GEOS dynamical core: Version 2

Max J. Suarez and Lawrence L. Takacs

Volume 6
April 1995

A Multiyear Assimilation with the GEOS-1 System: Overview and Results

Siegfried Schubert, Chung-Kyu Park, Chung-Yu Wu, Wayne Higgins, Yelena Kondratyeva, Andrea Molod, Lawrence Takacs, Michael Seablom, and Richard Rood

Volume 7
September 1995

Proceedings of the Workshop on the GEOS-1 Five-Year Assimilation

Siegfried D. Schubert and Richard B. Rood

Volume 8
March 1996

Documentation of the Tangent Linear Model and Its Adjoint of the Adiabatic Version of the NASA GEOS-1 C-Grid GCM: Version 5.2

Weiyu Yang and I. Michael Navon

Volume 9
March 1996

Energy and Water Balance Calculations in the Mosaic LSM

Randal D. Koster and Max J. Suarez

Volume 10 — April 1996
Dynamical Aspects of Climate Simulations Using the GEOS General Circulation Model
Lawrence L. Takacs and Max J. Suarez

Volume 11 — May 1997
Documentation of the Tangent Linear and Adjoint Models of the Relaxed Arakawa-Schubert Moisture Parameterization Package of the NASA GEOS-1 GCM (Version 5.2)
Weiyu Yang, I. Michael Navon, and Ricardo Todling

Volume 12 — August 1997
Comparison of Satellite Global Rainfall Algorithms
Alfred T.C. Chang and Long S. Chiu

Volume 13 — December 1997
Interannual Variability and Potential Predictability in Reanalysis Products
Wie Ming and Siegfried D. Schubert

Volume 14 — August 1998
A Comparison of GEOS Assimilated Data with FIFE Observations
Michael G. Bosilovich and Siegfried D. Schubert

Volume 15 — June 1999
A Solar Radiation Parameterization for Atmospheric Studies
Ming-Dah Chou and Max J. Suarez

Volume 16 — November 1999
Filtering Techniques on a Stretched Grid General Circulation Model
Lawrence Takacs, William Sawyer, Max J. Suarez, and Michael S. Fox-Rabinowitz

Volume 17 — July 2000
Atlas of Seasonal Means Simulated by the NSIPP-1 Atmospheric GCM
Julio T. Bacmeister, Philip J. Pegion, Siegfried D. Schubert, and Max J. Suarez

Volume 18 — December 2000
An Assessment of the Predictability of Northern Winter Seasonal Means with the NSIPP1 AGCM
Philip J. Pegion, Siegfried D. Schubert, and Max J. Suarez

Volume 19 — July 2001
A Thermal Infrared Radiation Parameterization for Atmospheric Studies
Ming-Dah Chou, Max J. Suarez, Xin-Zhong Liang, and Michael M.-H. Yan

Volume 20 — *The Climate of the FVCCM-3 Model*

August 2001 — Yehui Chang, Siegfried D. Schubert, Shian-Jiann Lin, Sharon Nebuda, and Bo-Wen Shen

Volume 21 — *Design and Implementation of a Parallel Multivariate Ensemble Kalman Filter for the Poseidon Ocean General Circulation Model*

September 2001 — Christian L. Keppenne and Michele M. Rienecker

Volume 22 — *A Coupled Ocean-Atmosphere Radiative Model for Global Ocean Biogeochemical Models*

August 2002 — Watson W. Gregg

Volume 23 — *Prospects for Improved Forecasts of Weather and Short-term Climate Variability on Subseasonal (2-Week to 2-Month) Time Scales*

November 2002 — Siegfried D. Schubert, Randall Dole, Huang van den Dool, Max J. Suarez, and Duane Waliser

Volume 24 — *Temperature Data Assimilation with Salinity Corrections: Validation for the NSIPP Ocean Data Assimilation System in the Tropical Pacific Ocean, 1993–1998*

July 2003 — Alberto Troccoli, Michele M. Rienecker, Christian L. Keppenne, and Gregory C. Johnson

Volume 25 — *Modeling, Simulation, and Forecasting of Subseasonal Variability*

December 2003 — Duane Waliser, Siegfried D. Schubert, Arun Kumar, Klaus Weickmann, and Randall Dole

Volume 26 — *Documentation and Validation of the Goddard Earth Observing System (GEOS) Data Assimilation System – Version 4*

April 2005 — Senior Authors: S. Bloom, A. da Silva and D. Dee

Contributing Authors: M. Bosilovich, J-D. Chern, S. Pawson, S. Schubert, M. Sienkiewicz, I. Stajner, W-W. Tan, and M-L. Wu

Volume 27 — *The GEOS-5 Data Assimilation System - Documentation of Versions 5.0.1, 5.1.0, and 5.2.0.*

December 2008 — M.M. Rienecker, M.J. Suarez, R. Todling, J. Bacmeister, L. Takacs, H.-C. Liu, W. Gu, M. Sienkiewicz, R.D. Koster, R. Gelaro, I. Stajner, and J.E. Nielsen

Volume 28
April 2012

The GEOS-5 Atmospheric General Circulation Model: Mean Climate and Development from MERRA to Fortuna

Andrea Molod, Lawrence Takacs, Max Suarez, Julio Bacmeister, In-Sun Song, and Andrew Eichmann

Volume 29
June 2012

Atmospheric Reanalyses – Recent Progress and Prospects for the Future.

A Report from a Technical Workshop, April 2010

Michele M. Rienecker, Dick Dee, Jack Woollen, Gilbert P. Compo, Kazutoshi Onogi, Ron Gelaro, Michael G. Bosilovich, Arlindo da Silva, Steven Pawson, Siegfried Schubert, Max Suarez, Dale Barker, Hirotaka Kamahori, Robert Kistler, and Suranjana Saha

Volume 30
December 2012

The GEOS-iODAS: Description and Evaluation

Guillaume Vernieres, Michele M. Rienecker, Robin Kovach and Christian L. Keppenne

Volume 31
March 2013

Global Surface Ocean Carbon Estimates in a Model Forced by MERRA

Watson W. Gregg, Nancy W. Casey and Cécile S. Rousseaux

Volume 32
March 2014

Estimates of AOD Trends (2002-2012) over the World's Major Cities based on the MERRA Aerosol Reanalysis

Simon Provencal, Pavel Kishcha, Emily Elhacham, Arlindo M. da Silva, and Pinhas Alpert

Volume 33
August 2014

The Effects of Chlorophyll Assimilation on Carbon Fluxes in a Global Biogeochemical Model

Cécile S. Rousseaux and Watson W. Gregg

Volume 34
September 2014

Background Error Covariance Estimation using Information from a Single Model Trajectory with Application to Ocean Data Assimilation into the GEOS-5 Coupled Model

Christian L. Keppenne, Michele M. Rienecker, Robin M. Kovach, and Guillaume Vernieres

Volume 35
December 2014

Observation-Corrected Precipitation Estimates in GEOS-5

Rolf H. Reichle and Qing Liu

Volume 36 *Evaluation of the 7-km GEOS-5 Nature Run*

March 2015 Ronald Gelaro, William M. Putman, Steven Pawson, Clara Draper, Andrea Molod, Peter M. Norris, Lesley Ott, Nikki Prive, Oreste Reale, Deepthi Achuthavarier, Michael Bosilovich, Virginie Buchard, Winston Chao, Lawrence Coy, Richard Cullather, Arlindo da Silva, Anton Darmenov, Ronald M. Errico, Marangelly Fuentes, Min-Jeong Kim, Randal Koster, Will McCarty, Jyothi Nattala, Gary Partyka, Siegfried Schubert, Guillaume Vernieres, Yuri Vikhliaev, and Krzysztof Wargan

Volume 37 *Maintaining Atmospheric Mass and Water Balance within Reanalysis*

March 2015 Lawrence L. Takacs, Max Suarez, and Ricardo Todling

Volume 38 *The Quick Fire Emissions Dataset (QFED) – Documentation of versions 2.1, 2.2 and 2.4*

September 2015 Anton S. Darmenov and Arlindo da Silva

Volume 39 *Land Boundary Conditions for the Goddard Earth Observing System Model Version 5 (GEOS-5) Climate Modeling System - Recent Updates and Data File Descriptions*

September 2015 Sarith Mahanama, Randal Koster, Gregory Walker, Lawrence Takacs, Rolf Reichle, Gabrielle De Lannoy, Qing Liu, Bin Zhao, and Max Suarez

Volume 40 *Soil Moisture Active Passive (SMAP) Project Assessment Report for the Beta-Release L4_SM Data Product*

October 2015 Rolf H. Reichle, Gabrielle J. M. De Lannoy, Qing Liu, Andreas Colliander, Austin Conaty, Thomas Jackson, John Kimball, and Randal D. Koster

Volume 41 *GDIS Workshop Report*

October 2015 Siegfried Schubert, Will Pozzi, Kingtse Mo, Eric Wood, Kerstin Stahl, Mike Hayes, Juergen Vogt, Sonia Seneviratne, Ron Stewart, Roger Pulwarty, and Robert Stefanski

Volume 42 *Soil Moisture Active Passive (SMAP) Project Calibration and Validation for the L4_C Beta-Release Data Product*

November 2015 John Kimball, Lucas Jones, Joseph Glassy, E. Natasha Stavros, Nima Madani, Rolf Reichle, Thomas Jackson, and Andreas Colliander

Volume 43 — September 2015

MERRA-2: Initial Evaluation of the Climate

Michael G. Bosilovich, Santha Akella, Lawrence Coy, Richard Cullather, Clara Draper, Ronald Gelaro, Robin Kovach, Qing Liu, Andrea Molod, Peter Norris, Krzysztof Wargan, Winston Chao, Rolf Reichle, Lawrence Takacs, Yury Vikhliaev, Steve Bloom, Allison Collow, Stacey Firth, Gordon Labow, Gary Partyka, Steven Pawson, Oreste Reale, Siegfried Schubert, and Max Suarez

Volume 44 — February 2016

Estimation of the Ocean Skin Temperature using the NASA GEOS Atmospheric Data Assimilation System

Santha Akella, Ricardo Todling, Max Suarez

Volume 45 — October 2016

The MERRA-2 Aerosol Assimilation

C. A. Randles, A. M. da Silva, V. Buchard, A. Darmenov, P. R. Colarco, V. Aquila, H. Bian, E. P. Nowottnick, X. Pan, A. Smirnov, H. Yu, and R. Govindaraju

Volume 46 — October 2016

The MERRA-2 Input Observations: Summary and Assessment

Will McCarty, Lawrence Coy, Ronald Gelaro, Albert Huang, Dagmar Merkova, Edmond B. Smith, Meta Sienkiewicz, and Krzysztof Wargan

Volume 47 — May 2017

An Evaluation of Teleconnections Over the United States in an Ensemble of AMIP Simulations with the MERRA-2 Configuration of the GEOS Atmospheric Model.

Allison B. Marquardt Collow, Sarith P. Mahanama, Michael G. Bosilovich, Randal D. Koster, and Siegfried D. Schubert

Volume 48 — July 2017

Description of the GMAO OSSE for Weather Analysis Software Package: Version 3

Ronald M. Errico, Nikki C. Prive, David Carvalho, Meta Sienkiewicz, Amal El Akkraoui, Jing Guo, Ricardo Todling, Will McCarty, William M. Putman, Arlindo da Silva, Ronald Gelaro, and Isaac Moradi

Volume 49 — March 2018

Preliminary Evaluation of Influence of Aerosols on the Simulation of Brightness Temperature in the NASA Goddard Earth Observing System Atmospheric Data Assimilation System

Jong Kim, Santha Akella, Will McCarty, Ricardo Todling, and Arlindo M. da Silva

Volume 50
March 2018

The GMAO Hybrid Ensemble-Variational Atmospheric Data Assimilation System: Version 2.0

Ricardo Todling and Amal El Akkraoui

Volume 51
July 2018

The Atmosphere-Ocean Interface Layer of the NASA Goddard Earth Observing System Model and Data Assimilation System

Santha Akella and Max Suarez

Volume 52
July 2018

Soil Moisture Active Passive (SMAP) Project Assessment Report for Version 4 of the L4_SM Data Product

Rolf H. Reichle, Qing Liu, Randal D. Koster, Joe Ardizzone, Andreas Colliander, Wade Crow, Gabrielle J. M. De Lannoy, and John Kimball

Volume 53
October 2019

Ensemble Generation Strategies Employed in the GMAO GEOS-S2S Forecast System

Siegfried Schubert, Anna Borovikov, Young-Kwon Lim, and Andrea Molod

Volume 54
August 2020

Position Estimation of Atmospheric Motion Vectors for Observation System Simulation Experiments

David Carvalho and Will McCarty

Volume 55
February 2021

A Phenomenon-Based Decomposition of Model-Based Estimates of Boreal Winter ENSO Variability

Siegfried Schubert, Young-Kwon Lim, Andrea Molod, and Allison Collow

Volume 56
June 2021

Validation Assessment for the Soil Moisture Active Passive (SMAP) Level 4 Carbon (L4_C) Data Product Version 5

John S. Kimball, K. Arthur Endsley, Tobias Kundig, Joseph Glassy, Rolf H. Reichle, and Joseph V. Ardizzone

Volume 57
July 2021

Tendency Bias Correction in the GEOS AGCM

Yehui Chang, Siegfried Schubert, Randal Koster, and Andrea Molod

Volume 58
August 2021

Soil Moisture Active Passive (SMAP) Project Assessment Report for Version 5 of the L4_SM Data Product

Rolf H. Reichle, Qing Liu, Randal D. Koster, Joseph V. Ardizzone, Andreas Colliander, Wade Crow, Gabrielle J. M. De Lannoy, and John S. Kimball

Volume 59
November 2021

Observation-Corrected Land Surface Precipitation for the SMAP Level 4 Soil Moisture (Version 6) Product and the GEOS R21C Reanalysis

Rolf H. Reichle and Qing Liu

Volume 60
January 2022

Soil Moisture Active Passive (SMAP) Project Assessment Report for Version 6 of the L4_SM Data Product

Rolf H. Reichle, Qing Liu, Randal D. Koster, Joseph V. Ardizzone, Andreas Colliander, Wade Crow, Gabrielle J. M. De Lannoy, and John S. Kimball

Volume 61
April 2022

Validation Assessment for the Soil Moisture Active Passive (SMAP) Level 4 Carbon (L4_C) Data Product Version 6

John S. Kimball, K. Arthur Endsley, Tobias Kundig, Joseph Glassy, Rolf H. Reichle, and Joseph V. Ardizzone

Volume 62
September 2022

Climate Characteristics of the Atmospheric Analysis Increments from the GEOS S2S V3 AOGCM Replayed to MERRA-2

Yehui Chang, Siegfried Schubert, Randal Koster, Andrea Molod, and Yong-Kwon Lim

Volume 63
October 2022

GEOS aerosol optical table calculation package GEOSmie

Osku Kemppinen, Peter R. Colarco and Patricia Castellanos